J-Aggregates

DOI: 10.1002/anie.201002307

J-Aggregates: From Serendipitous Discovery to Supramolecular Engineering of Functional Dye Materials

Frank Würthner, Theo E. Kaiser, and Chantu R. Saha-Möller*

Keywords:
aggregation · cyanines · dyes/pigments · self-assembly · supramolecular chemistry

Dedicated to Professor Siegfried Hünig on the occasion of his 90th birthday

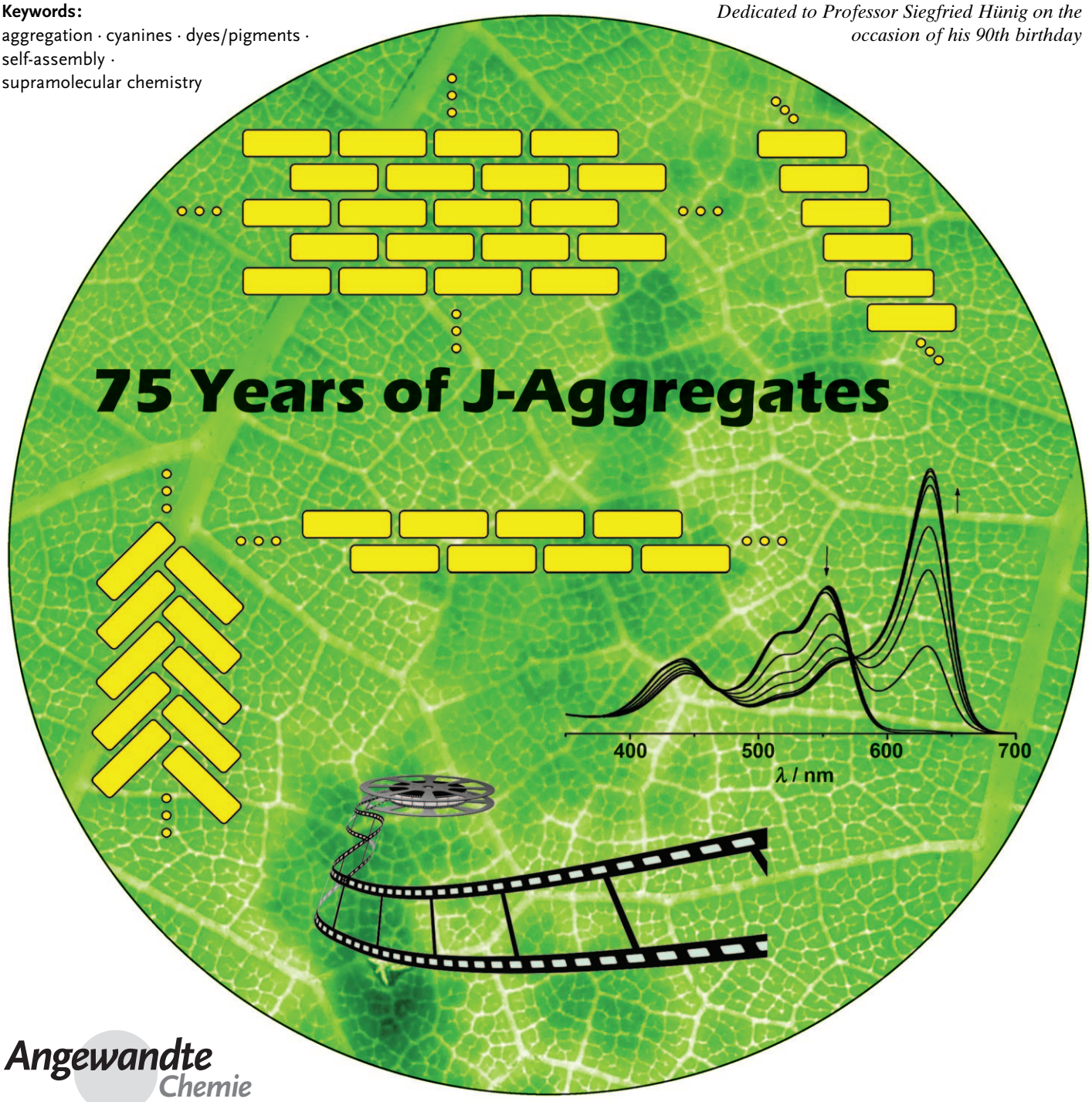

J-aggregates are of significant interest for organic materials conceived by supramolecular approaches. Their discovery in the 1930s represents one of the most important milestones in dye chemistry as well as the germination of supramolecular chemistry. The intriguing optical properties of J-aggregates (in particular, very narrow red-shifted absorption bands with respect to those of the monomer and their ability to delocalize and migrate excitons) as well as their prospect for applications have motivated scientists to become involved in this field, and numerous contributions have been published. This Review provides an overview on the J-aggregates of a broad variety of dyes (including cyanines, porphyrins, phthalocyanines, and perylene bisimides) created by using supramolecular construction principles, and discusses their optical and photophysical properties as well as their potential applications. Thus, this Review is intended to be of interest to the supramolecular, photochemistry, and materials science communities.

From the Contents

1. Introduction

More than 70 years ago, Scheibe et al.[1] and Jelley[2] observed independently an unusual behavior of pseudoisocyanine chloride (also known as 1,1′-diethyl-2,2′-cyanine chloride, PIC chloride, **1**; Figure 1) in aqueous solutions.[3] Compared to the spectra of this dye in other solvents, such as

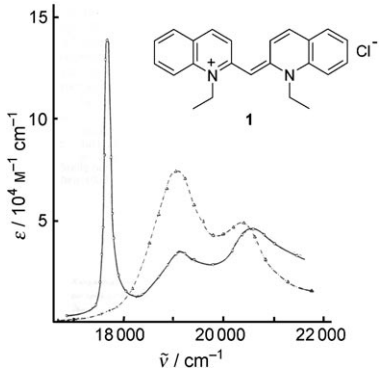

Figure 1. Absorption spectra of PIC chloride aggregates in water (——) and its monomers in ethanol (-----), as well as the structure of PIC chloride (**1**). Modified from Ref. [4a].

ethanol, the absorption maximum was shifted to lower energies—at around $\tilde{\nu} = 17500\ cm^{-1}$ ($\lambda_{max} = 571$ nm)—upon increasing the concentration above 10^{-3} M in water, and at higher concentration (ca. 10^{-2} M) this band became more intense and sharp; hence large deviations from the Lambert–Beer law were observed (Figure 1).[4] The addition of sodium chloride into an aqueous solution of **1** resulted in similar spectral changes as observed upon increasing the dye concentration. The characteristic features of this new absorption band is its sharpness with a small value for the full width at half maximum (fwhm) of about 200 cm^{-1} and a very high absorption coefficient ε. Concomitantly, a strong fluorescence with very small Stokes shift (maximum at 575 nm) was observed. In 1937, Scheibe et al. had already correctly interpreted the behavior of PIC under these conditions as an indirect result of desolvation upon (supramolecular) polymerization of the dye, and that the absorption spectrum was changed by the "vicinity effect" of the adjacent molecules.[1a–c] In contrast, Jelley observed a rapid precipitation of PIC from the ethanol solution upon addition of nonpolar solvents or a 5 M aqueous solution of sodium chloride, and a loss of the high fluorescence as the dye passes into the crystalline state. This might be the reason why Jelley ascribed the spectral changes misleadingly to the dye molecules, rather than to their aggregates.[2] Both Scheibe et al. and Jelley found that the spectral changes are reversible upon heating and cooling of the dye solutions, which indicates the self-assembly of PIC dyes.

Nowadays, dye aggregates with a narrow absorption band that is shifted to a longer wavelength (bathochromically shifted) with respect to the monomer absorption band and a nearly resonant fluorescence (very small Stokes shift) with narrow band are generally termed Scheibe aggregates or J-aggregates (J denotes Jelley) in accord with the name of their inventor.[5–7] Aggregates with absorption bands shifted to shorter wavelength (hypsochromically shifted) with respect to the monomer band, in contrast, are called H-aggregates (H denotes hypsochromic) and exhibit in most cases low or no fluorescence.[5a] These basic and easily recognizable spectral changes—for many J-aggregates, bathochromic shifts of about 100 nm are observed—already indicate that the molec-

[*] Prof. Dr. F. Würthner, Dr. T. E. Kaiser, Dr. C. R. Saha-Möller
Universität Würzburg, Institut für Organische Chemie and
Röntgen Research Center for Complex Material Systems
Am Hubland, 97074 Würzburg (Germany)
Fax: (+49) 931-31-84756
E-mail: wuerthner@chemie.uni-wuerzburg.de

ular properties of the building blocks are significantly altered upon aggregation. More sophisticated studies on the electronic properties of J-aggregates reveal that excited states are formed by extended domains of coherently coupled molecular transition dipoles, which advocates for J-aggregation as the archetype phenomenon for an emerging systems property on the supramolecular or nanoscale level.

The great significance of J-aggregates was recognized once such aggregates found application in spectral sensitization of the photographic process with silver halides.[5j,k] Since then, scientific interest in J-aggregates has grown continuously, and an enormous number of cyanine dye aggregates have been prepared and their optical, photophysical, and structural properties studied intensively.[5–7] During the last two to three decades, J-aggregates of other dyes, such as merocyanines, squaraines, synthetic and semisynthetic model compounds of natural light-harvesting pigments (chlorophylls), and functional dyes such as perylene bisimides, have been developed. The objective of this Review is to provide an overview on J-aggregates from a supramolecular perspective, beginning with their serendipitous discovery up to the current state, with an emphasis on the rational design of J-type functional aggregates. The Review is focused on the J-aggregation phenomena of the above-mentioned major classes of dye molecules in solution, and only a few examples of dye arrangements in the crystalline state are included to illustrate important packing motifs that could be elucidated with crystallographic precision. Owing to space limitations, neither all dye molecules that have been reported to form J-aggregates nor numerous J-type excitonic coupling phenomena that have been observed upon dye aggregation at surfaces and interfaces are included, for example, the seminal work of Kuhn and Möbius on Langmuir–Blodgett (LB) films,[5b,l] and J-aggregation phenomena in lyotropic or thermotropic mesophases or in amorphous π-conjugated materials such as conducting polymers. This holds true also for the most important application of J-aggregates as spectral sensitizers of silver halide crystals in photographic films.[5j,k]

2. Cyanine Dyes

Cyanine dyes were known long before the discovery of J-aggregates by Scheibe and Jelley. Williams was most probably the first chemist to come across a cyanine dye when in 1856 he reacted crude quinoline with alkyl (ethyl, amyl) iodides followed by treatment with silver oxide, as he observed a compound with "*a blue of great beauty and intensity*".[8] In 1860, Williams named the dye with a brilliant blue shade that he obtained by the reaction of quinoline with amyl iodide and subsequent base treatment as cyanine (*cyanos* = blue).[8b,9] Through detailed investigations of the cyanine dye, Hofmann recognized in 1862 that this dye was composed of quinoline and lepidine (4-methylquinoline) derivatives, which was not a surprise because the crude quinoline used by Williams contained lepidine as an impurity in great quantity.[8,10]

In the following years, similar chromophores with pronounced blue color were produced and cognate names such as cryptocyanine, isocyanine, pseudoisocyanine, and pinacyanol were introduced.[11] However, it was only decades later that the constitutions (structures) of these dyes, including that of Williams' cyanine, could be reliably clarified.[12] It was then realized that all of these dyes have one feature in common, namely, they consist of two heterocyclic units, which are connected by an odd number of methine groups $(CH)_n$ (with $n = 1, 3, 5, \ldots$). König introduced the term polymethine dyes in the 1920s, and he recognized for the first time that the color of these dyes is mainly determined by the length of the polymethine chain.[12c,13] The general structures of polymethine dyes are shown in Scheme 1.[11a,b] The predominantly aromatic heterocyclic donor (D) and acceptor (A) groups are connected by polymethine chains of various lengths. The ideal polymethine state is characterized by the alternation of the π-electron density on the polymethine chain (indicated by partial charges in structure **2**, Scheme 1) and equal π-bond orders (in contrast to the polyene state, which is characterized by the equalization of the π-electron density on the carbon atoms of the methine groups along the chain and a bond order alternation of single and double bonds).[14] The high oscillator strength of the dye in the polymethine state leads to the pronounced color. Cyanines can be cationic (cationic polymethines **3**–**5**), anionic (anionic polymethines, not shown), or neutral (neutro-polymethines **6**, also called merocyanines). The alternating π-electron density distribution is independent of whether the molecule is carrying a charge, or not.[15] A selection of various polymethine dyes with their trivial names (notice, the substituents at the nitrogen atoms are variable) are shown in Scheme 2.[11a,b] Although the term polymethine

Frank Würthner, born in 1964, studied chemistry at the University of Stuttgart, Germany, where he received his PhD with F. Effenberger. After postdoctoral research at MIT in Cambridge (USA) with J. Rebek, Jr., two years at BASF Central Research in Ludwigshafen (Germany), and a Habilitation in organic chemistry at the University of Ulm (2001), he became full professor at the University of Würzburg in 2002. His research interests include dye chemistry, noncovalent synthesis of functional nanostructures, and applications of organic materials in electronics and photonics.

Theo E. Kaiser was born in Würzburg, Germany, in 1979. He studied chemistry at the University of Regensburg, where he received the diploma in 2004. He then joined the group of Frank Würthner at the University of Würzburg, where he received his PhD in 2009. In the same year, he became a R&D manager at the Rent a Scientist GmbH, Regensburg, Germany.

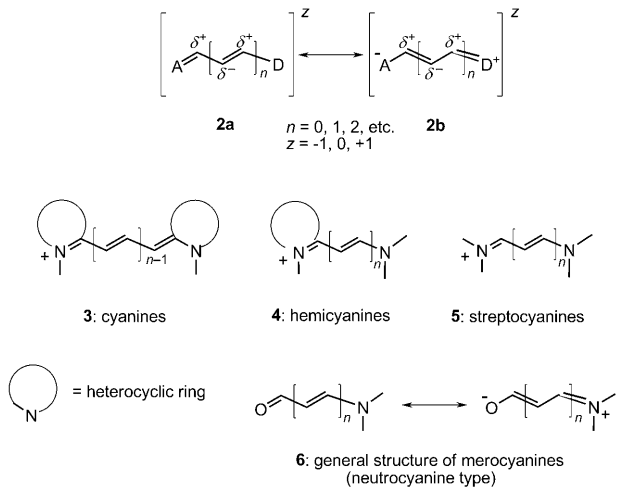

Scheme 1. General structures of polymethine dyes with their trivial names. The partial positive and negative charges on the atoms of the polymethine chain in the ground state are indicated by δ^+ and δ^- (see **2a**,**b**), respectively, according to Ref. [11b]. A general structure of merocyanines **6**, which are neutral cyanines, is also shown.

dye is systematically more correct, the term cyanine dye is still widely used,[16] and will also be used preferentially in this Review.

2.1. Aggregate Structures of Cyanine Dyes: PIC as a Prime Example

The elucidation of the structure and morphology of J-aggregates of cyanine dyes has been an active research field over the past few decades. One of the most thoroughly studied cyanine dyes in this context is pseudoisocyanine (PIC; see Figure 1). Thus, we have selected this cyanine dye as a prime example to illustrate how the search for the structure and morphology of J-aggregates developed. Aggregate structures of PIC dyes were initially studied by absorption and fluorescence spectroscopy. In 1938, Scheibe and Kandler had already performed flow anisotropy measurements on solutions of PIC chloride, and concluded the existence of long aggregates. They suggested the aggregates to have coin-pile (*Geldrollen*) like structures, in which the long axis of the

Chantu R. Saha-Möller, born in 1955 in Bangladesh, studied chemistry in Germany (PhD in 1986, University of Hamburg, with W. Walter). He then worked as a postdoctoral associate with Eric Block (SUNY Albany, USA). Since 1987 he has been a senior research associate at the University of Würzburg, Germany. He has co-authored about 180 publications in the field of organic chemistry.

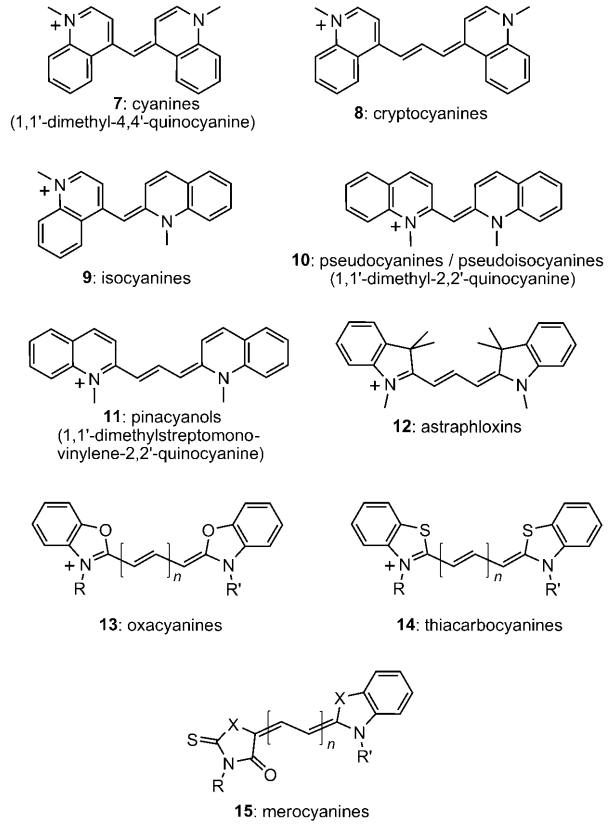

Scheme 2. Basic structures of various polymethine dyes **7**–**15** and their trivial names. The methyl substituent on the nitrogen atoms is shown as a representative group, but can be replaced by other alkyl groups. An example of a merocyanine dye **15** (a neutrocyanine) is shown for structural comparison with cationic polymethines **7**–**14**.

monomers is oriented perpendicular to the aggregation direction.[17] For the aggregation process, Scheibe suggested a reversible formation of dimers and their subsequent transformation into higher aggregates that are in equilibrium with the dimers.[4] Scheibe et al. also analyzed the length of the aggregates by fluorescence quenching experiments by using 1,2-dihydroxybenzene (pyrocatechol) as the quencher and found that, depending on the concentration of the dye molecules, one quencher molecule is needed to quench the fluorescence of 10^3–10^6 PIC dye molecules.[18] This finding was explained in terms of the extended chains of PIC molecules formed upon reversible aggregation containing up to one million of dye molecules. In these chains, the excitation energy is absorbed at any position and transferred to any other position in the chain until a quencher molecule is met. Therefore, Scheibe et al. proposed that an energy transfer across the aggregate over thousands of dye molecules should be possible.[18] It was also concluded that the aggregate length increases as the dye concentration increases, since fewer quenching molecules are required to decrease the fluorescence of more concentrated solutions. The efficient fluorescence quenching of J-aggregates of the PIC dye found by Scheibe et al. was later observed not only for other dye aggregates, but also for conjugated polymers, and was termed "superquenching".[19a–d,20]

Scheibe and Kandler showed by flow linear dichroism experiments that the sharp absorption band at 572 nm of J-aggregates of PIC is polarized parallel to the aggregate axis.[17a] From this result, Förster concluded in 1946 that the monomers in the aggregate are not perpendicularly oriented with their long axis with respect to the aggregate direction, but are aligned parallel (inclined) to the aggregate direction.[21] Moreover, Förster suggested that the monomers are helically disposed with respect to the aggregate axis, which in turn should lead to optically active assemblies (Figure 2).

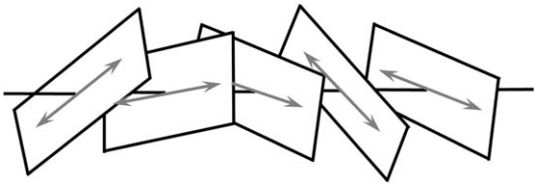

Figure 2. Schematic representation of the PIC aggregate model according to Förster.[21] The tilt of the molecular planes to the aggregate direction and the helical arrangement is shown. The gray double arrows symbolize the transition dipole moments. Modified from Ref. [21].

In 1964, Mason observed circular dichroism (CD) effects upon addition of a concentrated solution of PIC chloride in ethanol to an aqueous (+)-tartrate solution (Figure 3).[22] According to Scheibe et al., these CD effects originate from the close contact of the cationic aggregate with the optically active tartrate anion, whereby a small local distortion within the dye assembly takes place.[23]

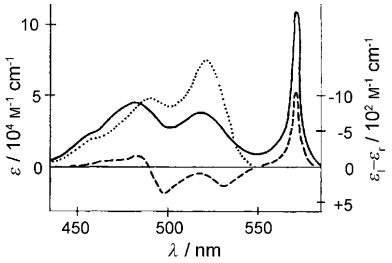

Figure 3. Absorption spectra of PIC chloride in ethanol (monomer: •••••) and in aqueous solution (aggregate: ——), as well as the circular dichroism (CD) spectrum (dashed line) of the aggregate in aqueous dipotassium (+)-tartrate solution. Reproduced from Ref. [22] with permission. Copyright (1964) The Royal Society of Chemistry.

X-ray analyses of crystals of different cyanine dyes revealed that the dye molecules are not planar, as initially assumed by Scheibe et al. Instead, the two quinolinium rings of the cyanine dyes are twisted at an angle of 50° with respect to each other.[7b,24] This observation led to a new explanation for the optical activity of the J-aggregates of cyanine dyes, namely, that the CD effect originates from the twist within the monomers.[7b,c] According to Scheibe et al., the tight binding of tartrate counterions to the polycationic PIC aggregate affords diastereomeric complexes that are biased towards one atropisomer. The proposed aggregate model is illustrated in Figure 4.[7b] In this context it is noteworthy that the nature of the counterions also affects the structure and the stability of the aggregates,[7b,25] with the stability decreasing in the order: $SO_4^- > Cl^- \approx F^- \gg Br^-$. As this order resembles the so-called Hoffmeister series quite well, it is tempting to relate the counterion-dependent stability of PIC J-aggregates to the Hofmeister effect.[26]

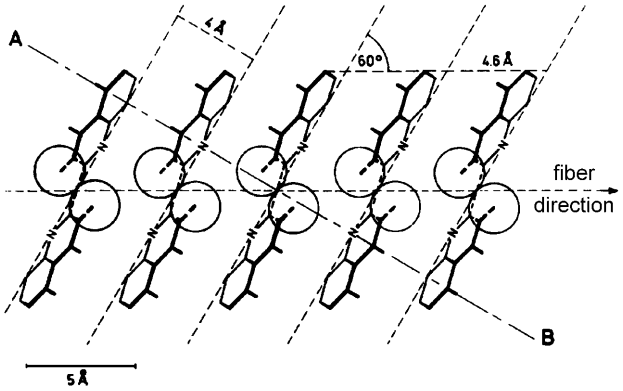

Figure 4. Aggregate model of PIC proposed by Scheibe et al. in 1970,[7b] assuming similar conformations of the monomers in crystals and in aggregate solutions. Reproduced from Ref. [7b] with permission. Copyright (1970) Elsevier Science Ltd.

Notably, the model shown in Figure 4 is not consistent with excitonic coupling theory of Kasha and co-workers,[27,28] which describes the excitonic interaction of the transition dipole moments of chromophores with respect to their geometrical arrangement as a point dipole approximation (Figure 5). According to this theory, a much more pronounced displacement of the dyes is needed to afford bathochromically shifted J-type absorption bands. However,

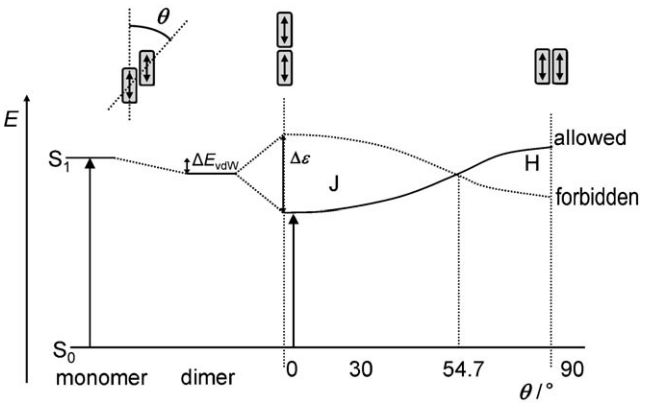

Figure 5. A schematic energy diagram for aggregated dimers with coplanar inclined transition dipoles. The geometry and the slip angle θ are illustrated above. Note that for parallel aligned dimers the optical excitation is only allowed from the ground state to one of the two excitonic states depending on the angle θ. For $\theta < 54.7°$ the lower energy state is allowed (leading to a bathochromically shifted J-band), while for $\theta > 54.7°$ the allowed state is at higher energy (leading to a hypsochromically shifted H-band). ΔE_{vdW} = difference in van der Waals interaction energies between ground and excited states.[27]

it should be noted that, although the model of Kasha and co-workers is very instructive for explaining the spectral shifts of dye aggregates, this model has some clear limitations, as discussed in several publications.[7a,29] In particular, this model seems to overestimate the magnitude of energy shifts.[29]

In 1970, Cooper observed a splitting of the J-band by temperature-dependent absorption studies of solutions of PIC bromide at temperatures below 253 K (Figure 6).[30] The

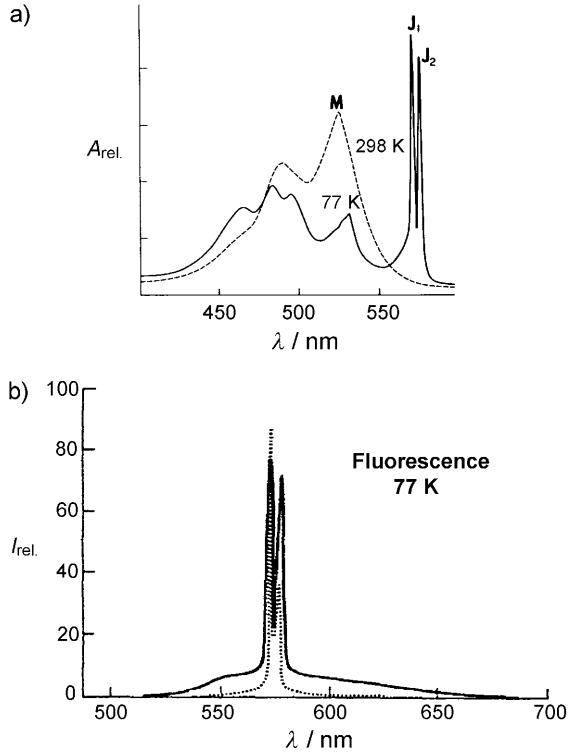

Figure 6. a) Absorption and b) fluorescence spectra of PIC bromide solutions ($c = 4 \times 10^{-3}$ M in a 1:1 ethylene glycol/water mixture) at 298 K and 77 K (as indicated); M = monomer. In (b), the emission spectra are depicted for excitations at 498 nm (——) and 565 nm (-----). (a) and (b) are modified from Refs. [5a] and [30], respectively.

presence of two extremely sharp bands of almost equal intensity resembles the line-shaped spectra of molecules in the gas phase rather than typical band-shaped solution spectra. The splitting is barely 151 cm^{-1} and the fwhm values for the bands are about 50 cm^{-1} at 77 K and 30 cm^{-1} at 4 K. Excitation of the J-band at different wavelengths resulted in different ratios of the fluorescence intensities of the two split J-bands (Figure 6b). Accordingly, it was suggested that the fluorescence originates from two distinct electronic transitions that are associated with two geometric conformations of the J-aggregate.

However, as pointed out by Bird and co-workers, an exact agreement between experimental data and calculated spectral shifts is not possible with Kasha's exciton theory. While Bird and co-workers suggested a refinement by means of a higher order, instead of the first order, perturbation theory,[31] Kuhn and co-workers were in favor of a first order perturbation treatment, and related the deficiencies of Kasha's exciton theory to the point dipole approximation.[7a,32] By using an extended dipole model, these authors could indeed demonstrate that the calculated values are in proper agreement with those obtained by experiments. By including steric considerations, Kuhn and co-workers proposed a brickwork arrangement (Figure 7a) for the PIC J-aggregates in which both a tight packing with J-type coupling as well as a parallel alignment of the monomer long axes along the aggregate direction is realized. The latter feature contradicts the previously postulated ladder or staircase arrangements (Figure 7b,c), but is in aggreement with the experimental results.[17a,21]

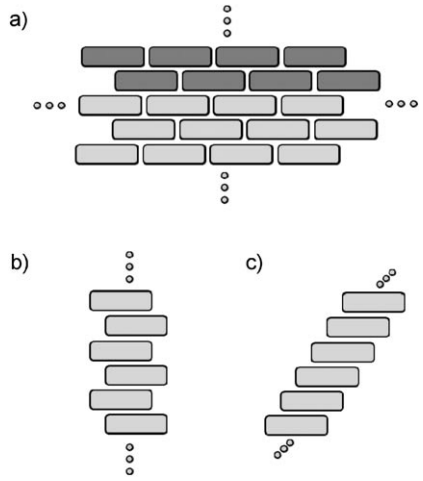

Figure 7. Schematic representation of the possible arrangements of dye molecules in J-type aggregates. a) Brickwork arrangement, b) ladder arrangement, and c) staircase arrangement. The most likely arrangement of the monomers in PIC J-aggregates according to Bücher and Kuhn is shown in (a).[32] Each rectangle represents the contours of a pseudoisocyanine (PIC) cation. A double-string chain unit of the brickwork arrangement is indicated by dark gray rectangles.

The brickwork model suggested by Kuhn and co-workers prompted Scheibe et al. to reconsider their original model, depicted in Figure 4.[7b] Daltrozzo, Scheibe et al. then proposed the threaded double-string models for PIC aggregates, as shown in Figure 8, which illustrates two possible optically active (a2, b2) and two optically inactive (a1, b1) aggregate structures.[7c] It is noteworthy that a double-string subunit of the brickwork model (Figure 7a, dark gray) properly complies with the rectified model of Daltrozzo et al., which additionally takes into account the steric peculiarities of twisted PIC chromophores (Figure 8).

Besides a refined structural model, a two-step mechanism for the aggregation of PIC was suggested by Daltrozzo and Scheibe on the basis of concentration- and temperature-dependent absorption studies. The first step is the nucleation process, in which a nucleus is formed that is energetically disfavored, relative to both the monomer and higher aggregates, up to a minimum size of seven assembled monomers. In the second step (the growth process), the aggregate size rises

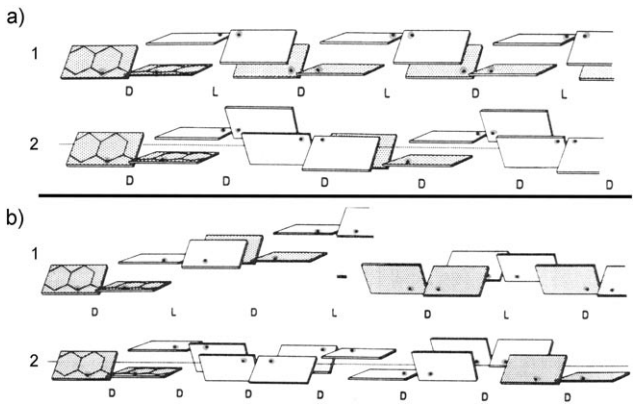

Figure 8. Schematic representation of structural models for J-aggregates of PIC proposed by Daltrozzo, Scheibe et al. with nitrogen atoms of the quinolinium rings on opposite (a) and on the same site (b).[7c] The black dots symbolize the nitrogen atoms. Structures a1 and b1 constitute optically inactive, while a2 and b2 optically active aggregates. Modified from Ref. [7c].

quickly with increasing concentration, whereas the number of independent aggregates remains constant.[7c] CD measurements on PIC solutions containing different amounts of (+)-tartrate revealed optical activity, as shown for the first time by Mason in 1964,[22] thereby illustrating a probable helical arrangement of the aggregates that is induced by optically active tartrate anions, and results from the twist of about 50° between the two quinolinium rings in the monomer.

More than a decade later, Nolte proposed some different models for the aggregate of PIC.[33] At that time, when the structural arrangement in these dye aggregates was a subject of high controversy, Marchetti et al. compared the optical spectra of aggregate solutions of PIC dyes with those of their crystals. Since the spectra were very similar, they concluded that the dye aggregates are probably microcrystals, whose aggregate bands originate from crystal transitions (so-called Davydov splitting).[34,35]

In 1993, Kobayashi and co-workers investigated highly oriented J-aggregates of PIC dispersed in polymer films.[36] The linear dichroism spectra of oriented J-aggregates confirmed that the J-band is polarized mainly parallel to the direction of alignment. On the basis of the linear and nonlinear optical properties of oriented J-aggregates, Kobayashi and Misawa proposed a model for a hierarchically structured material consisting of mesoaggregates and macroaggregates.[37] The former is characterized by coherent excitation over the aggregate and the latter is an inhomogeneous ensemble of mesoaggregates (for details see Ref. [37]).

In 1996, several studies were published concerning the characterization of concentrated PIC solutions with high viscosity. By using polarizing microscopy at moderately low temperatures (0–20 °C) and at dye concentrations higher than 0.2 wt % (ca. 6×10^{-3} M), Stegemeyer and Stöckel observed an optical texture that is characteristic for a nematic liquid-crystalline phase.[38] These observations support the proposal of Daltrozzo et al. of a double-stranded model for PIC aggregates.[7c] Rheology experiments performed by Rehage et al. with PIC chloride in aqueous solutions at 25 °C revealed an enormous increase in the viscosity at concentrations higher than 1×10^{-2} M, and a permanent birefringence was observed above a concentration of 2×10^{-2} M.[39] Polarization microscopy studies at room temperature showed that the texture of the liquid-crystalline phase of PIC possesses similarities to that of the nematic rod phase reported by Stegemeyer and Stöckel.[38] However, the observed maltese crosses are usually absent in nematic rod phases. Therefore, Rehage et al. concluded that the observed texture is characteristic of a smectic C phase, which consists of crystalline smectic layers with monomers in tilted positions, as found in thermotrophic systems. Thus, the viscoelastic dye solutions tend to form rod-shaped or tubular aggregates within supramolecular network structures, which exhibit appreciable elasticity properties.

In 2000, von Berlepsch et al. visualized for the first time the rodlike morphology of a closely packed network of PIC chloride J-aggregates directly by using cryo-transmission electron microscopy (cryo-TEM).[7f] For a 12.5×10^{-3} M aqueous solution of this dye, an average aggregate length of at least 350 nm could be found, which corresponds to about 3000 dye molecules in an aggregate, and a rod diameter of about 2.3 nm was estimated The distance between adjacent rods decreases as the concentration increases, leading to a dense packing. Based on the observation of highly ordered line patterns in the cryo-TEM images, von Berlepsch et al. presumed that these patterns were a signature of nanometer-sized PIC crystals. Comparison of the electron diffraction pattern of the rods with single-crystal X-ray diffraction data confirmed the supposition that there is a two-phase state of coexisting J-aggregates and nanocrystals. However, no experimental data to gain insight into the molecular structure of the J-aggregates interior could be obtained by these methods. Since the J-aggregates composing the network are very closely packed at higher concentration (12.5×10^{-3} M), isolated J-aggregates could not be studied at such a high concentration. Thus, von Berlepsch et al. performed further cryo-TEM investigations on solutions of PIC chloride with dye concentrations in the range of 2.5×10^{-4} to 6.1×10^{-4} M in 200 mM NaCl, which confirmed the formation of network superstructures consisting of isolated fibers and complex fiber bundles.[7g] More of the isolated threadlike J-aggregates could be made visible by diluting the solution; these aggregates are characterized by a diameter of 2.3 nm, a length of several hundreds of nanometers, and a high stiffness. No concentration-dependent growth of the J-aggregates, that is, elongation of aggregate length, could be observed at the higher concentration. Hence, the sudden occurrence of the J-band within the narrow concentration regime from 2.5×10^{-4} to 6×10^{-4} M was assumed to be mainly the result of an increase in the concentration of the aggregates, and not because of their growth.[7g] Studies by Huber and co-workers on the aggregation of PIC chloride in aqueous NaCl solution by time-resolved static light scattering are consistent with the results of von Berlepsch et al. obtained by cryo-TEM investigations.[40]

The dichroic absorption spectra of the aggregate solution revealed that there was a strong similarity between the spectra in the region of the J-band and those of a PIC single

crystal, as calculated from measured polarized reflection spectra.[41] Thus, a similar arrangement of adjacent chromophores in the J-aggregates in solution and in single crystals was assumed, and a structure model for PIC aggregates was suggested,[7f] which is close to the model proposed by Daltrozzo, Scheibe et al.[7c] In the model of von Berlepsch et al., a quasi-one-dimensional threadlike aggregate composed of two monomers per unit length was proposed, in which the quinoline rings of adjacent chromophores adopt a sandwich-like arrangement, but with a large displacement of the monomers (Figure 9 a,b).[7f,41] To account for the cross-sectional diameter of 2.3 nm, it was suggested that the rods are composed of six individual threadlike strands (Figure 9 c,d).

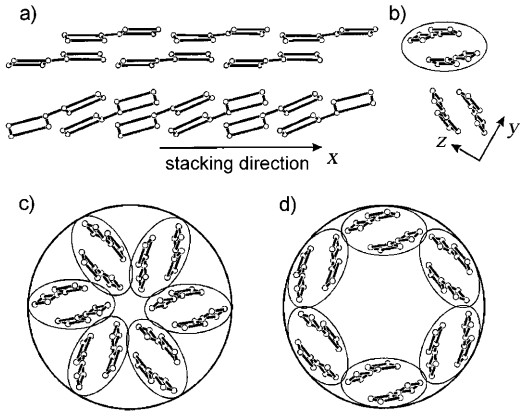

Figure 9. Structural model of threadlike-arranged PIC molecules proposed by von Berlepsch et al.[7f] This model (a,b) was derived from the stacking of molecules in single crystals. Adjacent molecules that form one strand are arranged along the *x*-axis of the crystal. Two such single strands with oppositely oriented molecules form a double strand with a herringbone-like arrangement (a,b). Assuming the same mass density as in the single crystal, the volume of a cylindrical particle with a cross-sectional diameter of 2.3 nm can be filled by approximately six "unit strands". Two highly symmetrical ones are shown in (c,d), whereby (d) shows a hollow brickwork chimney model. Reproduced from Ref. [7f] with permission. Copyright (2000) American Chemical Society.

Regarding the publications in the current decade, there is still an ongoing discussion on the "true" structure of PIC aggregates. In 2001 and 2002, Tani and co-workers performed polarized reflection microspectroscopy with simultaneous atomic force microscopy (AFM) analysis to explore the absolute orientations of exciton transition dipole moments of PIC J-aggregates locally.[42] These studies indicated a wide range of directions, from parallel to perpendicular, with respect to the long axis of the fibers, thus implying that a new structural model has to be conceived to explain the observed phenomena.

In the search for the structure of the PIC aggregates, the coherent length of excitonically coupled monomers within the aggregate has also been explored and sometimes confused with the length of the aggregate, that is, the number of monomers comprising the aggregate. It should be mentioned in this regard that all spectroscopic investigations just determine the virtual size of the exciton delocalization, which only provides a lower limit for the physical size of the aggregates. The simplest spectroscopic approach applies mass action considerations, where $\lg(c_{mon})$ is plotted versus $\lg(n\,c_{agg})$ to show a linear relationship with a slope of n; c_{mon} and c_{agg} are the concentrations of the monomer and aggregate, respectively. With this approach, the value of n was estimated to be very small for PIC aggregates, and initially thought to be the number of molecules constituting the aggregate.[5a] However, viscosity[4] and fluorescence quenching[18] studies performed with aggregates of PIC by Scheibe et al. in the 1930s had already revealed the existence of much longer aggregates. Similarly, Hillson and McKay proposed on the basis of diffusion constant measurements by polarographic techniques that PIC aggregates consist of hundreds of repeating units.[43] Moreover, J-aggregates of PIC and related dyes can be concentrated by centrifugation, that means, they behave like high-molecular-weight species of colloidal dimensions. Therefore, it was suggested that the aggregation number n does not correlate with the physical size of the aggregate, but only to the number of molecules in the aggregate that undergo mutual spectral perturbation. Thus, only a few molecules were considered to constitute the repeating spectroscopic unit cell of the J-aggregate, which relate to the double-string chains of brickwork-type structure of J-aggregates proposed by Kuhn and co-workers (Figure 7 a).[32,44]

On the basis of spectral analysis (especially the line width of the J-band) and theoretical models, Knapp suggested an exciton coherence length of at least 60 monomer units in PIC J-aggregates.[45] Sundström et al. performed exciton annihilation experiments and showed that excitons can migrate over up to 10^4 molecules in the PIC aggregates.[7e] By using a variety of nonlinear optical measurement techniques, combined with numerical calculations and treating the PIC J-aggregate in terms of a one-dimensional model of a Frenkel exciton, while considering also static disorder of the molecular arrangement, Wiersma and co-workers proposed a delocalization of the excitonic states in the PIC aggregates over approximately 100 molecules and with great oscillator strength.[46] A similar coherence domain of about 70 molecules (exciton delocalization) was observed by pump-probe spectroscopy experiments for PIC aggregates at 1.7 K.[47,48]

Recently, methods have become available to study individual aggregates. Higgins and Barbara have applied the near-field imaging technique for the first time to polyelectrolyte-bound J-aggregates of PIC.[49] The long rodlike aggregates with an estimated length of several micrometers were photobleached and revealed an upper limit of 50 nm for the exciton migration distance. A few years later, scanning near-field optical microscopy (SNOM) studies were carried out by Kobayashi and Fukutake on PIC J-aggregates, and revealed an average aggregate size of 30 ± 5 molecules and a coherent domain size also of about 30,[50] which is in agreement with the values reported in earlier publications. In 2007, Tani et al. conducted SNOM experiments with improved sample preparation on PIC J-aggregate fibrils in thin film matrices and with modified microscope optics.[51] On the basis of their new results, the authors considered a zigzag-type molecular

structure as a suitable model for PIC J-aggregates. Individual J-aggregates of cyanine dyes have been studied not only by imaging techniques as mentioned above, but also by single-molecule spectroscopy. Köhler and co-workers have investigated aggregates of *amphi*-PIC (1-methyl-1′-octadecyl-2,2′-cyanine) at low-temperature (1.5 K) by single-molecule spectroscopy and obtained highly resolved fluorescence excitation spectra of individual J-aggregates.[52]

In 2008, Katoh and co-workers investigated the formation process of PIC J-aggregates by fluorescence detection of single aggregates in flowing solutions.[53] They observed a continuous signal for the fluorescence of a large number of mesoaggregates consisting of 20–100 PIC molecules each, as well as a pulsed signal for individual macroaggregates with a fiberlike shape, a length of a micrometer, and a diameter of 2–3 nm. These values are consistent with those obtained earlier by cryo-TEM studies.[7f,g] Katoh and co-workers concluded that the formation of PIC J-aggregates proceeds through the assembly of mesoaggregates in solution. Moreover, the nuclei of the macroaggregates appear to regerminate throughout the formation process.

As evident from the above discourse, the structure of PIC aggregates has often been discussed controversially, and diverse structural models for PIC J-aggregates have been proposed. It is remarkable that the observations made in the early years, when rather very modest instrumental techniques were employed, and the conclusions made on the basis of those observations are still valid. Undoubtedly, PIC aggregates self-assemble into extended supramolecular polymers in aqueous solution,[54] and these polymers exhibit spectacular functional properties, in particular, exciton migration over macroscopic distances. It is remarkable, however, that even the highly sophisticated NMR spectroscopy and electron microscopy techniques available nowadays can not reliably resolve the structural details of the molecular packing in these aggregates, and thus the much desired structure–property relationship still remains unexplored.

In our opinion, it is very likely that not only the aggregate size but also the aggregate structure of PIC dyes strongly depends on the experimental conditions, and that spectroscopic techniques are very sensitive to even subtle changes in the aggregate structure. Concentration-dependent studies of very dilute solutions show equilibria between H-aggregates (attributed to dimeric species) and J-aggregates (attributed to extended double-string chains, Figure 8). In more concentrated solutions these initial double-string chains may interact to form a larger nanofiber (Figure 9). Under different experimental conditions (temperature, pH value, ionic strength, etc.), however, the individual molecules might also reorganize into another packing motif (for example, brickwork; Figure 7a).

In this context it has to be taken into account that noncovalent interactions between PIC molecules depend merely on van der Waals forces. These forces are sufficiently strong to enable self-assembly, because of the high polarizability of cyanine molecules, but exhibit little directionality.[14] Thus, the hydrophobic effect may exert a strong influence on the packing of PIC molecules within these aggregates at different levels of structural hierarchy in aqueous solutions of PIC aggregates. Moreover, counterions of PIC dyes have to be accommodated into larger structures for electrostatic reasons, which affect the molecular arrangement in aggregate structures. Depending on the conditions used for the preparation of the aggregates, we may also anticipate the formation of kinetic products, that is, metastable aggregates, which could not equilibrate under the applied experimental conditions. Such kinetically trapped aggregates become more probable the larger the aggregate structures grow.[55] It is, therefore, reasonable to anticipate that the apparently contradictory results on structural and spectroscopic features of PIC aggregates originate from the prevalence of different aggregate species because of the diverse preparation conditions used in different laboratories.

2.2. J-Aggregates of Other Cyanine Dyes

Although cyanine dyes were discovered much earlier than J-aggregates, this class of dyes gained their popularity only after the significance of J-aggregates for silver halide photography had become evident. The most prominent cyanine dye is undoubtedly pseudoisocyanine (PIC). However, a large variety of other cyanine dyes are known to form J-aggregates.

Systematic structural variations were already performed in the late 1930s to determine the structural features that enable J-aggregation. Scheibe replaced the quinoline ring of the pinacyanol **16** (1,1′-diethylstreptomonovinylene-2,2′-quinocyanine, also called quinocarbocyanine) by a benzothiazole or an indole ring to obtain thiacarbocyanine (**17**, 3,3′-diethylthiacyanine, benzthiocarbocyanine) or astraphloxin (**18**, indocarbocyanine; Scheme 3). He noticed that the

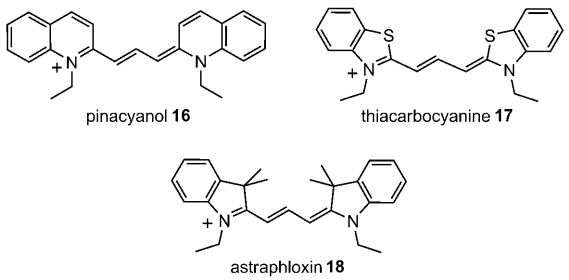

Scheme 3. Chemical structures of some cyanine dye cations with their trivial names (chemical names are given in the text).

aggregation tendency is decreased enormously by these structural variations.[4] However, thiacarbocyanine and astraphloxin were found to form dimeric and extended H-aggregates with strongly hypsochromically shifted absorption bands.[56,57]

Scheibe's co-worker Ecker changed the structure of PIC by introducing substituents at the quinoline ring (Scheme 4) and observed that the J-band shifts from 572 nm to higher wavelengths as the number of methyl groups increases (**19**, **20**).[57] This red-shift can further be increased up to 605 nm by anellation of the aromatic rings (**21**, **22**) instead of introducing methyl groups in the quinoline ring. However, the replace-

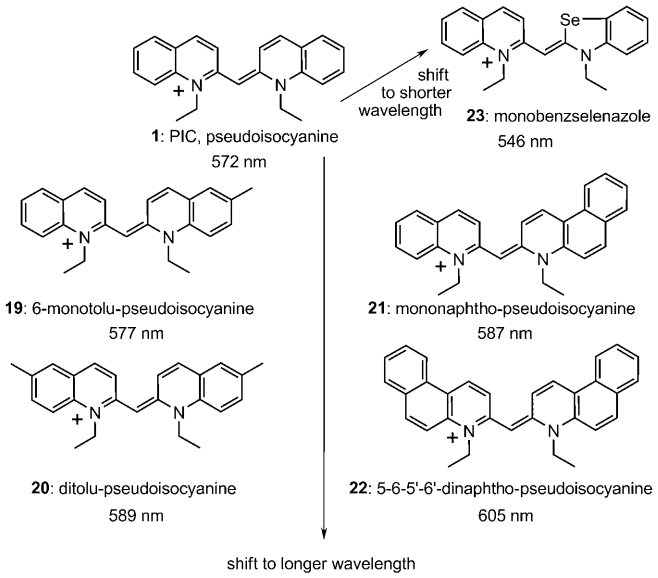

Scheme 4. Structures of PIC derivatives **19**–**23** and the absorption maxima of their J-bands.

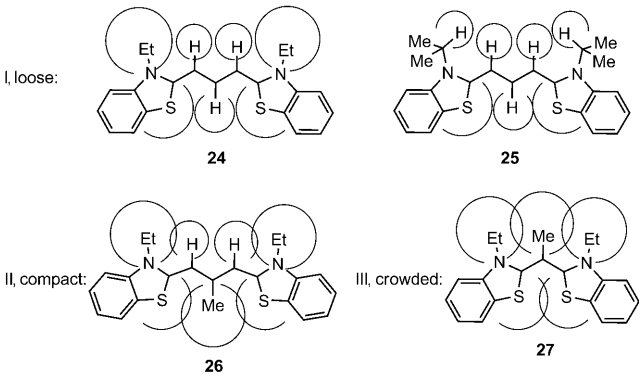

Figure 10. Classification of cyanine dyes based on their molecular flexibility according to Brooker et al.[60] Double bonds in the methine unites are omitted for simplicity.

ment of a quinoline ring of PIC by a benzselenazol heterocycle to give dye **23** leads to a J-aggregating derivative with a somewhat less-shifted J-band at 546 nm. Furthermore, it was observed that the absorption spectrum of a mixture of different J-aggregates is not a superposition of the corresponding absorption spectra of the sole aggregates.[4,58] Ecker then performed systematic aggregation studies on mixtures of different J-aggregates of these PIC derivatives and observed the formation of coaggregates with a strong interaction between the different dyes.[57] An alternating incorporation of the monomers into the aggregate was assumed, as known for mixed crystals. The dyes studied by Ecker initially formed sandwich-type dimers with H-coupling, and extended aggregates with J-type coupling were created only at higher concentration.[57] Concomitantly with the appearance of the J-band, those aggregate solutions showed high viscosity and elasticity, as well as thixotropy.

Scheibe et al. recognized in the 1960s that the hydrophobic effect (also called solvophobic effect for solvents other than water) is the main driving force for the aggregation of cyanine dyes in water.[23] Since dispersion forces between the dye molecules can neither explain the high values of free binding energy, nor the fact that these dyes aggregate only in water at room temperature, the hydrogen-bonding interactions within this solvent have to be considered. This means that the aggregation process of cyanine dyes can be understood in terms of hydrophobic interactions, with the energy being provided by the expulsion of water molecules from the first hydration shell.

Additional criteria for the aggregation strength of cyanine dyes are the size of their van der Waals surfaces and the freedom of torsional motions in the molecules;[23,59] the latter process is related to the steric demands of the dye substituents. Cyanine dyes were classified into three different types on the basis of steric bulk: I: loose, II: compact, and III: crowded (Figure 10).[59,60] In loose cyanine dyes (**24**, **25**), torsions and oscillations of the molecule counteract the aggregation, while in compact dyes (**26**) several units of the molecule are interlocked, thus rigidifying the molecule and hence resulting in a high tendency for aggregation. No planar molecular structure is possible in crowded dyes (**27**) because of steric congestions imposed by bulky substituents, thus molecular stacking is hindered and, as a consequence, the aggregation ability of such cyanine dyes is decreased. Thiacarbocyanine **27** does not even form dimers in water.[59] This classification indicates that the aggregation propensity of cyanine dyes increases as the steric hindrance increases up to a certain point and then diminishes again. This observation implies that a fine-tuning of the structural properties of cyanine dyes is necessary to attain optimized aggregation properties.

A large variety of cyanine dyes have been reported in the past decades,[61] and several of the J-aggregate-forming dyes have been given common abbreviations (Scheme 5). Particularly interesting examples are, besides 1,1′-diethyl-2,2′-cyanine (pseudocyanine **1**, PIC), the dyes 5,5′,6,6′-tetrachloro-1,1′-diethyl-3,3′-di(4-sulfobutyl)benzimidazolocarbocyanine (**28**, TDBC), 1,1′,3,3′-tetraethyl-5,5′,6,6′-tetrachloro-

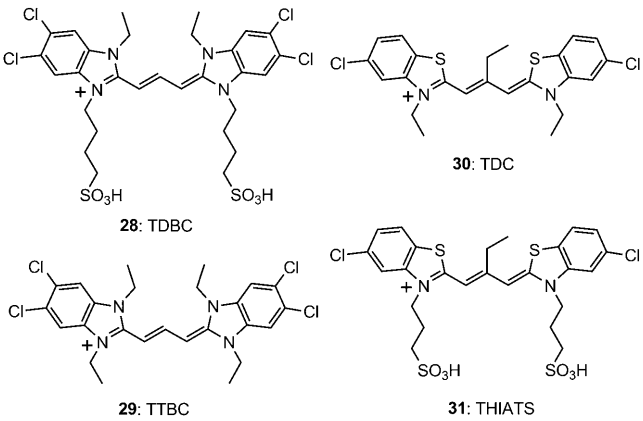

Scheme 5. Chemical structures and common abbreviations of the cyanines **28**–**31** (chemical names are given in the text).

benzimidazolocarbocyanine (**29**, TTBC), 3,3′,9-triethyl-5,5′-dichlorothiacarbocyanine (**30**, TDC), and 3,3′-bis(sulfopropyl)-5,5′-dichloro-9-ethylthiacarbocyanine (**31**, THIATS). The aggregation properties of TDBC and THIATS and the optical properties of their aggregates are discussed in the following as representative examples, since these dyes are the most thoroughly studied.

The cyanine dye TDBC exhibits a strikingly simple spectrum with isosbestic points that is much easier to explain than the spectra of PIC. Hence, TDBC was used for aggregation studies by concentration-dependent UV/Vis absorption measurements. Herz investigated for the first time the J-aggregates of the sodium salt of TDBC by concentration-dependent absorption spectroscopy to determine the number of monomers forming the assembly.[7d,e] In contrast to PIC dyes, TDBC shows a well-defined transition from monomers to J-aggregates without population of any intermediate dimer or H-aggregate (Figure 11). From consideration of the the mass action, in which it is assumed that n monomers form one aggregate [Eq. (1)] and the total dye concentration is given by c_0, Equations (2)–(4) can be obtained:

$$n\,\mathrm{M} \rightleftharpoons \mathrm{Agg}, \qquad K = c_{agg}/c_m^n \tag{1}$$

$$c_0 = c_m + n\,c_{agg} \tag{2}$$

$$c_0 - c_m = n\,c_{agg} = nKc_m^n \tag{3}$$

$$\lg n\,c_{agg} = \lg n\,K + n \lg c_m \tag{4}$$

c_m and c_{agg} are the concentrations of the monomeric and aggregated molecules, respectively, n is the number of monomer units in the aggregate, and K is the association constant.[7d,e] The concentration of the monomer c_m can be determined directly from the UV/Vis spectra by using the Lambert–Beer law. According to Equation (4), a plot of $\lg(n\,c_{agg})$ versus $\lg c_m$ should be linear with a slope of n, while the y-intercept allows evaluation of the association constant K. From this, an aggregation number of $n = 4$ was estimated for TDBC (Figure 11 a,b).[5a] As discussed before, however, this aggregation number does not relate to the physical size of the aggregate itself, but seems only to relate to the number of molecules in the aggregate that undergo mutual spectral perturbation (compare discussion for PIC in Section 2.1). Therefore, four molecules were considered to constitute the repeating spectroscopic unit cell of the J-aggregate of the cyanine TDBC (**28**).[62] Herz also studied the effect of surfactants on TDBC J-aggregates and found that J-aggregates of TDBC dissociate nearly completely into monomers upon addition of only 1 wt% of alkylphenoxy polyethyleneglycol surfactant (Figure 11 c).[7d]

Moreover, J-aggregates of TDBC were used to study the exciton delocalization by advanced spectroscopic methods, such as temperature- and wavelength-dependent fluorescence lifetime and accumulated photon-echo experiments.[63a] Studies performed by Wiersma and co-workers revealed that the temperature dependence of the fluorescence quantum yield and the dephasing behavior of TDBC are very similar to those of PIC. Pump-probe experiments showed that the delocalization of the exciton in TDBC J-aggregates was distributed over 30 to 45 molecules at $T = 1.5$ K. By using a motional narrowing model for disordered molecular aggregates, a correlation of several hundred molecules was deduced based on their data at 1.5 K.[63a] In the case of TDBC J-aggregates, the exciton delocalization length was determined at room temperature by femtosecond nonlinear optical experiments to be 16 molecules.[63b]

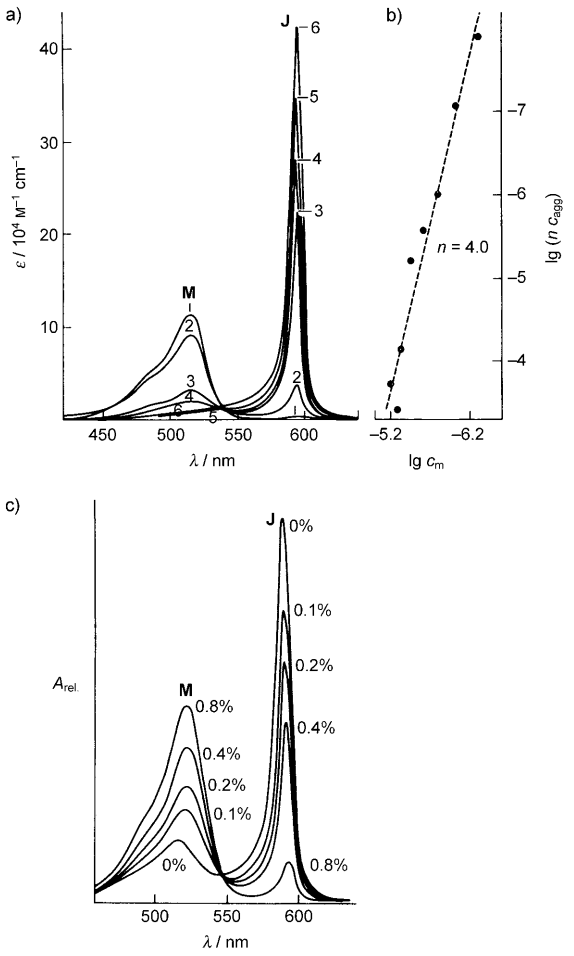

Figure 11. a,b) Concentration-dependent absorption of dye **28** at 25 °C. a) UV/Vis absorption spectra of **28** in aqueous NaOH ($c = 1\times10^{-3}$ M) solutions at different concentrations of: 1) 5.0×10^{-7} M, 2) 1.0×10^{-6} M, 3) 5.0×10^{-6} M, 4) 1.0×10^{-5} M, 5) 1.0×10^{-4} M, and 6) 4.0×10^{-4} M. b) The molar concentrations of the monomer (c_m) and aggregate (c_{agg}), which were derived from spectra in (a), are plotted to obtain the aggregation number n of the J-aggregate. c) Deaggregation of J-aggregates of **28** into monomers by aqueous surfactants at 25 °C. The spectra were obtained with 10^{-3} M solutions containing the indicated wt% (0.0–0.8%) of alkylphenoxy polyethyleneglycol surfactants. Reproduced from Ref. [5a] with permission. Copyright (1977) Elsevier Science B.V.

While amphiphilic cyanines such as derivatives of TDBC preferentially form tubular J-aggregates (for details, see Section 2.3), the dye TTBC (**29**) forms two-dimensional J-aggregates with a herringbone-type packing.[64] Such aggregates of TTBC are characterized by a broad H-band and a narrow J-band, and are attributed to Davidov splitting (Figure 12).

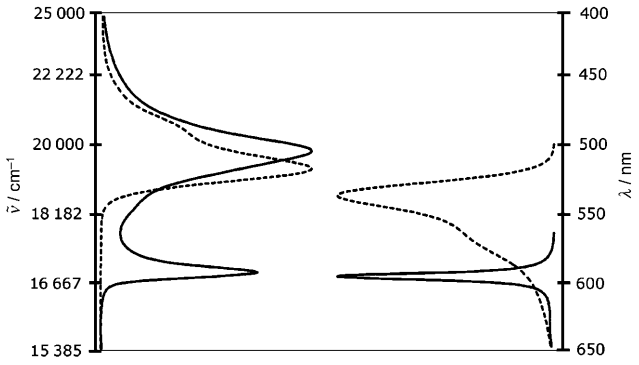

Figure 12. Normalized absorption (left) and fluorescence (right) spectra of dye **29**: —— aggregate, ••••• monomer. Reproduced from Ref. [64] with permission. Copyright (2006) American Chemical Society.

Hada et al. observed, depending on the preparation conditions, not only a broad H-band, but also three different J-bands for J-aggregates of TDC dye **30**.[65] Each band could be assigned to a different J-aggregate species (denoted as J_1, J_2, and J_3), which can be identified by 1) the position of the J-band in the absorption spectrum, 2) the width of the absorption and fluorescence bands, 3) the value of the Stokes shift, and 4) the shape of the entire absorption spectrum. Drobizhev et al. performed steady-state and time-resolved spectroscopy at low temperatures and found that only J_2- and J_3-aggregates were formed under these conditions.[66] The J_1-type aggregates have the lowest transition energy of these J-bands, and are relatively unstable. Upon optical excitation, the J_3-aggregates undergo a thermally activated transformation to J_2-aggregates.

Van der Auweraer, Vitukhnovsky, and co-workers compared the spectral properties of the aggregates of TDC dye (**30**) with those of the structurally related THIATS dye (**31**), and found that the latter also exhibits three different J-bands (Figure 13b, only one J-band is shown here).[67] They also observed a dependence of the fluorescence anisotropy of both TDC and THIATS aggregates on the excitation wavelength, which was rationalized in terms of a zigzag chain model with two molecules per unit cell. In this model, the transition dipole moment of each molecule is estimated to possess an angle of $\pm(65–70)°$ with respect to the chain direction. In a subsequent study, this model was modified to a double-chain model that could explain both the narrow J-band and broad H-band of THIATS aggregates.[68]

Fluorescence anisotropy as well as linear dichroism experiments performed by Scheblykin et al. on aligned aggregates of THIATS in a rotating cell provided evidence of the presence of two molecules per unit cell.[69a] Fluorescence quantum yields were measured across the entire exciton band, and values of 0.1 and 0.4 were found for excitations involving the upper and lower Davydov components, respectively, thus revealing an intraband exciton relaxation (Figure 14). Exciton–exciton annihilation experiments demonstrated an efficient exciton transport within this aggregated system, which suggested an exciton migration over 6×10^4 monomer units at room temperature and 6×10^6 monomers at 77 K before it decays.[69]

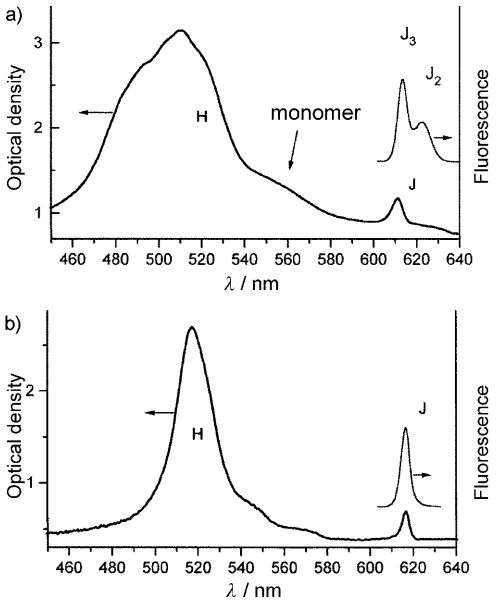

Figure 13. Absorption and fluorescence spectra of aggregates of a) TDC and b) THIATS in a water/ethylene glycol glass at 77 K at a concentration of 10^{-3} M. Reproduced from Ref. [67b] with permission. Copyright (1996) IOP Publishing Ltd.

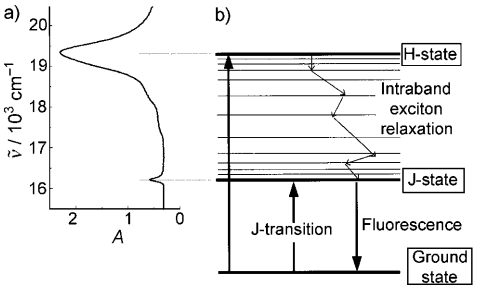

Figure 14. a) Absorption spectrum of THIATS J-aggregates at 77 K in relation to b) the energy diagram of a molecular aggregate with Davydov splitting of the exciton band, which shows intraband exciton relaxation. Reprinted from Ref. [70] with permission. Copyright (2000) Elsevier Science B.V.

In further studies, Scheblykin et al. investigated the temperature dependence of the optical and excitonic characteristics of J-aggregates of THIATS, in particular, the radiative lifetime and the coherence length of THIATS excitons, over a temperature range from 4.2 to 130 K.[70] The fluorescence quantum yields were found to increase as the temperature was decreased. It was concluded from comparative studies of PIC and THIATS aggregates at different temperatures that the coherence length of the PIC aggregates increases more rapidly than that of THIATS aggregates upon cooling. Moreover, it was demonstrated convincingly that the consideration of all the optically allowed Davydov components of the exciton band is important to estimate the exciton coherence length correctly. The temperature dependence of the exciton radiative lifetime of J-aggregates of THIATS can be rationalized, in contrast to PIC J-aggregates, within the framework of a one-dimensional model with two molecules

per unit cell. However, a two- or three-dimensional aggregate has to be present to account for the very efficient exciton migration observed for PIC aggregates through exciton–exciton annihilation. Only in this case does the density of states allow the observed temperature dependence at low temperature to be explained.[71]

The first systematic investigation on the temperature dependence of Stokes shifts of J-aggregates was performed with THIATS aggregates, along with studies on the temperature dependence of other excitonic and optical characteristics, such as absorption and fluorescence line broadening, exciton migration rate, and wavelength dependence of the fluorescence decay time.[7h] The line broadening was assumed to be the result of both static and dynamic disorder. To explain the temperature-dependent behavior, rather simple models for the static disorder such as the broken rod (BR) model, the model of continuous energy disorder (CED model), and the model of totally accessible density of states (DOS) were discussed.[72] It was revealed that there are three temperature ranges where a whole set of exciton and spectral properties of J-aggregates of THIATS exhibit different temperature dependences (Figure 15). Static disorder is the

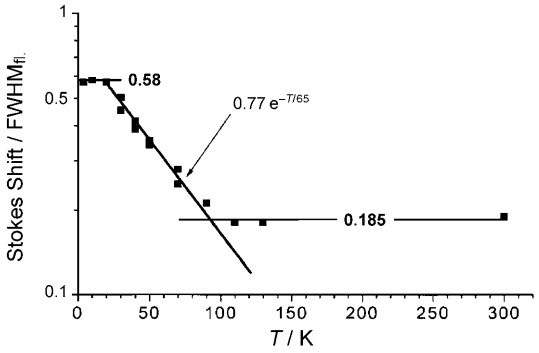

Figure 15. The temperature dependence of the Stokes shift relative to the fwhm of the fluorescence spectrum in the semilogarithmic scale reveals three temperature ranges. The functions plotted by bold lines are indicated. Reprinted from Ref. [7h] with permission. Copyright (2001) American Chemical Society.

main factor that limits the coherence length, exciton–exciton annihilation, and absorption band width in the static range ($T = 0$–20 K). The static to dynamic range ($T = 30$–70 K) is the transition range, where most of the excitonic properties change greatly. In the third range, the dynamic range ($T = 80$–300 K), the exciton migration is strongly slowed down by the scattering of optical phonons.[7h] The non-monotonous temperature dependence of the Stokes shift was modeled theoretically later on by Knoester and co-workers, and nicely agrees with the experimental data.[6c]

An interesting application of extended excitons has been introduced by Whitten and co-workers. They have intensively studied polylysine polymers with pendant cyanine dyes **32** (Scheme 6) to explore the potential of these cyanine-based polymers for fluorescence sensing.[19] They have shown that these cationic cyanine-pendant polymers exhibit characteristic J-aggregate absorption and fluorescence in aqueous

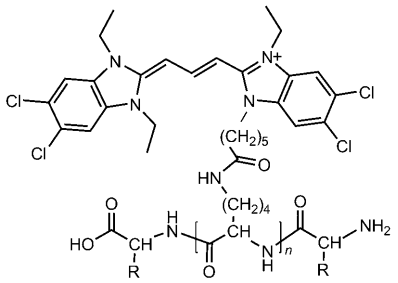

32

Scheme 6. General structure of the polylysines **32** with pendant TTBC cyanine dyes, as investigated by the Whitten research group.[19d,e]

solution and also after adsorption onto anionic supports. The fluorescence of such J-aggregated cyanine polylysines can be efficiently quenched by suitable small quencher molecules as well as by bio-macromolecules, and thus they can be used for biosensing.[19d,e] Moreover, the Whitten research group has found that cyanine dyes such as TTBC (**29**) and TDC (**30**) form J-aggregates in the presence of water-soluble organic polyelectrolytes, such as carboxymethylamylose (CMA), with characteristic absorption and fluorescence properties. Accordingly, these systems are also interesting for fluorescence-based biosensing.[19e,f]

2.3. Amphiphilic Cyanine Dyes

The most significant recent advancement in the field of J-aggregating cyanine dyes was the systematic functionalization of 5,5′,6,6′-tetrachlorobenzimidacarbocyanine (TBC) with hydrophobic and hydrophilic chains on the two sides of the chromophore by Dähne and co-workers.[5d,g,7j,73] In this way, the dyes became soluble amphiphilic molecules (in contrast to the cyanine dyes studied before by Kuhn and Möbius in LB layers) and were accordingly named as *amphipipes* (*amphi*philes with *p*igment *i*nteractions *p*erforming *e*nergy migration) by their inventors. The general structure **33** of TBC-based amphiphilic cyanine dyes is shown in Scheme 7, and interested readers are referred to an excellent and detailed recent review by Kirstein and Dähne that covers all the relevant findings on the structural and optical properties of this class of dye aggregates.[5g] The important advantage of these amphiphilic cyanine dyes is that their self-assembly in aqueous solution can be controlled by the relative size of the

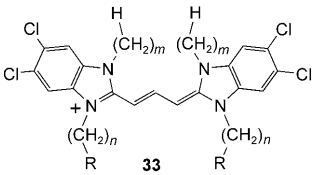

33

Scheme 7. General structure of amphiphilic cyanine dyes based on TBC (**33**) with R = COO^- (COOH) or SO_3^- (SO_3Na); $m = 2$–12 and $n = 1$–4 indicate the length of the alkyl chains in the hydrophobic and hydrophilic substituents, respectively.

hydrophobic side chains and the polar head groups. Accordingly, highly ordered J-aggregates of various morphologies became accessible from the same chromophore, and their characteristic optical properties could be related to the mutual orientations of the transition dipole moments of the dyes in the supramolecular arrangements.[5d,f,g,7j,73]

Studies with numerous derivatives of **33** have shown that the morphology of the aggregates of those amphiphilic cyanine dyes depends sensitively on the structural features of the hydrophobic and hydrophilic substituents. A short mnemonic code of the type C*m*R*n* was introduced to address different derivatives of **33**, where *m* and *n* indicate the length of the alkyl chains at the 1,1′- and 3,3′-positions, respectively, and R donates the ionic groups in the hydrophilic substituents. If R = COO^- or COOH, it is represented by O, and when R = SO_3^- or SO_3Na by S.[5g] It was observed that derivative C8O1 (that is, structure **33** with $m = 8$ and $n = 1$, and R = COOH) does not form any J-aggregates, while dyes with longer hydrophilic and hydrophobic chains, for example, dyes C8O3, C10O3, and C12O3, mostly form tubular aggregates. A selection of the investigated amphiphilic cyanine dyes, along with their mnemonic codes and observed aggregate morphology, can be found in Ref. [5g].

Two most extensively studied amphiphilic cyanine dyes are C8O3 and its sulfo analogue C8S3. Both dyes form tubular aggregates upon self-assembly. For C8O3, von Berlepsch et al. obtained direct evidence for the first time of tubular aggregates by cryo-TEM.[73] Ropelike structures were observed that consist of bundles of a distinct number of tubules, as shown in Figure 16 together with a computer simulation. The computer simulation shows hollow cylinders that are packed on a triangular lattice and intertwined. The observed tubules exhibit an outer diameter of 10 nm and the length of the ropelike bundles exceeds hundreds of micrometers. The thickness of the wall of the tubules was estimated to be approximately 4 nm, which led to the assumption that the wall is constructed of a bilayer of the amphiphilic dyes, similar to a lipid bilayer.

The tubules formed by self-assembly of the sulfobutyl-substituted dye C8S3 are, in contrast to those of C8O3, well separated, and only sporadically bundles of tubes are formed.[74] The diameter of the tubes of C8S3 is dependent on the solvent composition and preparation conditions, with values of 16 nm and 13 nm being observed in pure water and solutions containing more than 18 vol% methanol, respectively.[5g,74] In both cases,

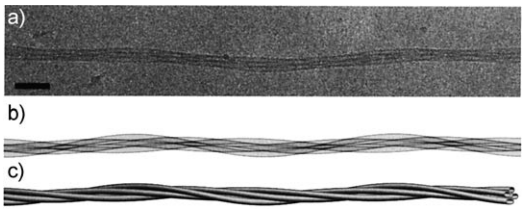

Figure 16. a) Cryo-TEM image of a single quadruple helix. The scale bar represents 50 nm. b) Simulated projection image of this helix and the c) corresponding three-dimensional view. Reprinted from reference [73] with permission. Copyright (2000) American Chemical Society.

the thickness of the walls of the aggregates was found to be on the order of 4 nm, which was taken as an indication that the wall consists of a bilayer, as in the case of C8O3. A high-resolution transmission contrast image was obtained by cryo-TEM on C8S3 aggregates, which revealed a double-walled tubular structure.[5g,75] A schematic model of the double-walled tubular J-aggregates of C8S3 is illustrated in Figure 17.[75b] Such J-aggregates could be immobilized on solid surfaces, which enabled the recording of high-resolution

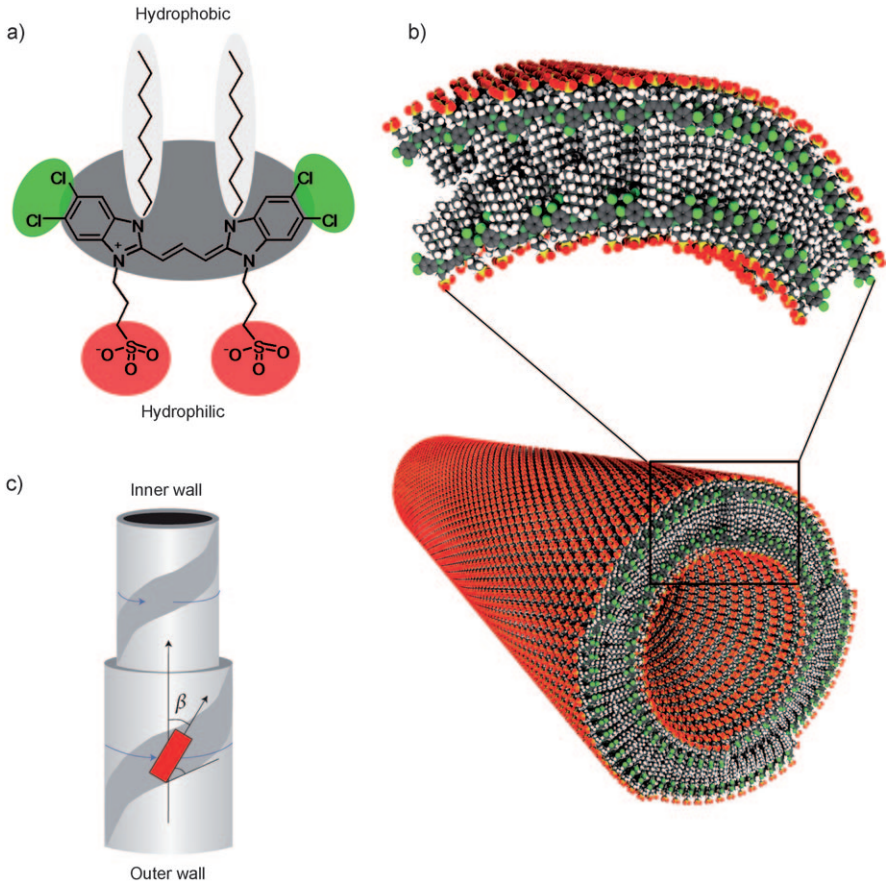

Figure 17. a) Structure of cyanine dye C8S3 with the most hydrophilic and hydrophobic regions marked. b) A model of the double-walled nanotube with the long alkyl chains in the interior of the bilayer. c) Schematic representation of the orientation β of the transition dipole of the monomer dye relative to the long axis of the nanotube. The gray band indicates the wrapping of the inner and outer walls of the bilayer tube by dye monomers. Reprinted from reference [75b] with permission. Copyright (2009) Nature Publishing Group.

images of the topography and measurement of the exciton fluorescence of individual J-aggregates by polarization resolved near-field scanning optical microscopy (NSOM).[75b]

Whilst planar ribbonlike J-aggregates of C8O4 feature simple narrow and red-shifted J-bands,[5g] complicated absorption spectra composed of several J-bands were observed for the cyanine dyes C8O3 and C8S3 in aqueous solutions (Figure 18).[5g,76] From a theoretical point of view, cylinder structures such as the one shown in Figure 17 are indeed predicted to show two exciton states with allowed

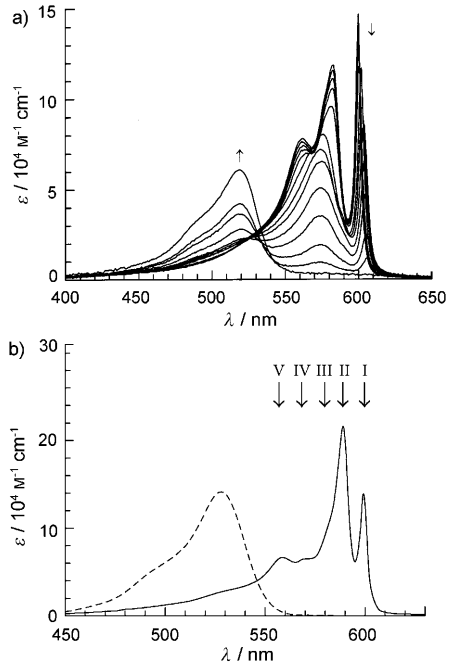

Figure 18. a) Change in the absorption spectra of an aqueous solution of C8O3 upon addition of MeOH. The arrows indicate the changes upon increasing the amount of MeOH from 0 to 34.4 vol%. b) Absorption spectra of an aggregate solution (aqueous NaOH with 16 wt% MeOH) of C8S3 (——) and a solution of monomers (-----) for comparison. The different J-bands are indicated by I–V. Reproduced from a) Ref. [76] with permission, copyright (2002) American Chemical Society, and b) Ref. [5g], copyright (2006) Hindawi Publishing Corporation.

optical transitions, both shifted towards lower energies compared to the monomer transitions.[5f] Accordingly, because of the dependency of the transition energies on the diameter of the cylinder, up to four excitonic states can arise for a bilayer tubule. Digrada et al. have clarified the relation between the molecular aggregate structure and the shape of the absorption spectrum by linear dichroism (LD) studies on oriented samples of C8O3 and C8S3.[74,77] The two absorption bands with lowest energy (labeled as I and II in Figure 18b) are polarized along the aggregate axis, while the third band at higher energy (III) is polarized perpendicular to the axis. The origin of the less intensive absorption bands IV and V is still not completely understood, as they are not, or only weakly, polarized.

The band with the lowest transition energy is very narrow and leads to fluorescence emission without notable Stokes shift, independent of the excitation wavelength. Thus, similar to J-aggregates of PIC and other cyanine dyes, fairly delocalized excitonic states are formed in the C8O3 and C8S3 aggregates. The size of the coherently coupled domain in the C8O3 tubular aggregates was determined by two-color pump-probe experiments to involve about 95 molecules at 1.5 K.[77c] This value is slightly larger than those of the cyanine dyes TDBC (30–45) and PIC (ca. 70) obtained under the same experimental conditions.[48]

Surprisingly, the formation of optically active tubules was already observed by CD spectroscopy on J-aggregates of some achiral amphiphilic TBC derivatives.[78a] This observation was explained by an unequal distribution of left- and right-handed helicity of J-aggregates. Moreover, it was shown that ionic surfactants such as sodium dodecyl sulfate (SDS) and trimethyltetradecylammonium bromide (TTAB) affect the morphology of the J-aggregates of these amphiphilic cyanine dyes.[73a,79] This was expressed by distinct changes in the visible region of the spectra upon addition of such surfactants to solutions of the aggregates. In the case of C8O3/SDS mixtures, single-walled tubules of 15 nm diameter and 300–600 nm length were formed, which were completely transformed into thick multilamellar tubes of micrometer length after several days. In contrast, C8O4/SDS mixtures remained stable for several weeks. The cationic surfactant TTAB first induces the formation of vesicles of the cyanine dye C8O3, which later transforms again into tubular aggregates of nanometer thickness and micrometer length. For C8O4/TTAB mixtures, however, aggregation leads to precipitation and eventually to the formation of needle-like microcrystals. The addition of chiral surfactant alcohols resulted in the formation of J-aggregates with defined helical chirality.[80]

Although amphiphilic cyanines possess many desirable properties, it has to be noted that these chromophores readily degrade in the presence of oxygen upon extensive exposure to light.[5d] Investigations on tubular J-aggregates of C8S3 revealed that irreversible oxidation of the J-aggregates appears to occur primarily along the outer wall of the tubular structure.[75a] Electrochemical and chemical reaction steps, in which dimerization and subsequent dehydrogenation take place, result in the formation of a new dehydrogenated dimeric oxidation product.

The modest photostability and ionic character of cyanine dye aggregates limit their scope for applications. These aggregates have mostly been used for photosensitization of silver halides in color photography.[5j,k] However, with the advent of digital photography, the significance of this application is diminishing. More recently, the advantageous fluorescence and exciton transport properties of cyanine dye aggregates have been utilized for biosensing applications, which rely on the efficient fluorescence quenching of cyanine J-aggregates by minute amounts of analytes.[19] The pronounced color changes that occur upon aggregation/deaggregation or structural reorganization, that is, from H-type to J-type aggregation, have been utilized to explore the interactions of cyanine dyes with a variety of biomacromolecules, including DNA,[81] polypeptides,[19d,e,82] and polysacchari-

des.[19f] Undoubtedly, all these applications benefit from the cationic character of cyanine dyes, and hence their solubility in water. On the other hand, it is exactly this ionic character that limits the application of cyanine dyes in other fields where the excellent exciton transport properties of J-aggregates are of interest, for example, organic photovoltaics. Notably, a salt composed of a cationic and an anionic polymethine dye has recently been applied in a bulk heterojunction (BHJ) solar cell.[83] J-Aggregates of neutral molecules that are discussed in the following sections might be more promising for this area of high technological relevance.

3. Merocyanine and Squaraine Dyes

The structurally most closely related dyes to cyanines are merocyanines and squaraines. Both of these classes of dyes contain linear and highly polarizable polymethine chains but, in contrast to cyanines, they are not ionic. Therefore, these dyes are interesting candidates for the photovoltaic applications mentioned in Section 2.3.[84] As a consequence of their significant zwitterionic character, and thus strong dipole moments (Figure 19a), merocyanine dyes have been widely studied for nonlinear optical (NLO) and photorefractive (PR) applications.[85] Those investigations have concentrated mainly on monomers. However, numerous studies were performed during the last few decades on merocyanine aggregates in films, such as LB films, where in some cases J-type assemblies were formed. A comprehensive overview on this particular subject has recently been published by Kuroda,[86] thus this aspect is not discussed here.

While many kinds of cyanines form J-aggregates in solution or in silver halide emulsions, only a few examples of merocyanine J-aggregates in solution have been reported. The reason for this might be that highly dipolar merocyanine dyes preferentially form face-to-face-stacked centrosymmetric dimers (Figure 19b) with H-type excitonic coupling.[87] Occasionally, a weak J-band and fluorescence from the lower excitonic state have been observed (Figure 19c), which are attributed to a rotational displacement of two dye molecules in the dimers.[87c] The strong electrostatic interactions have resulted in these sandwich-type dimers exhibiting the highest Gibbs binding energies of the dye aggregates reported so far.[88] Interestingly, functionalization of the electron-donor moiety with bulky substituents can induce displacement of the monomers into a slipped stacking arrangement in the solid state (Figure 20).[89]

Nevertheless, a few merocyanine dyes with J-type aggregation behavior in solution were reported in the 1980s. Mizutani et al. observed J-type aggregation of the merocyanine dye **36** bearing a long alkyl chain (Scheme 8) in methanolic aqueous solutions containing KOH and nonionic surfactant Triton X-100.[91] The two low-energy absorption bands observed for this dye at about 595 and 630 nm were tentatively assigned to a tetramer and a hexamer species, respectively. The corresponding merocyanine **37** containing a sulfonate group (Scheme 8) and its derivatives with various lengths of the alkyl chain and differerent counterions were studied intensively by Balli and co-workers, and they

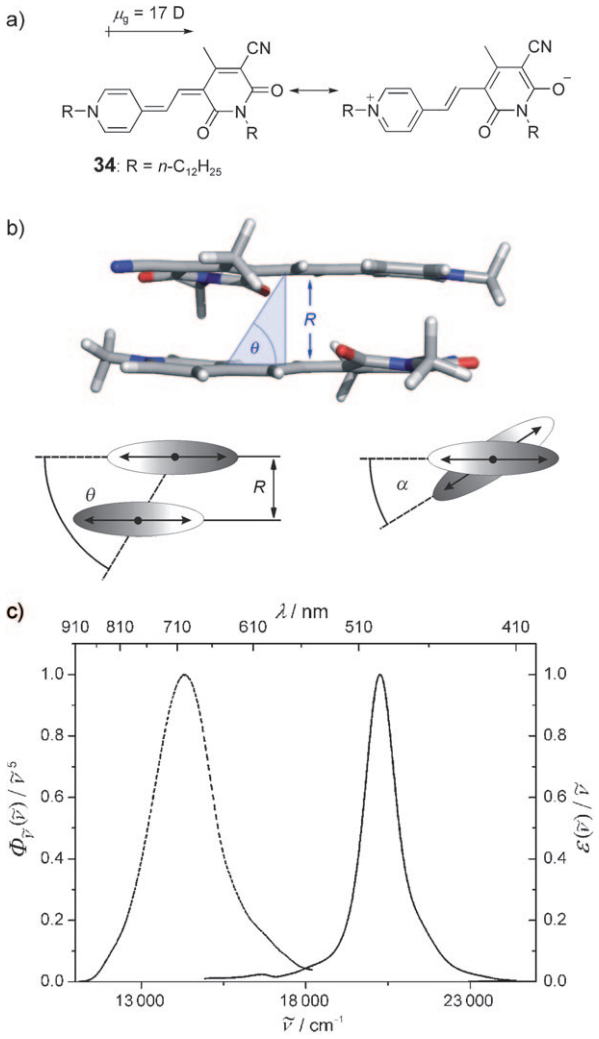

Figure 19. a) Mesomeric structures of the highly dipolar merocyanine dye **34** with its dipole moment. b) Top: MP2/6-31G(d,p)-minimized structure of the dimer aggregate of **34** with $\theta = 58°$ and $R = 3.25$ Å (all alkyl substituents were replaced by methyl groups in the calculation); gray C, white H, blue N, red O. Bottom: structural model (left, side view; right, top view) for the calculation of the exciton coupling between the transition dipole moments indicated as double arrows in the dimer aggregates. c) UV/Vis absorption (——) and fluorescence (-----) spectra for dimers of **34** in dioxane at room temperature ($\lambda_{ex} = 21\,505$ cm^{-1}).[87c]

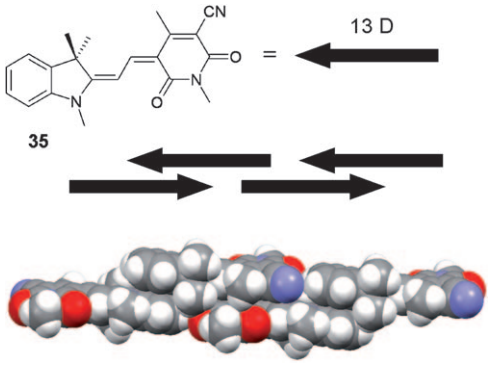

Figure 20. Dipolar merocyanine dye **35** (IDOP)[90] and double-string aggregate motif observed for this dye in the solid state by single-crystal X-ray analysis; gray C, white H, blue N, red O.[89]

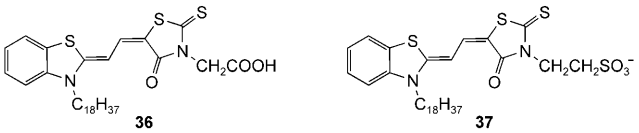

Scheme 8. Structures of J-aggregate-forming merocyanine dyes reported by Mizutani et al. (**36**)[91] and Balli and co-workers (**37**).[92]

observed that these merocyanines form J-aggregates in water or DMSO/water mixtures without the addition of any salt.[92] Moreover, a bathochromically shifted absorption band, presumably because of J-aggregation, was observed when related bismerocyanine dyes aggregated in water in the presence of starch.[92e]

In the early 1980s, Kalisky and Williams suggested, on the basis of N_2-laser transient spectroscopy studies, a photo-induced formation of J-aggregate stacks of a merocyanine and its ring-closed form spiroindolinebenzopyran.[93] Recently, Yagai et al. reported the creation of binary hydrogen-bonded supramolecular polymers composed of a bismelamine and barbiturate-type merocyanine dye in aliphatic solvents.[94] These supramolecular polymers exhibit well-defined one-dimensional fibrous structures that form, as a result of interchain association, two-dimensional sheetlike macroscopic structures. The latter show a weakly red-shifted absorption band at higher concentration relative to that of the monomer in dilute solution.

Squaraine dyes **38** (also called squarylium dyes) are derivatives of squaric acid (also called quadratic acid), and consist of an oxocyclobutenolate core with aromatic or heterocyclic components at both ends of the molecule (Scheme 9).[95] These dyes were first synthesized in the 1960s,[96] and they show intense absorption and often also fluorescence emission, typically in the red and near-infrared region. With these characteristic features, they have attracted much attention from the viewpoint of technological application.[95] However, J-aggregates of this class of dyes have been reported sparsely, and most investigations were performed on films, for example, LB films.[97]

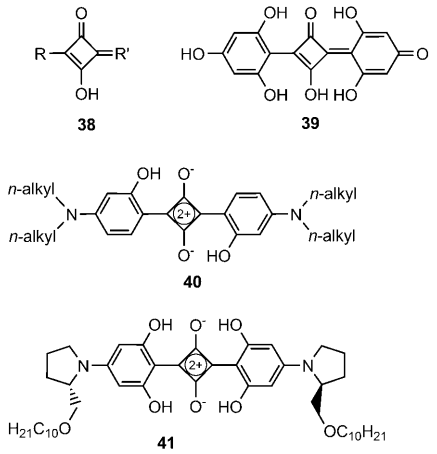

Scheme 9. General structure of squaraine (**38**), where R and R′ are aromatic or heterocyclic components. Examples of J-aggregating squaraine dyes **39**–**41** with alkyl = butyl, octyl, or dodecyl in dye **40**.

Only a few squaraine dyes have been reported to form J-aggregates in solution. During concentration-dependent absorption studies on bis(2,4,6-trihydroxyphenyl)squaraine (**39**) in dry acetonitrile a narrow bathochromically shifted band was observed that was attributed to a J-type dimer formed by hydrogen bonds.[98] In a more recent study, the authors confirmed that changes in the absorption spectra were due to aggregation of the dye molecules, and not caused by the presence of spurious amounts of acid or water.[99] On the other hand, it was observed for the class of *N*-alkyl squaraines **40** that the formation of J-type or H-type aggregates depends on the DMSO/water solvent composition.[100] J-Aggregates were formed in water with a low percentage of DMSO, whereas H-aggregates were created in solvent mixtures containing a high percentage of DMSO. For the intermediate range, a conversion from J-type to H-type aggregates of such squaraine dyes could be observed over time, thus pointing at a thermodynamically only metastable J-aggregate state. Furthermore, UV/Vis absorption and CD spectroscopic studies showed that the chiral squaraine dye **41** formed J-aggregates in acetonitrile upon addition of at least 10 vol% water.[101]

4. Chlorophyll Dyes and Structurally Related Macrocyclic Tetrapyrroles

The predominant "pigments" in natural light-harvesting (LH) systems are chlorophylls and bacteriochlorophylls, which can be considered as derivatives of the tetrapyrrole macrocycle porphyrin.[102] These natural LH pigments are constructed from a chlorin or bacteriochlorin (Scheme 10)

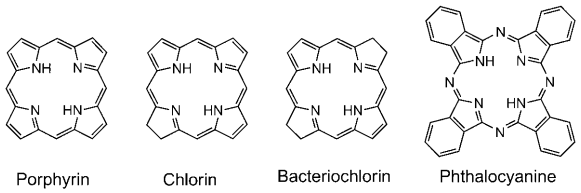

Scheme 10. Basic structures of porphyrin and its derivatives chlorin and bacteriochlorin, in which one or two pyrrole double bonds, respectively, are reduced. The structure of the most important tetraazaporphyrin derivative phthalocyanine is also shown.

skeleton containing an additional five-membered ring with a keto function and a central metal ion (magnesium), which is coordinated to the pyrrole nitrogen atoms. The chemical structures of light-harvesting chlorophylls and bacteriochlorophylls are shown in Scheme 11.

The structures of chlorophylls (Chls) *a* and *b* as well as bacteriochlorophylls (BChls) *c*, *d*, and *e* are based on a chlorin structure, while those of BChls *a* and *b* are derived from a bacteriochlorin. It is noteworthy that the term "bacteriochlorophyll" for BChls *c*, *d*, and *e* is somewhat misleading, as these BChls contain a chlorin structure, and not a bacteriochlorin. However, the trivial name "bacteriochlorophyll" was assigned to these chromophores long before their chemical structures were completely elucidated, and originated from

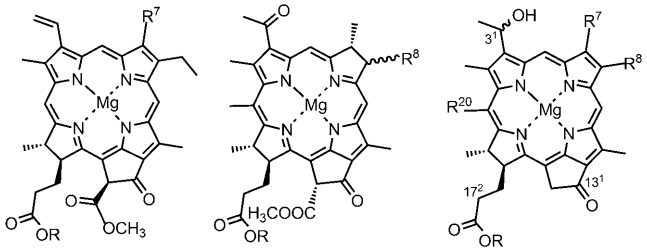

Scheme 11. Chemical structures of most frequently occurring natural chlorophylls (Chls) and bacteriochlorophylls (BChls). The substituent R in the chlorophylls is a phytyl group, while in the bacteriochlorophylls R is variable (for example, phytyl, farnesyl, or stearyl group). Substituent R^8 in BChls *c–e* can be a methyl, ethyl, propyl, isobutyl, or neopentyl group.[103]

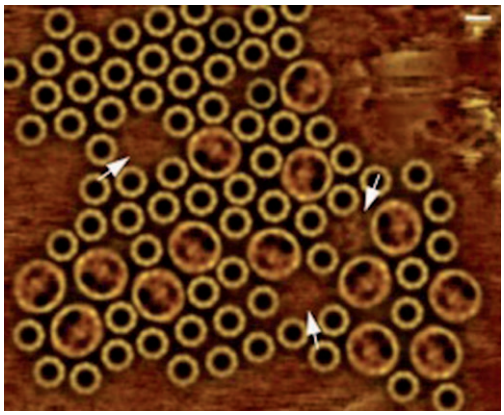

Figure 22. Organization of the bacterial photosynthetic apparatus in a membrane. Scale bar: 3 nm; arrows indicate regions that might contain other membrane proteins. Reprinted from Ref. [108] with permission. Copyright (2004) National Academy of Sciences USA.

their natural occurrence in bacteria. For example, light-harvesting complexes II (LH II) of purple bacteria *Rhodopseudomonas (Rps.) acidophila*[104] and *Rhodospirillum (Rs.) molischianum*[105] contain 27 and 24 BChl *a* chromophores, respectively, which are organized in a circular arrangement in a protein scaffold into the so-called B800 and B850 rings, which are named according to their absorption maxima at around 800 nm and 850 nm, respectively. The structures of LH II of *Rs. molischianum* and light-harvesting complex I (LH I) of *Rhodobacter* (*Rb.*) *sphaeroides*, together with the transfer of excitation energy in the bacterial photosynthetic unit is shown in Figure 21.[106] In the B850 manifold, 18 and 16 BChl *a* dyes are positioned in a slipped stacking arrangement that affords J-type coupling. This spatial organization ensures ultrafast exciton transport within the cyclic array (ca. 100 fs) and efficient excitation energy transfer to other LH II or LH I complexes (both within a few ps)[106,107] that are located in proximity in photosynthetic membranes (Figure 22).[108] The

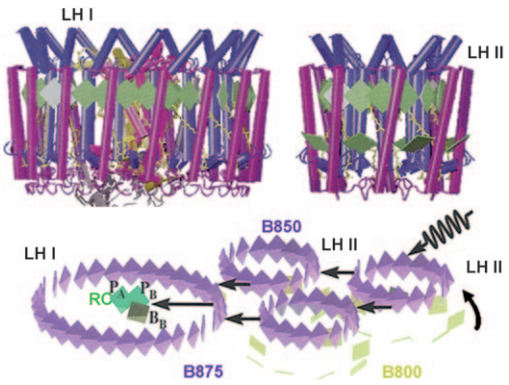

Figure 21. Top: Structures of LH I and LH II complexes of *Rb. sphaeroides* and *Rs. molischianum*, respectively. Bottom: Schematic representation of the transfer of excitation energy in a bacterial photosynthetic unit.[106] Reprinted from Ref. [106a] with permission. Copyright (1997) American Institute of Physics.

directionality of the LH II→LH I energy transfer process is ensured by the more bathochromically shifted J-band (B875) of LH I, which arises from a larger number of BChl *a* dyes that are organized in a more distorted cycle.[106,107b]

Inspired by the fascinating beauty and pivotal functions of such arrays of natural cyclic dyes in the photosynthetic apparatus, a multitude of artificial cyclic dye arrays—in particular based on porphyrin and metalloporphyrin dyes—have been constructed over the past few decades to mimic the functional features of the natural archetypes. As comprehensive reviews on artificial cyclic dye arrays have been published in recent years,[109] those systems are not discussed in detail in this Review.

In contrast to the LH complexes of purple bacteria, LH systems in chlorosomes of green sulfur bacteria (*Chlorobi*) and green non-sulfur bacteria (*Chloroflexi*) contain a large number of mainly BChl *c–e* molecules (there can be more than 200000 dye molecules per chlorosome), whose defined arrangement is controlled and stabilized only by dye–dye interactions,[110] and not by the protein matrix, as in the case of purple bacteria. Chlorosomes are oblong bodies with a size of up to $200 \times 100 \times 30\ nm^3$ that are attached to the inner side of the cytoplasmic membrane (Figure 23).

Unfortunately, no crystal structure of chlorosomal LH systems has been determined, which would provide clear information on the molecular arrangement of BChl aggregates in chlorosomes. Thus, in vitro self-assembly of BChl *c* and semisynthetic model compounds, particularly zinc chlorin **42a** (see Scheme 12, Section 4.1),[111a–e] have been intensively studied to explore the structural features of chlorosomal LH systems. This has led to different structural models for the macroscopic organization and the local supramolecular arrangement of adjacent BChl dyes having been proposed and controversially discussed.[110,111] Since even chlorosomes of the same species may contain BChls *c–e* in different ratios with variable side chains and as stereoisomers (Scheme 11) depending on the growth conditions and the development stage of the cell, it seems likely that the organization of the pigment is not limited to one particular arrangement, but is

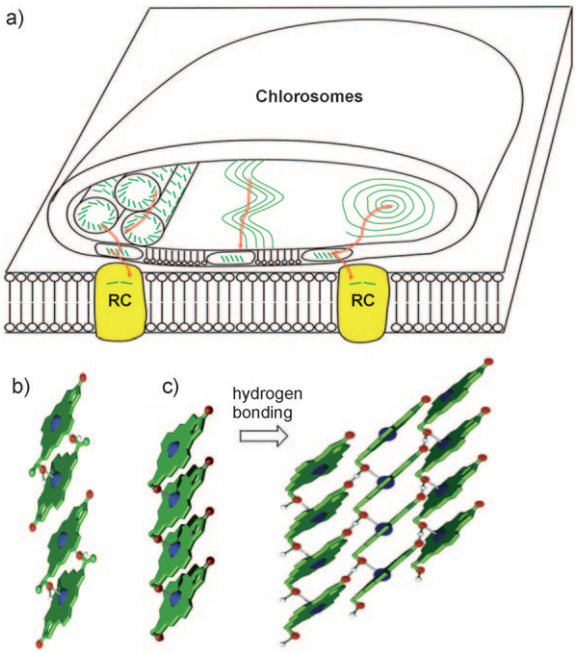

Figure 23. Models for the chlorosomes of green photosynthetic bacteria. a) Schematic representation of the macroscopic organization of BChl *c–e* pigments in the ellipsoidal bodies of chlorosomes for which tubular rod (left), lamellar (middle), and spiral (right) arrangements have been suggested.[112,113] The red arrows indicate the pathways for the energy transfer to the reaction centers (RC). b,c) Two of the many models that have been suggested for the organization of adjacent BChl *c–e* dyes. In (b), two BChl molecules form an antiparallel dimeric unit held together by two magnesium–oxygen coordinative bonds and π–π stacking. Further assembly is governed by π–π stacking and hydrogen bonding (not shown), which may lead to a variety of structures of similar thermodynamic stability. In (c), slipped stacks are formed by magnesium–oxygen coordination and π–π stacking, and further self-assembly by hydrogen bonding affords the curvature that is a characteristic feature of the chromosomal BChl aggregates observed by electron microscopy.

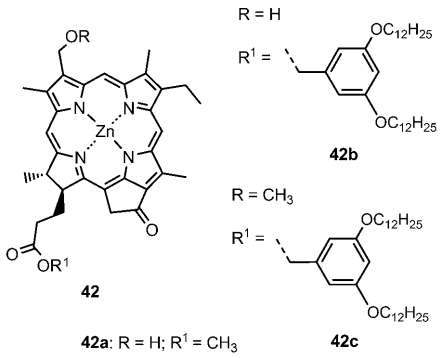

Scheme 12. Structures of semisynthetic zinc chlorins **42a–c**.

adaptive so as to provide just the required energy supply for the cell.

Figure 23 illustrates the three proposed structure models for the macroscopic organization of BChl aggregates in chlorosomal LH antennae: the tubular nanorod model suggested by Holzwarth and Schaffner,[112a] the lamellar organization model favored by Pšenčík et al.,[113a,b] and the most recent multilayer cylinder or spiral model by Oostergetel et al.[113c,d] All the models are based primarily on cryo-TEM investigations, and thus the latest studies with the highest resolution appear to be the most convincing. Nevertheless, these studies have also revealed differences between wild-type *Chlorobium tepidum* green bacteria and mutants that indicate the coexistence of different arrangements, as discussed above.

A favorable interplay between three different weak noncovalent interactions between the BChl molecular units has been recognized and confirmed for the local supramolecular organization of BChls *c–e* by various spectroscopic methods, including infrared and Raman spectroscopy as well as solid-state NMR spectroscopy. These interactions are π–π stacking interaction, metal–ligand coordination, and hydrogen bonding, the last being specific to this special type of natural chlorophylls (Scheme 11).[112] The combination of π–π stacking of the extended aromatic core of BChls and coordination of the central metal ion to the oxygen atom of the 3^1-hydroxy group of a neighboring BChl molecular unit can lead to either the formation of closed dimers (antiparallel model, Figure 23b) or to one-dimensional stacks (parallel model, Figure 23c). For the latter case a J-type slipped arrangement is defined for the whole stack, whilst quite different 1D and 2D arrangements are feasible for the former because the packing of the dimeric units relies on nondirectional van der Waals forces (π–π stacking). Accordingly, it is much easier to predict the further organization of the parallel stacks that are closely attached to each other by hydrogen bonding between the 3^1-hydroxy group and the 13^1-keto group. This results in a curvature that is the prerequisite for tubular or spiral-type macroscopic structures (Figure 23c).[112b]

Holzwarth, Schaffner et al. have used time-resolved fluorescence spectroscopy to investigate intensively the energy-transfer processes in zinc chlorin aggregates as model systems for chromosomal LH systems by coaggregation with various kinds of quencher molecules.[112b,114] These studies revealed that the energy-transfer processes from the antenna aggregate of zinc chlorin to the trap are within the picosecond range (7–9 ps) and substantial fluorescence quenching occurred in the antenna aggregate under reducing as well as nonreducing conditions. On the basis of the strong increase in the radiative rate of aggregates versus monomeric chlorins, it was concluded that the excitation is delocalized over at least 10–15 pigment molecules in the aggregates at room temperature.[114]

4.1. Biomimetic Zinc Chlorin Dyes

As mentioned in Section 4, the zinc chlorin (ZnChl) chromophore **42a** (Scheme 12) has served as a very useful model compound for natural BChl *c* to elucidate the structural and functional features of chlorosomal LS systems in green bacteria.[111a–c,112a] Zinc chlorins possess the three functional units (a hydroxy group, a central metal ion, and a keto function) relevant for the self-assembly found in their natural counterpart BChl *c*. The advantages of ZnChls over natural BChl *c* are: an easier availability from Chl *a* by a semi-

synthetic approach using standard chemical transformations,[111c,115] and the higher chemical stability of zinc chlorins compared to the magnesium chlorins present in natural BChls. However, the aggregates of simple zinc chlorins, such as ZnChl **42a**, are poorly soluble and thus prone to undefined agglomeration.[116] Similar to their natural counterpart BChl *c*, zinc chlorin dye **42a** forms π stacks with J-type coupling by metal-ion-mediated self-assembly. However, it is unlikely that tubular structures can evolve in the absence of solubilizing peripheral substituents. Therefore, Würthner and co-workers have developed new zinc chlorin derivatives, for example, zinc chlorins **42b,c**, bearing variable numbers of long alkyl chains on the 17^2 carboxylic acid substituent (see Scheme 12). It was shown that ZnChl derivatives with two or three peripheral dodecyl chains self-assemble into well-defined J-aggregates with good solubility and long-lasting stability in nonpolar solvents, thereby enabling spectroscopic and microscopic investigations aimed at elucidating the aggregate structure.[117] Detailed studies with ZnChl **42b**, which has a hydroxy group at the 3^1-position and two long alkyl chains on the carboxylic acid at the 17^2-position, revealed a fully reversible self-assembly process from monomers into extended aggregates that have excellent solubility in nonpolar solvents. Furthermore, the spectroscopic properties of these aggregates closely match those of BChl *c–e* aggregates in natural chlorosomes, namely, a red-shifted (about 100 nm) Q_y-band (Figure 24).[117a,b] The aggregation of

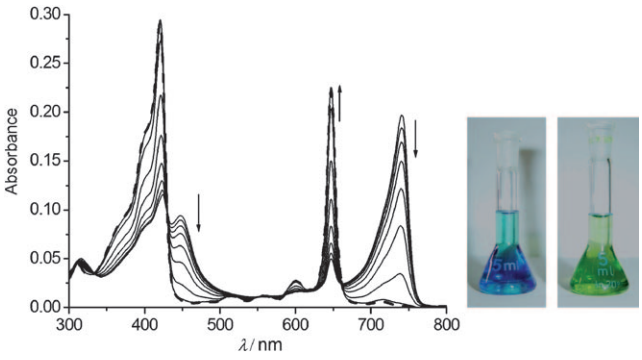

Figure 24. Left: Temperature-dependent UV/Vis spectra of zinc chlorin **42b** in a 20:80 mixture of di-*n*-butyl ether/*n*-heptane (3×10^{-6} M). The arrows indicate the spectroscopic changes upon increasing the temperature from 15 °C up to 95 °C (bold dashed line: monomer spectrum at 95 °C). Modified from Ref. [117]. Right: Photographs of solutions of monomeric **42b** in THF (blue) and its aggregate in *n*-hexane (green).

ZnChl **42b** can be observed with the naked eye, as the blue solution of the monomeric dye in di-*n*-butyl ether or tetrahydrofuran (THF) turns green upon initiation of the aggregation by addition of a nonpolar solvent such as *n*-heptane or *n*-hexane (Figure 24, right). The morphology of aggregates of zinc chlorins was elucidated by AFM studies, which revealed well-defined nonoscale rod structures, with **42b**, for example, having a height of about 6 nm (Figure 25).[117a,b] This value is in good agreement with the tubular model (described in the previous section) and the electron microscopy data for chlorosomal BChl *c* aggregates.[112,118]

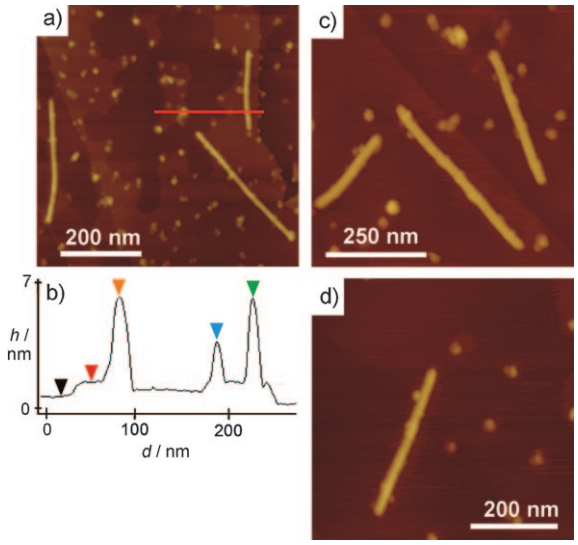

Figure 25. AFM images of aggregates of zinc chlorin **42b** on highly oriented pyrolytic graphite (HOPG). Different areas and magnified images are shown in (a), (c), and (d); b) the height profile along the red line in (a). The samples were prepared by spin-coating from a solution of **42b** in *n*-hexane/THF (100:1) on HOPG and measured in air. Reprinted from Ref. [117b] with permission.

Several research groups have studied the self-assembly of ZnChl derivatives in which the 3^1-OH group is replaced by a methoxy group, hence eliminating the possibility of hydrogen bonding that interconnects the one-dimensional (1D) chlorin stacks into a tubular structure.[112e,117c] The formation of extended π stacks was also confirmed for these dyes by concentration- and temperature-dependent UV/Vis and circular dichroism (CD) spectroscopic studies. A pronounced bathochromic shift (about 80 nm) of the Q_y-band was indicative of a J-type arrangement of the chlorin molecules in a slipped π stack.[117c] The self-assembly of such 3^1-methoxy zinc chlorins, in particular **42c**, to give highly ordered 1-D π-stacks of zinc chlorins could also be achieved on HOPG surfaces, as revealed by high-resolution AFM and scanning tunneling microscopy (STM) studies. Two types of π-stacked aggregates (single and double stacks) were observed, depending on the concentration of **42c**.[117c]

Very recently, de Groot, Würthner, and co-workers have elucidated the molecular packing of self-assembled ZnChls **42b** and **42c** in the solid state by magic angle spinning (MAS) NMR spectroscopy in conjunction with X-ray powder diffraction, DFT calculations, and molecular modeling studies.[119] It was found that zinc chlorins, containing either a 3^1-OH or methoxy functionality, self-assemble in the solid state in planar layers composed of antiparallel π stacks (Figure 26).[119]

Despite the fact that the tubular aggregates of BChl *c* and ZnChl are very efficient exciton transport systems, they cannot absorb the significant green region of the solar spectrum. Thus, biomimetic LH systems based on ZnChl with covalently appended naphthalene bisimide (NBI) dyes as auxiliary light-harvesting chromophores for the green region were developed to bridge the "green gap".[120] Several

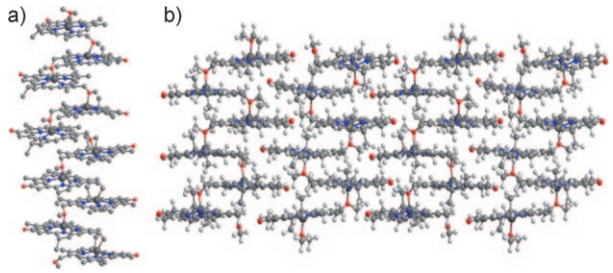

Figure 26. Proposed model based on MAS NMR spectroscopy, MM+ calculations, and X-ray diffraction data for the three-dimensional packing of **42c** in the solid state in an alternating antiparallel π-stack arrangement:[119] a) A single stack model and b) a multiple stack model; light gray C, white H, blue N, red O, dark gray Zn.

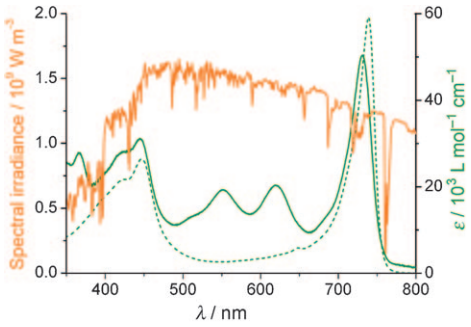

Figure 27. a) UV/Vis absorption spectra (green) of aggregates of the ZnChl–NBI–NBI' triad (**43**; ——) in cyclohexane/tetrachloromethane (99:1) and the corresponding aggregates of **42b** (•••••) in cyclohexane/tetrachloromethane/THF (99:1:0.1).[120b] The solar irradiance (orange line, source: http://rredc.nrel.gov/solar/spectra/am1.5/) is also shown to indicate the very significant green light region.

ZnChl–NBI dyads and triads were synthesized and their self-assembly properties were studied by UV/Vis, CD, and steady-state emission spectroscopy. The absorption spectra of the aggregate of the ZnChl–NBI–NBI′ triad (**43**) and that of the respective ZnChl, together with the solar irradiance, are shown in Figure 27 to illustrate the coverage of the "green gap" by J-aggregates of such triads. Self-assembly studies on these multichromophore systems revealed the formation of rodlike antennae by noncovalent interactions between ZnChl units, while the appended NBI dyes do not aggregate at the periphery of the rod antennae.[120] A schematic illustration of the proposed model for rod antennae self-assembled from triad **43** is shown in Figure 28.

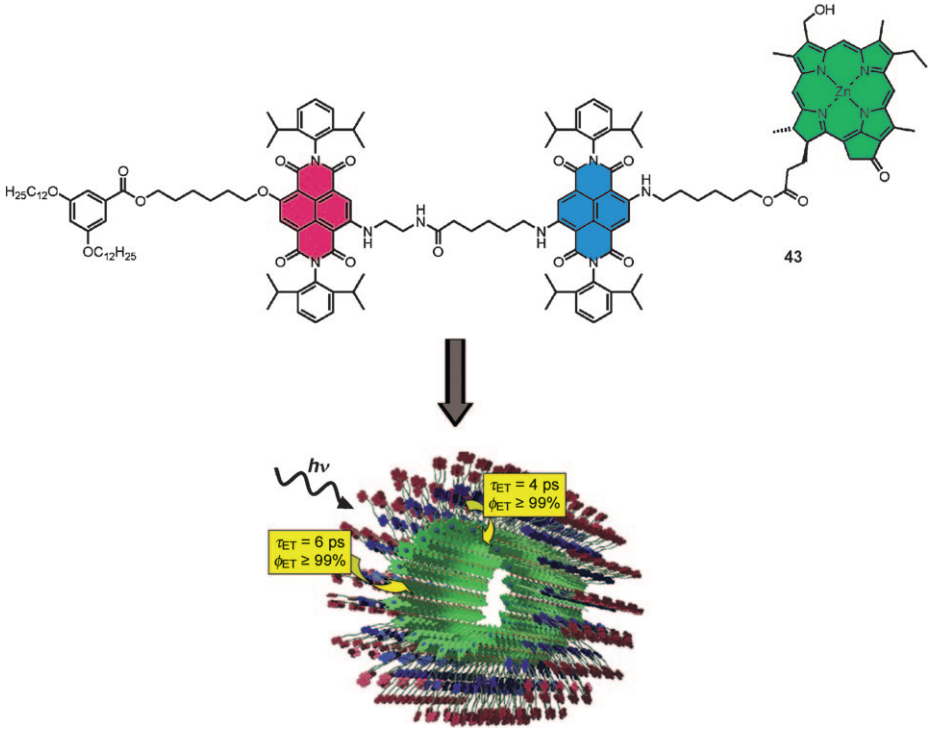

Figure 28. Top: the ZnChl-NBI-NBI′ triad **43** and bottom: schematic structural model for rodlike antennae with the fluorescence energy transfer (ET) rates and efficiencies Φ_{ET}.[120b]

Furthermore, picosecond time-resolved fluorescence spectroscopy of these rod antennae revealed a highly efficient fluorescence resonance energy transfer (nearly 100%) to the inner zinc chlorin stack upon photoexcitation of the peripheral NBI units. The efficiencies of such rod aggregates of ZnChl for the harvesting of solar light are, thus, markedly increased up to 63% (for triad **43**) compared to the light-harvesting capacity of the monochromophoric aggregates of the ZnChl model system.[120b] Most recently, Tamiaki and co-workers constructed remarkably efficient Grätzel cells (also called dye-sensitized solar cells) with light-sensitive bacteriochlorin J-aggregates and titanium dioxide (solar energy conversion efficiency of 6.6%).[121]

4.2. Porphyrin and Phthalocyanine Dyes

Natural (bacterio)chlorophyll dyes can be considered as derivatives of porphyrin since they contain a porphyrin structure as the core, with one or two double bonds of tetrapyrrol rings reduced. It appears to be questionable, however, whether porphyrins and their J-aggregates can serve as artificial counterparts of natural chlorin systems, as the latter exhibit lower energy Q_y-bands of high oscillator strength, whereas these transitions are almost forbidden in porphyrins. As a consequence, exciton coupling, which is proportional to the oscillator strength (or, more precisely, to

the square of the transition dipole moment), is very small for the Q_y-states in π–π-stacked porphyrins compared to those of chlorins. The excitonic coupling between porphyrins is thus typically evaluated on the basis of the very intensive higher energy B-band (Soret band), which is, however, irrelevant for exciton transport.

The structurally very appealing self-assembled porphyrins with a slipped face-to-face stacking geometry have been developed by Kobuke and co-workers. This research group found in the early 1990s that meso-imidazolyl-substituted zinc porphyrins had a pronounced Gibbs dimerization enthalpy.[122a] Since then, they have created a wide variety of fascinating molecular architectures, including supramolecular polymers and cyclic arrays with close structural resemblance to the dye arrays found in LH systems of purple bacteria, have been realized (Figure 29).[122b] Despite the low intensity of the Q_y-bands of porphyrins, Kim and co-workers found photophysical results of high significance for these very defined aggregates by employing time-resolved spectroscopy.[123]

In the absence of strong metallosupramolecular interactions, however, porphyrins typically self-assemble in to weak, only slightly slipped face-to-face columnar arrangements with H-type excitonic coupling.[124] Tetrakis(4-sulfonatophenyl)-porphyrin **44** ($TPPS_4$, sometimes also abbreviated as H_2TPPS or TSPP; Figure 30) is possibly the most intensively studied J-aggregating porphyrin derivative. The presence of J-bands in the UV/Vis absorption spectra of porphyrins was first reported in the early 1970s for $TPPS_4$ in acidic solutions.[125] It was found that pH 4.8, which is about the pK_a value of **44b**, is a threshold value for aggregation. The pH-dependent aggregation process, which is not observed for related metalloporphyrins, could be attributed to the protonation of the central pyrrole nitrogen atoms of the free-base form **44a** to give **44b**. A subsequent aggregation process is mediated by ion pair contacts between the cationic porphyrin centers and the anionic sulfonate groups at the periphery.[126] Only at rather low concentrations of $<10^{-5}$ M was the monomeric diacid form **44b** observed, whose transformation into the aggregate could be induced by increasing the concentration or increasing the ionic strength. The latter process is shown in Figure 31, which depicts the formation of two J-bands—a sharp one at 491 nm from the Soret band (B-band) of monomeric **44b** (434 nm) and a broad one at 707 nm from the longest wavelength Q_1-band of monomeric **44b**. In comparison to **44b**, the absorption spectra of the deprotonated monomeric form of **44a** consist of an intense Soret band at 413 nm and four very weak Q-bands at 648, 580, 552, and 515 nm (Q_1, Q_2, Q_3, and Q_4, respectively), which is typical for free-base porphyrins.[121a]

As shown in Figure 31, aggregation of **44b** is induced by the addition of salts such as NaCl, KCl, or $NaClO_4$. It is assumed that the counterions form a "cloud" around the J-aggregate, and thus reduce the electrostatic

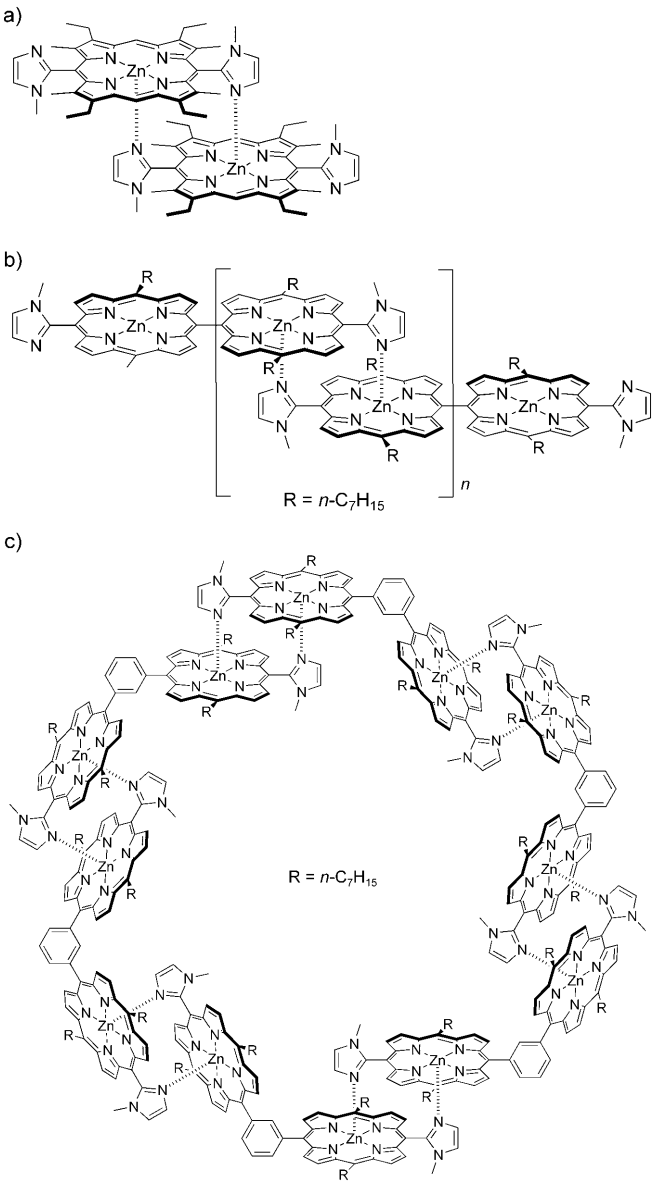

Figure 29. Structures of an a) imidazolyl-zinc porphyrin dimer, b) polymer, and c) macrocycle, as representative examples for architectures constructed by the Kobuke research group.[122]

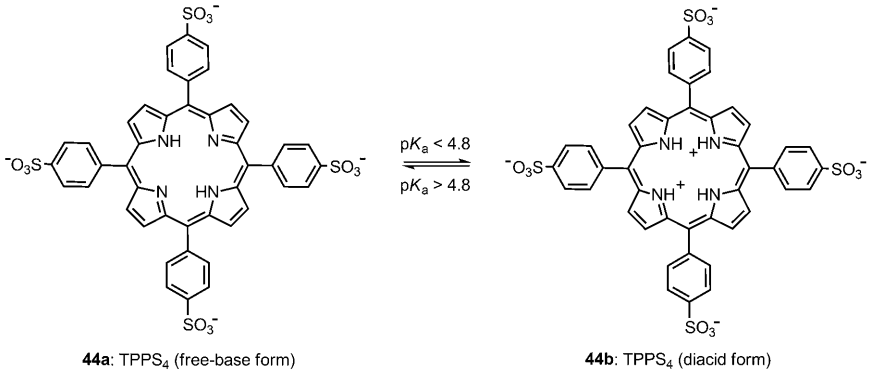

44a: $TPPS_4$ (free-base form) **44b**: $TPPS_4$ (diacid form)

Figure 30. Two ionic forms of $TPPS_4$ in aqueous solution: deprotonated (free-base) form **44a** and protonated (diacid) form **44b**.

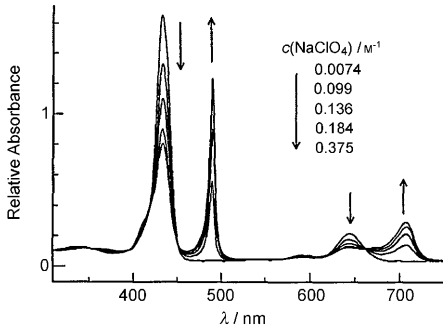

Figure 31. UV/Vis absorption spectra of $TPPS_4$ at a constant concentration of 7.2×10^{-6} M in acidic aqueous solution. The arrows indicate the changes upon addition of $NaClO_4$, which leads to the formation of J-aggregates. Reproduced from Ref. [126a] with permission. Copyright (1993) American Institute of Physics.

repulsion between the divalent porphyrin anions **44b**.[127] Upon aggregation, the fluorescence quantum yield and the fluorescence lifetime are reduced from 27% and 4.0 ns, respectively, in the absence of a salt, to 17% and 3.0 ns in the presence of NaCl.[126a]

Linear dichroism (LD) spectroscopic studies of **44b** aggregates revealed that the characteristic transitions, denoted by the J-bands at 491 and 707 nm, originate from oscillations that are polarized along the long axis of the rodlike aggregate.[126a] The addition of L-tartaric acid or a mechanical swirling flow in the period of aggregate growth resulted in induction of circular dichroism, as observed by CD spectroscopic studies.[126a,128] It is assumed that the monomers are arranged in the aggregate in a slipped face-to-face stacking arrangement, thereby forming planar, linear J-type assemblies, as shown in Figure 32 b,c. Such achiral structures are easily transformed into helical assemblies by external driving forces such as chiral counterions or vortices because of the lack of directionality between the ion pair contacts (Figure 32 d).

In a resonance light scattering (RLS) study the width of the J-band (which relates to the exciton delocalization length) and size of the $TPPS_4$ J-aggregates were found to be controllable by the concentration of ammonium ions.[129] The highest spectroscopic aggregation number—a coherence length of 12.9 molecules—obtained from the width of the 490 nm band was realized for an aggregate with a hydrodynamic radius of 56 nm. A similar exciton delocalization over about 10 molecules was estimated for the narrow high-energy J-band at 490 nm by ultrafast transient absorption and fluorescence spectroscopy.[130] However, as revealed by this study, the exciton becomes rapidly localized on only one to two molecules after its relaxation to the lowest exciton J-band at 707 nm, where propagation is only possible in a non-coherent way. These results are in reasonable agreement with expectations based on simple line-width analysis for these two J-bands. The same two-band Frenkel exciton system has been subjected to sub-5 fs spectroscopy, which revealed their coupling to a coherent molecular vibration and explained the unusually intense J-band at 707 nm by a dynamic intensity borrowing from the intense B-transition to the weak Q-

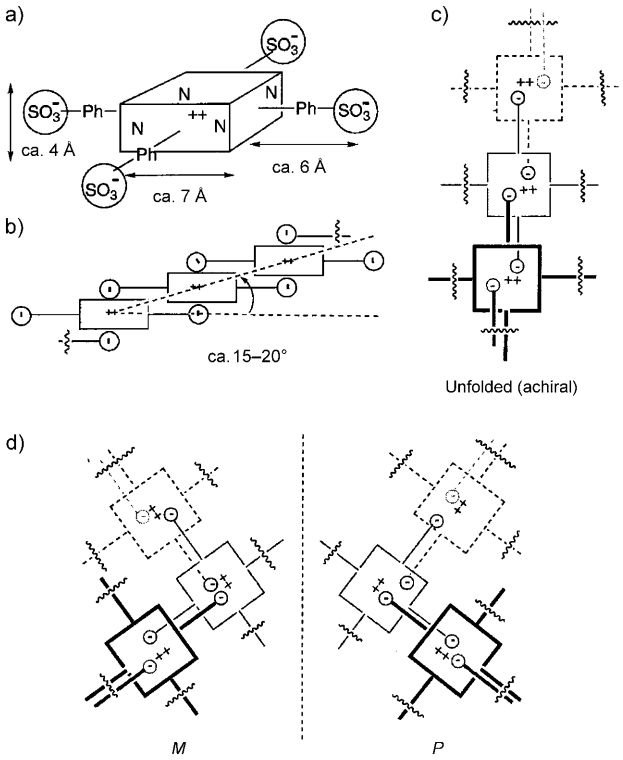

Figure 32. Proposed model of the J-aggregate of protonated $TPPS_4$ which forms a supramolecular chain. a) Schematic representation of $TPPS_4$; b) side view of the chain, illustrating the angles between the chain alignment and the porphyrin plane are 15–20°; c) top view of the achiral chain and d) *M* and *P* conformers of a chiral chain arising from stirring. Reproduced from Ref. [128b] with permission.

transition through a ruffling mode with a frequency of 244 cm^{-1}.[131]

Porphyrin nanorods could be observed by AFM upon deposition of aggregates of the diacid form of $TPPS_4$ onto substrates such as mica.[132] The individual rods exhibit a diameter of 3.8 nm and lengths of 0.77–20 μm (Figure 33). The remarkably straight nanorods with a well-defined height are also observed to form larger structures with the same height. UV/Vis spectroscopy and dynamic light scattering (DLS) measurements have shown that the aggregates were already formed in solution, and not during deposition onto the surface of the substrate.

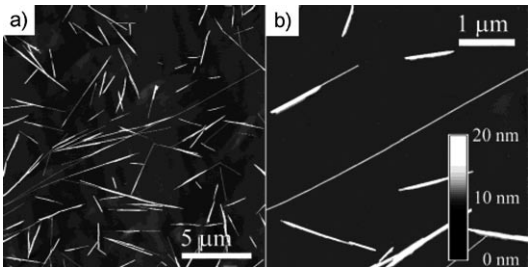

Figure 33. AFM images from aqueous solutions of $TPPS_4$ (5×10^{-3} M) containing 3×10^{-4} M HCl adsorbed onto mica. a,b) Single rods and b) larger structures composed of those single rods. Reproduced from Ref. [132] with permission. Copyright (2003) American Chemical Society.

In 2008, amphiphilic derivatives of $TPPS_4$ were also reported to self-assemble into J-aggregates.[133] In these derivatives, one of the four sulfonic acid groups in $TPPS_4$ is replaced by a methoxy, octyloxy, or octadecyloxy chain as the hydrophobic site. For the octyloxy derivative **45**, a regular leaflike structure was observed by AFM, which corroborates the results obtained by absorption and DLS measurements. The proposed bilayer structure, in which the hydrophobic alkoxy groups are oriented inside the bilayer and interdigitated with each other while the hydrophilic porphyrin moieties are exposed outside, is shown in Figure 34.

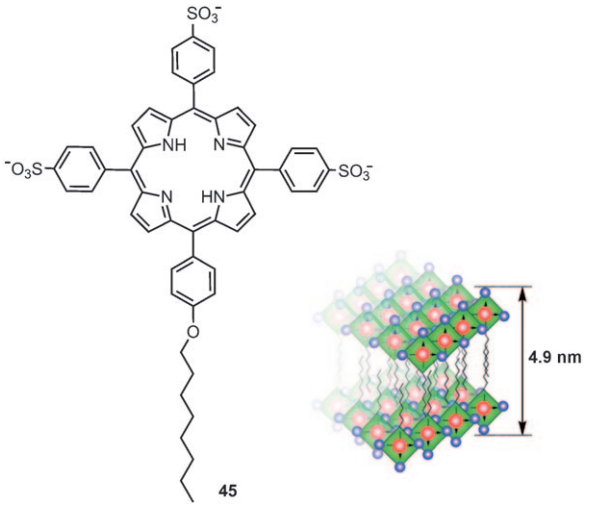

Figure 34. Structure of the octyloxy derivative of $TPPS_4$ **45** (left) and the proposed bilayer model for the porphyrin J-aggregate with a thickness of 4.9 nm (right). Reproduced from reference [133] with permission. Copyright (2008) American Chemical Society.

Further examples of J-aggregates of synthetic porphyrins are the heteroaggregates of Shellnut and co-workers composed of the divalent anionic diacid form of **44b** and the respective cationic protonated tetrapyridyl derivative **46**, which was found to form hollow porphyrin nanotubes upon aggregation (Figure 35),[134] and a dendronized porphyrin of Aida et al. that forms J-type aarrangements (Figure 36).[135] The latter contains two bulky dendron groups and two carboxylic acid groups as well as a central zinc ion (Figure 36a,b). This zinc porphyrin was found to initially form linear chains by hydrogen bonding with either a short and oblique or long and non-oblique slip of the monomers, which further assemble into a 2D J-aggregate that can be transformed into a chiral assembly by spin coating.[135]

Similar to most porphyrins, phthalocyanines typically self-assemble into H-aggregates in solution because the slipping angle resulting from the equilibration of dispersion and electrostatic interactions clearly favors sandwich face-to-face contacts with strongly overlapping π surfaces rather than the more slipped arrangements required for J-type coupling.[136] Accordingly, only a few examples of phthalocyanine J-aggregates have been reported, and in most cases these aggregates are assisted by the complexation of a metal ion.[137] An anomalously broad and strongly red-shifted Q-band

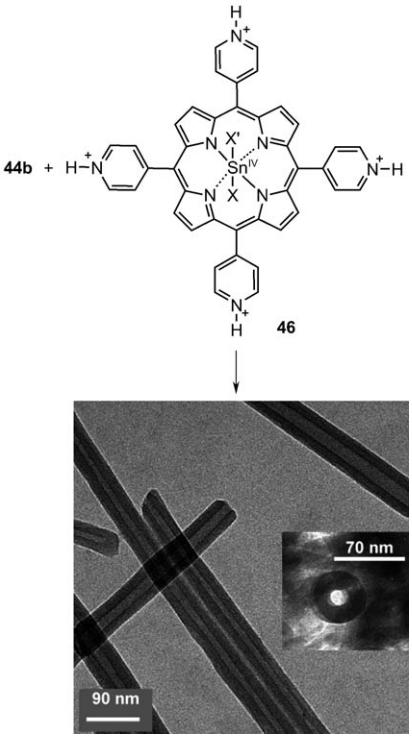

Figure 35. Structure of the tetrakispyridyl derivative **46** (X, X′ = Cl^-, OH^-, H_2O) and TEM image of the porphyrin nanotubes formed by the co-self-assembly with anionic porphyrin **44b**. Inset: Tube trapped in a vertical orientation by a thick mat of tubes. Reprinted from Ref. [134] with permission. Copyright (2004) American Chemical Society.

($\lambda_{max} = 870$ nm) was observed for an antimony(III)–phthalocyanine complex upon aggregation in dichloromethane, thus indicating a J-type coupling of the transition dipole moments in the assembly. A structurally better characterized example of a phthalocyanine J-dimer was reported by Kobuke and co-workers, again through the appropriate positioning of imidazole ligands, which control the displacement of the two phthalocyanine dyes within a dimer aggregate (Figure 37).[138a] The J-type coupling in this dimer is supported by a small bathochromic shift of the Q_y-band and high fluorescence yields of up to 76%. A related zinc ion mediated J-type dimer of phenoxy-substituted phthalocyanines has been achieved by coordinating oxygen ligands.[138b] Similar to their natural BChl *c* counterparts and zinc chlorins **42**, the addition of coordinating solvents such as methanol caused dissociation of these dimers, which implies that the absence of coordinating solvents is essential for J-aggregation of these dyes.

Slipped π–π-stacking arrangements with bathochromically shifted J-bands are also of crucial importance in the major application of phthalocyanine chromophores as solid-state materials, that is, as color and functional pigments.[139] Among the many know metal complexes of phthalocyanines, the blue copper complexes (CuPc) are the most important ones and are manufactured on a large scale. Depending on their packing arrangements in the solid state, different polymorphs are formed that are able to satisfy different coloristic needs. A polymorph named as the β modification is

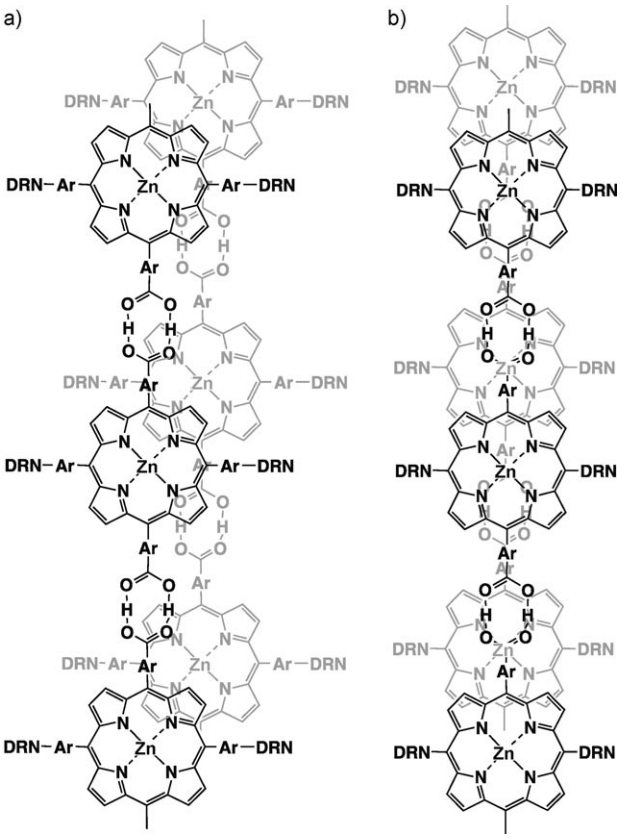

Figure 36. a,b) Structures of the J-aggregates of a dendron (DRN) functionalized zinc porphyrin with a) short, oblique slip and b) long, non-oblique slip. Reproduced from Ref. [135] with permission.

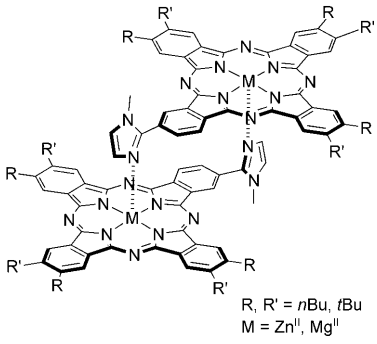

Figure 37. Dimers of imidazolyl-metallophthalocyanines with J-type coupling developed by Kobuke and co-workers.[138a]

the thermodynamically most stable one, and is able to provide the cleanest shades of turquoise blue, as required for the cyan ink in three- and four-color printing. Whilst the basic absorption properties of the monomeric CuPc—that is, a sharp and intense absorption band at 678 nm (Q-band)—are a promising starting point for achieving a pure cyan hue, it is the broadening and bathochromic shift of the absorption band in the aggregate that makes this pigment an outstanding cyan colorant (marketed as a pigment with color index C. I. Pigment Blue 15:3). Both effects can be related to the excitonic coupling of the monomeric dyes in the crystal,

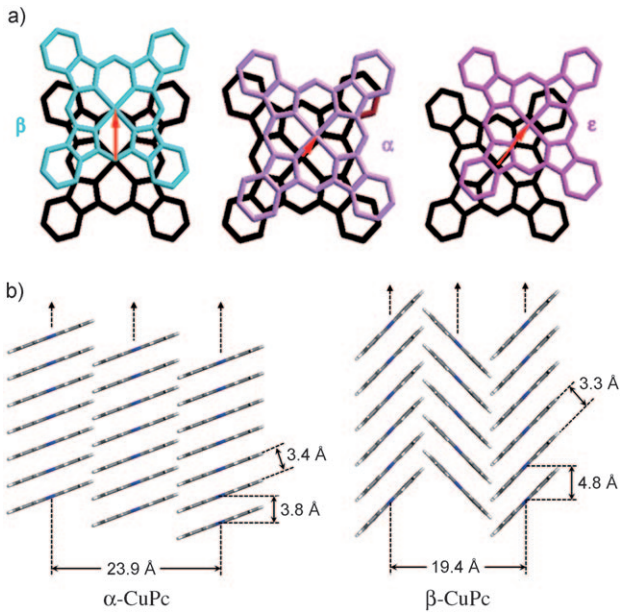

Figure 38. a) Packing of CuPc molecules in the π stacks of α, β, and ε polymorphs according to single-crystal structure analyses. The displacement vector is shown in red and the color of the pigment is indicated by the upper phthalocyanine molecule. b) Arrangement of the planar and almost square phthalocyanine molecules in one-dimensional stacks (similar to rolls of coins) in the α and β modifications. Note that the different angles between the staple axis and the molecular plane lead to a different displacement and coupling between the transition dipole moments.

where a major effect (bathochromic shift) arises from the coupling between adjacent dyes within the one-dimensional π stacks (Figure 38a) and minor effects (band broadening) arise from the coupling to more distant dyes that are located in the neighboring π stacks (Figure 38b). Different coloristic properties are accessible from the same dye molecule as a consequence of the different packing of the CuPc monomers in other polymorphs (Figure 38a). Thus, the α and the ε modifications exhibit a more reddish blue hue, which is desirable for automotive finishes in both solid and metallic shades (α-CuPc) and for blue color filters of liquid-crystal displays (ε-CuPc).

Another phthalocyanine pigment, titanylphthalocyanine (TiOPc), has evolved to be the most applied photoconductor for laser printers.[140] For this application, J-type excitonic coupling is crucial for enabling an efficient transportation of excitons to the interface and a proper adjustment of the absorption band to the wavelength of commercial NIR laser diodes (750–850 nm). The central Ti=O unit is responsible for the strong displacement of the chromophores in the solid state, as has been observed for several polymorphs of TiOPc (Figure 39).[141] A particularly pronounced band broadening and bathochromic shift of the originally very narrow absorption band of TiOPc monomers in solution (at ca. 700 nm) enabled the commercial application of the solid-state polymorph Y-TiOPc (absorption band from 600 to 900 nm with a maximum at ca. 800 nm).[142] It is noteworthy that this structural arrangement of the dyes and its effect on the absorption properties are both reminiscent of photosynthetic

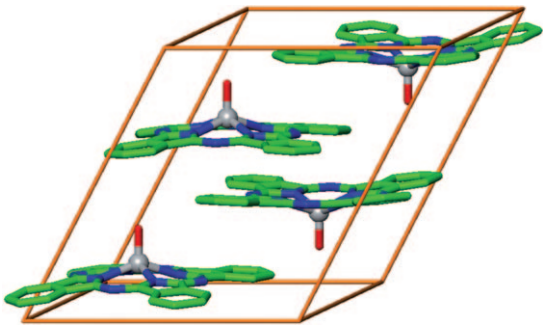

Figure 39. Packing of TiOPc molecules in the Y-polymorph of the charge-generating layers of xerographic photoreceptors; green C, blue N, red O, gray Ti. This Figure was made available by P. Erk (BASF SE), as a courtesy.

(bacterio)chlorophyll pigments in purple and green bacterial light-harvesting systems. The structural details of these natural LH systems were, however, unknown at the time when TiOPc photoconductors were developed.

5. Perylene Bisimide Dyes

As a consequence of their outstanding optical properties, in particular exceptional fluorescence with quantum yields up to unity, perylene bisimide (PBI)[143] dyes are a highly interesting class of chromophores for J-aggregates with promising functional properties. Similar to phthalocyanines, the major application of PBI dyes is as high-performance color pigments with shades ranging from red to violet, maroon and black,[139] which is again attributable to the arrangement of the molecules in the crystal and the resulting excitonic coupling. Remarkably, despite their outstanding fluorescence properties in solution, no fluorescence is typically observed for theses dyes in the solid state. The reason for this might be attributed to the packing arrangement in the pigments, which is mostly of H-type character.[143,144] Nevertheless, strongly emitting microcrystalline powders of PBI dyes are accessible, as shown in Figure 40.[145] For dye **47d** with the bulky *tert*-butylphenoxy bay substituents, a high solid-state fluorescence quantum yield of 70% was measured, which might be rationalized by the fact that these substituents prohibit the formation of close π–π contacts (with H-type coupling). However, quite intense fluorescence was also observed for the sterically less demanding chlorine-functionalized PBI (**47c**) and even for the core-unsubstituted dyes **47a**,**b**[146] (solid-state quantum yield of 40% for both **47b** and **47c**).[145]

In solution, perylene bisimides without bay substituents prefer to aggregate in columnar stacks whose major absorption band is hypsochromically shifted, thus indicating predominant H-type excitonic coupling.[147] However, as a consequence of a rotational displacement between neighboring dyes, the optical transition into the lower energy exciton state becomes allowed,[27] as evidenced by a second absorption band at longer wavelength. The particular arrangement and the concomitant photophysical properties of the aggregates are strongly dependent on the imide substituents. For PBIs bearing electronically active rather innocent trialkylphenyl substituents, a relatively long-lived excited state with an appreciably high fluorescence quantum yield of 47% has been reported,[147] which was attributed to the relaxation of the exciton into an excimer.[148]

In 2001, Würthner et al. reported perylene bisimide dye aggregates that exhibit predominant J-type character.[149,150] Such J-aggregating PBIs, for example, **48a**, have 3,4,5-tridodecyloxyphenyl substituents at the imide N atoms and

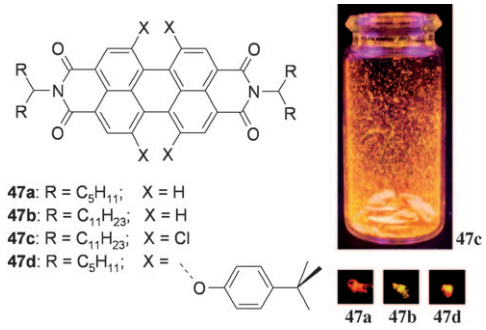

Figure 40. Left: Structures of PBI dyes **47a–d** that strongly fluoresce in the solid state. Right: Photographs of fluorescent powders of **47c** (in a glass vial) and other PBI pigments **47a**,**b**,**d** (upon illumination with UV light at 366 nm).[145]

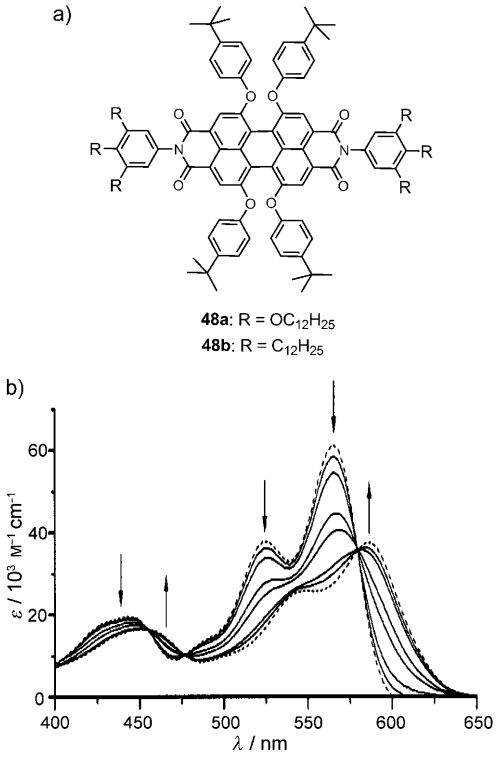

Figure 41. a) Structures of PBIs **48a**,**b** that form aggregates with J-type character. b) Concentration-dependent UV/Vis absorption spectra of **48a** in methylcyclohexane (MCH). The arrows indicate the changes in the spectra with increasing concentration. The dotted lines represent spectra for the free and the aggregated chromophores, calculated from the respective data set. Reproduced from Ref. [149] with permission.

aryloxy substituents in the four bay positions (Figure 41). A rather broad but red-shifted absorption band was observed upon self-assembly in low-polarity solvents. Although this red-shift indicates the presence of slipped chromophores, the broadness of the absorption band and the rather large Stokes shift might be taken as an indication of a less ideal system that is influenced by disorder and phonon coupling[151] caused by the bulky aryloxy substituents. In addition, the fluorescence of these compounds was quenched both in the monomeric ($\Phi_{Fl} = 21\,\%$) and the aggregated state as a result of a photoinduced electron transfer from the electron-rich trialkoxyphenyl substituents to the electron-poor perylene bisimide.[152] For this reason, PBI **48b** was synthesized and revealed significantly improved fluorescence properties ($\Phi_{Fl} = 95\,\%$) while maintaining the J-type character of the aggregates.[153] The presence of dimeric aggregate species in 0.001–0.01 M solutions of PBI dye **48b** was confirmed by vapor pressure osmometry. Notably, a whole series of trialkyl- and trialkyloxyphenyl-substituted PBIs were shown to exhibit columnar liquid-crystalline mesophases over a broad temperature range.[153]

Structurally related PBI derivative **49a**, which contains hydrogen atoms instead of trialkyoxyphenyl groups in the imide positions (Figure 42a), formed J-aggregates with very characteristic optical properties, which are comparable to those of the well-studied classical cyanine J-aggregates, and thus represent the first genuine J-aggregating PBI.[154] UV/Vis and fluorescence spectroscopic studies on **49a** in the nonpolar solvent methylcyclohexane revealed the reversible formation of these J-aggregates (Figure 42b,c) and the strong narrowing of the red-shifted absorption band from a full-width-at-half-maximum (fwhm) value of 2393 cm^{-1} down to 885 cm^{-1}. In addition, a narrowing of the fluorescence band from 1660 cm^{-1} to 878 cm^{-1} was observed, and a concomitant increase in the fluorescence quantum yield from 93% to 96%. As expected for J-type-coupled chromophores with a significantly enhanced transition dipole for the $S_0 \rightarrow S_1$ transition, the fluorescence lifetime is decreased for the aggregate (2.6 ns) compared to that of the monomer (6.8 ns).[154]

This J-type aggregation of functional perylene bisimide chromophores could be achieved by the design of monomeric building blocks that encode the desired slipped face-to-face arrangement by the mutual effects of hydrogen bonding and π–π interaction, while preventing aggregation into columnar stacks because of their twisted π-conjugated core and sterically demanding substituents in the bay area. The proposed model for the formation of aggregates is shown in Figure 43. In-depth investigations on the series of PBIs **49a–c** (Figure 42a) revealed the formation of a dimeric nucleus (Figure 43c) prior to elongation into double-string cablelike J-aggregates (Figure 43d), with the monomers aligned with translational offset (Figure 43e).[154b] This cooperative nucleation–elongation mechanism is in contrast to the isodesmic (or equal K) model, which was used previously to described the aggregation process for common assemblies of PBIs. Equilibrium constants for dimerization (= nucleation, Figure 43c) of $K_2 = (13 \pm 11)\ M^{-1}$ and for elongation of $K = (2.3 \pm 0.1) \times 10^6\ M^{-1}$ in methylcyclohexane (MCH) were obtained by applying the nucleation–elongation model to concentration-dependent absorption studies. Accordingly, for this system, dimeric species should not show up in significant quantities as, for example, observed for the PIC dye. Instead, an instantaneous growth into extended nanofibers will occur at a critical temperature and concentration. Furthermore, the nonlinearity of chiral amplification in PBI heteroaggregates composed of achiral and chiral PBIs **49b** and **49c**, respectively, directed by the sergeants-and-soldiers principle was demonstrated by CD spectroscopy.[154b,155]

Very recently, exciton transport along these J-aggregates has been studied by spectroscopy at low temperatures (from 300–5 K)[156] and by single-molecule spectroscopy.[157] For individual PBI J-aggregates, fluorescence blinking corresponding to the collective quenching of up to 100 PBI monomers has been observed, which could be related to an exciton diffusion length of up to 70 nm in these aggregates at

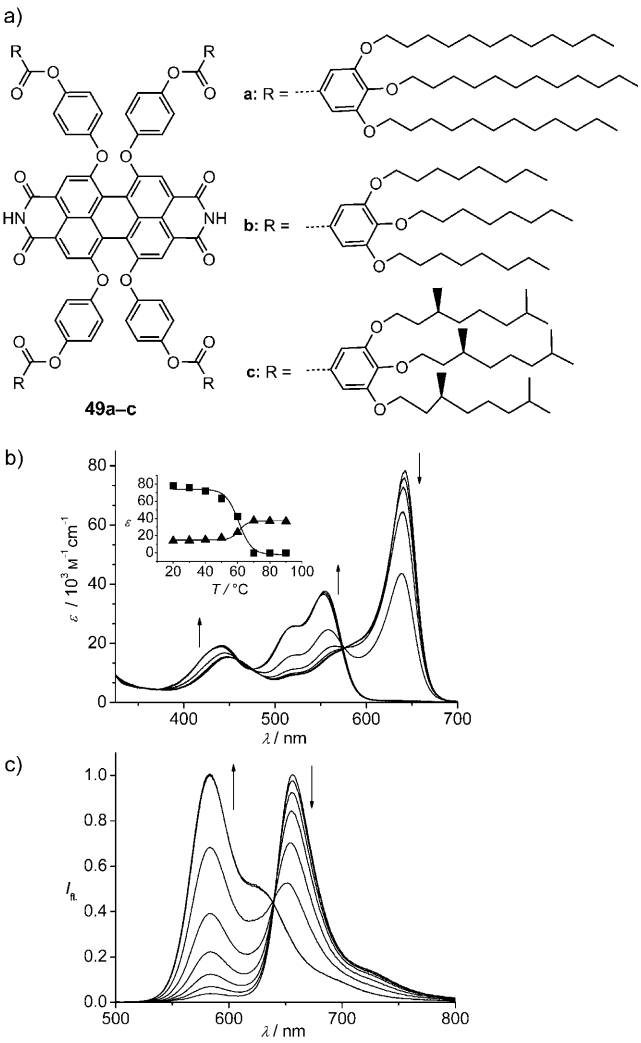

Figure 42. a) Structures of PBI dyes **49a–c**. b) Temperature-dependent UV/Vis spectra of **49a** in MCH (1.5×10^{-5} M) at 20–90 °C. The arrows indicate the changes in the spectra with increasing temperature. Inset: changes in the absorption at 642 nm (■) and 553 nm (▲). c) Temperature-dependent fluorescence spectra of **49a** in MCH (6×10^{-7} M, $\lambda_{ex} = 476$ nm) at 15–50 °C; the arrows indicate the changes in the spectra with increasing temperature. b,c) Reproduced from Ref. [154a] with permission.

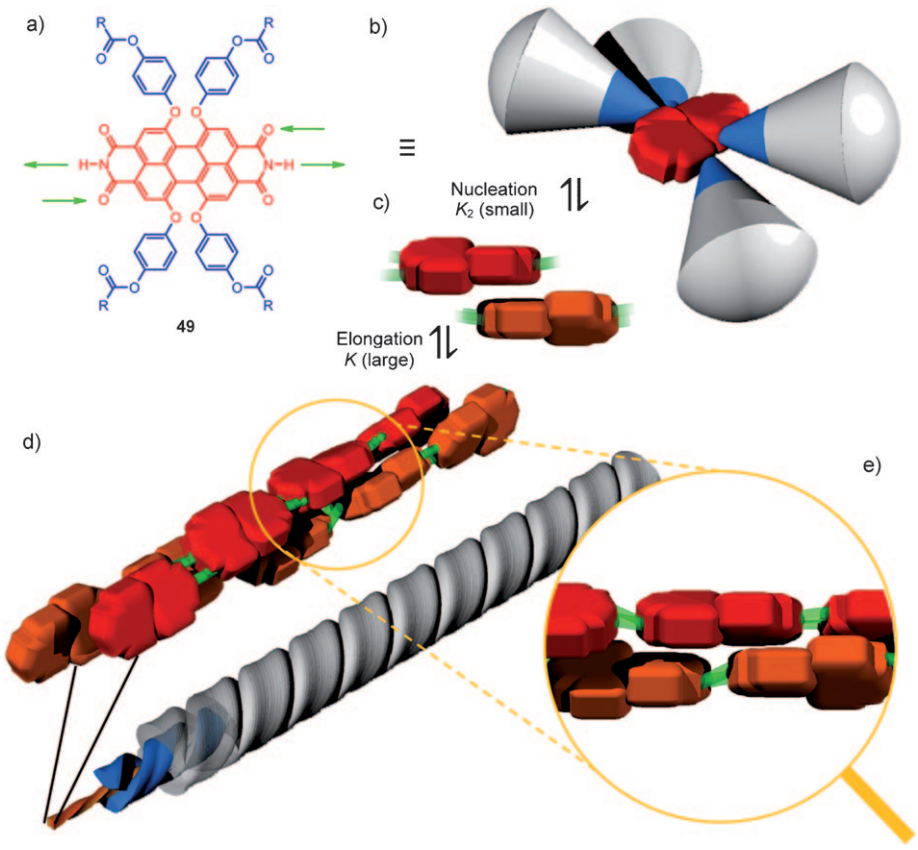

Figure 43. Schematic illustration of the self-assembly of the perylene bisimide dyes **49** into J-aggregates. a) Structure of **49** (substituents R are defined in Figure 42a) and b) graphical representation of the monomer. c) Schematic representation of the π-stacked dimeric nucleus and d) that of an extended hydrogen-bonded J-aggregate of **49**. Red (and orange) twisted blocks represent the perylene bisimide cores (in the adjacent chain), gray cones with a blue apex represent the bay substituents, and green lines represent hydrogen bonds. The dyes **49** self-assemble in a helical fashion, as shown in the magnification (substituents are omitted and only the left-handed helical structure is shown for simplicity). e) The magnification shows the side view of the J-type arrangement of the perylene bisimide core units in a double-string cable. Reprinted from Ref. [154b] with permission. Copyright (2009) American Chemical Society.

room temperature. These values already approach the highest reported singlet exciton diffusion lengths for organic crystals, for example, 100 nm in diindenoperylene.[158] Recently, the supramolecular strategy for PBI displacement by means of core twisting and hydrogen bonding was applied to the crystal engineering of solid-state materials to afford organic thin-film transistors with exceptional n-type charge-transport properties under ambient conditions.[159]

Core-unsubstituted PBI derivatives **50** (Scheme 13) with amide functionalities, and with trialkoxyphenyl groups at the

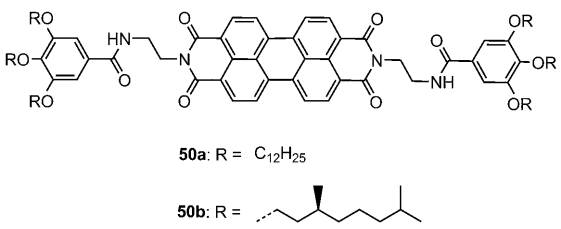

Scheme 13. Structure of PBIs **50** that form organogels with H- or J-type character.

imide positions, were shown to form aggregates that exhibit either H- or J-type absorption spectra depending on the peripheral alkoxy chains.[160,161] These amide-functionalized PBIs form long fibers by hydrogen-bond-assisted self-assembly that are able to immobilize a broad variety of solvents to give organogels. Remarkably, whilst the PBI derivative **50a** with simple *n*-alkyl chains at the periphery forms red-colored H-type aggregates, as expected for core-unsubstituted PBIs, aggregates of dye **50b** bearing chiral, branched alkyl chains exhibit a strongly bathochromically shifted broad J-band in solution (Figure 44) as well as in the organogel state. The aggregates of **50b** are almost black and possess an even more pronounced gelation ability than the aggregates of **50a**. This feature has been exploited for the gelation of p-type semiconducting polymers.[162] It is indeed very intriguing that the aggregation mode (that is, H- or J-type) of PBI chromophores could be altered by a subtle variation of the peripheral substituents. A broad series of structurally related PBIs with different alkyl chains at the periphery have been investigated to explore in detail the effects of peripheral

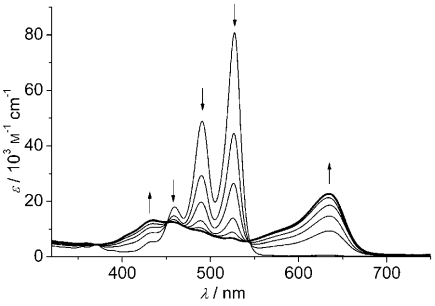

Figure 44. Solvent-dependent UV/Vis absorption spectra of chiral PBI **50b** in MCH/$CHCl_3$ solvent mixtures of 50:50 to 80:20 at a constant concentration of 10^{-5} M. The arrows indicate changes in the spectra with increasing amounts of nonpolar MCH. Modified from Ref. [161].

substituents on the gelation capability and self-assembly properties.[163] These studies revealed that the steric nature of the peripheral side chains dictates the type of self-assembly of these core-unsubstituted PBI dyes. Derivatives bearing linear alkyl chains (less steric demand) form H-type assemblies, while J-type assemblies prevail for dyes containing branched

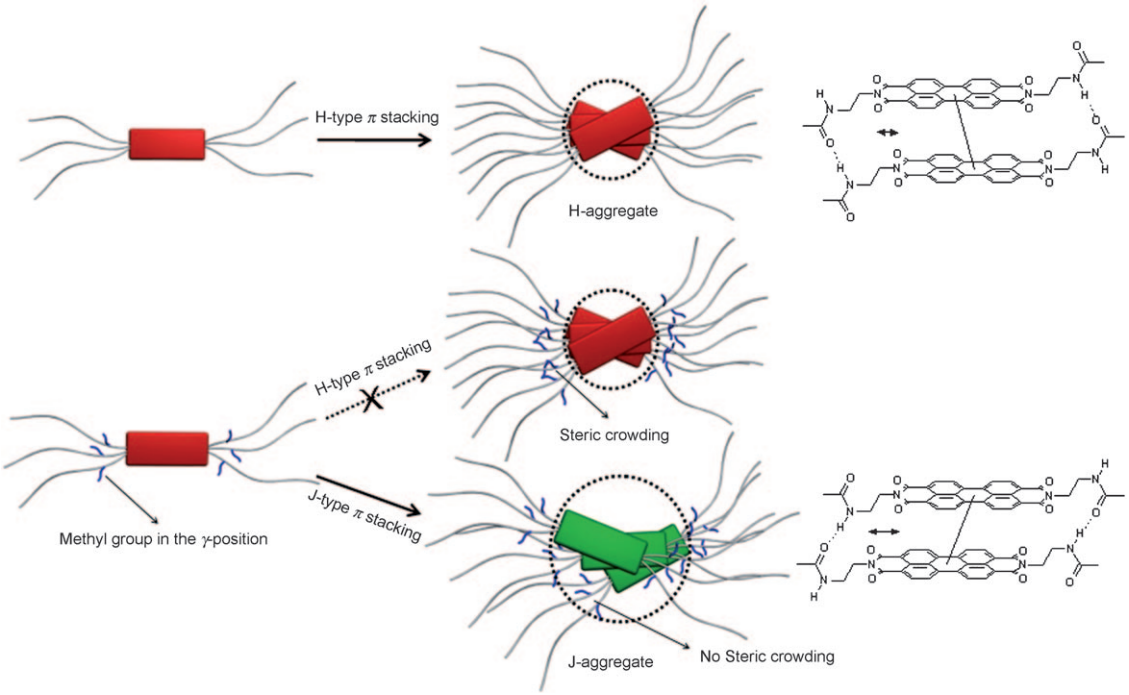

Figure 45. Left: Schematic representation of PBI chromophores **50** with linear (top) and branched (bottom) alkyl substituents. Middle: The transition from H- (top) to J-type (bottom) π stacking with increasing steric demand of the peripheral alkyl side chains. Right: Proposed packing model for H- (top) and J-type (bottom) π stacking. In both cases, additional rotational offsets are needed to enable both close π–π contact and hydrogen bonding. Reprinted from Ref. [163] with permission.

alkyl chains (high steric demand). Simplified packing models proposed for the J-type and H-type assemblies of these PBIs are illustrated in Figure 45. It is interesting to note that alteration of the chromophore **50a** by introducing *tert*-butylphenoxy substituents at all four bay positions afforded a PBI organogelator that forms lyotropic mesophases and shows a rather sharp J-type absorption band with a high fluorescence quantum yield.[164]

A few more examples of PBI aggregates with J-type character have been reported that exhibit in general rather broad J-bands (comparable to those of PBI **48a**; Figure 41).[165] Not only homoaggregates of PBI chromophores, but also heteroaggregates consisting of PBI and other π systems, for example, melamine derivatives, have been reported.[166] A triple hydrogen-bonding motif from perylene bisimide to the melamine derivative (ADA–DAD; A = acceptor and D = donor) together with π–π interactions of the adjacent PBIs led to the formation of extended fluorescent PBI–melamine networks.[166] The long alkyl chains of the melamine facilitate the solubility of the assemblies, and the van der Waals interactions between the aliphatic chains further stabilize the network. Absorption spectroscopy revealed a small bathochromic shift of the J-band, which is assumed to originate from a slightly slipped arrangement of the chromophores.

Well-ordered J-type aggregates were formed by the self-assembly of hydrogen-bonded and covalent donor–acceptor–donor arrays of bay-substituted PBIs as acceptors and oligo(*p*-phenylene vinylene)s (OPVs) with chiral side chains as donors. Concentration- and temperature-dependent absorption spectroscopy revealed a bathochromic shift of the PBI bands of these aggregates compared to that of the respective PBI monomer.[167] Further investigations by circular dichroism, photoluminescence, and femtosecond pump-probe spectroscopy revealed the formation of chiral arrangements, in which the PBI monomers are arranged in a slipped J-type arrangement (similar to the "green" J-aggregates; Figure 45), and ultrafast photoinduced charge transfer from the OPVs to the PBIs.[167b,d] Recently, a related system was reported where the OPV was replaced by azobenzenes.[168] A unique example of a melamine-functionalized, core-unsubstituted PBI that self-assembles upon additon of 0.5 equivalents of ditopic cyanurate into H-type dimers was reported by Yagai et al. Interestingly, the addition of 1 equivalent of cyanurate transforms the H-dimers into J-type aggregates with a strongly red-shifted absorption band (>100 nm) compared to that of the monomeric PBI.[169] Such a concept for the control of H- and J-type aggregation indeed has the potential to generate responsive J-type aggregates for fluorescence sensors.

6. Summary and Outlook

Strong excitonic coupling between fluorescent dyes that are significantly slipped with respect to each other yields the characteristic and desired features of J-aggregates, such as a narrow absorption band that is bathochromically shifted relative to the monomer band, high fluorescence intensity with small Stokes shift, and exceptional exciton transport

capability. In this Review, we have given an overview of the major classes of colorants that have been demonstrated to form J-aggregates. A prime goal of this Review was to illustrate supramolecular principles that govern the transformation from the more often encountered sandwich-type face-to-face stacking[88a] with H-type coupling to highly slipped dye arrangements with J-type coupling. In the case of perylene bisimide (PBI) dyes, the distortion of the dyes' π system in combination with directional hydrogen bonds is a successful approach for the noncovalent synthesis of double-string J-aggregates with unprecedented fluorescence quantum yields. For merocyanine and phthalocyanine dyes, sterically demanding substituents provide the repulsive forces for displacement of the chromophore in the solid state, which is required for efficient photoconductive and photovoltaic layers. For chlorin and porphyrin dyes, metallosupramolecular coordination to the central metal ion was discussed as a highly suitable strategy to afford a slipped dye stack with J-type coupling. This strategy is biomimetic in the sense that this supramolecular motif is found ubiquitously in light-harvesting complexes of photosynthetic bacteria, where it results in absorption bands above 700 nm and even above 800 nm for naturally abundant chlorophyll and bacteriochlorophyll chromophores, respectively.

It needs, however, to be emphasized that these examples of supramolecular and crystal engineering are still rather special examples, while the largest class of known J-aggregates is still based on serendipitously discovered cyanine dye aggregates. Since several reviews on J-aggregates of cyanine dyes are available, we have neither featured all the cyanine dyes that form J-aggregates in this article nor discussed all of the important photophysical studies on those, but have focused on archetype examples such as the historically most significant pseudoisocyanines (PIC) and the recently most intensively investigated derivatives of benzothiazol- and benzoimidazol-based trimethine dyes. The latter also played an important role as photosensitizers in silver halide photography,[5] and were thus the first supramolecular dye systems with widespread technological applications. A superb ability to adsorb onto colloidal silver halides (AgX) together with the absorption of visible light in a very narrow spectral range and efficient energy transfer to AgX particles was mandatory for applications in the photographic process. From a supramolecular perspective, it is remarkable that the exact aggregate structure of the first J-aggregate, that is, PIC aggregate, is still a matter of debate 75 years after its discovery, and will remain a topic of future research.

Even more remarkable from a functional point of view than the cyanine J-aggregates, are those of the natural bacteriochlorophylls *c*, *d*, *e* in the chlorosomes of green bacteria, which constitute the most efficient light-harvesting system found in nature. As a consequence of the unique metallosupramolecular interaction between the hydroxy functionality and the magnesium ion of BChl *c*, *d*, *e*, an ideal displacement of the π-stacked dyes is accomplished to ensure absorption of light in the NIR spectral region and rapid exciton transport—requirements that are needed to catch and utilize the few traces of stray light in extreme habitats such as the depths of ponds or the ocean.[170] The absence of proteins in chlorosomal light-harvesting complexes ensures the highest possible pigment density among all the natural photosynthetic apparatus and offers the opportunity to reconstruct these light-harvesting antenna from BChl *c*, *d* or their semisynthetic analogues in the laboratory by self-assembly in aqueous or even in organic media.

In recent years, dye assemblies with J-type coupling have received considerable attention in two major fields of research: biomolecular science and organic solid-state science. For biomolecular science, water solubility is of relevance and thus it is not surprising that cationic cyanine dye aggregates were the dyes of choice for the development of novel fluorescent and colorimetric sensing schemes, for example, by the connection of cyanine dyes to peptides or by DNA-templated J-aggregation. The strong absorption of light and efficient exciton transport to analyte traps provide these dye aggregates with an ultrahigh sensitivity. The same virtues of these J-aggregates may serve for artificial photosynthesis, if trap sites with appropriate photocatalytic properties become accessible. The recently observed photoinduced reductions of noble metal ions to metal nanoparticles on tubular J-aggregates[171] and the generation of molecular hydrogen by water cleavage with the help of pseudoisocyanine aggregates, viologen electron acceptors, and EDTA as a sacrificial agent[172] are the first steps in this direction.

The beneficial properties that arise from J-type brickwork arrangements of the dye molecules in organic solid-state materials have been well recognized, not only for exciton transport but also for hole or electron transport. This is because brickwork arrangements provide not only J-type excitonic coupling with high exciton transfer rates but also two-dimensional percolation pathways for hole and electron charge carriers. For applications of organic semiconductors in thin-film devices, such as in organic field effect transistors, such 2D transport pathways eliminate the severe alignment problems encountered with columnar one-dimensional π stacks.[173] Notably, 2D percolation pathways may also help to reduce the serious problems of charge or exciton trapping in organic semiconductors because a trap site consisting of an impurity or a degraded molecule is not necessarily an insurmountable barrier as in 1D transport systems. From this perspective, it appears quite logical that the natural light-harvesting antennae in chlorosomes contain the quite sensitive bacteriochlorophyll dyes in two-dimensional cylindrical or lamellar arrangements.

Beyond these two fields of application, we see a bright future for J-aggregates in many areas of nanophotonics. Accordingly, J-aggregates could operate in molecular plasmonic devices,[174] where they would feed nanostructures with absorbed light energy or serve as self-assembled optical microcavities.[175] Strong coupling between J-aggregate and microcavity states has already been demonstrated by embedding J-aggregates in an organic light-emitting microcavity device, which is an important step towards polariton lasers or other cavity quantum electrodynamical (QED) devices.[176] Bright prospects for the application of J-aggregates in high-speed optical switching, optical computing, and quantum computing[177] are, therefore, highly justified.

We are deeply indebted to our co-workers and collaboration partners who have diligently contributed to this research, and whose names are mentioned in the respective literature cited herein. Generous financial support by the Deutsche Forschungsgemeinschaft (DFG), Volkswagen-Stiftung, and Alexander von Humboldt-Stiftung are gratefully appreciated. We express their gratitude to PD Dr. Stefan Kirstein for his valuable suggestions and discussions concerning cyanine dye aggregates.

Received: April 19, 2010

[1] a) G. Scheibe, *Angew. Chem.* **1937**, *50*, 51; b) G. Scheibe, L. Kandler, H. Ecker, *Naturwissenschaften* **1937**, *25*, 75; c) G. Scheibe, *Angew. Chem.* **1937**, *50*, 212 – 219; the first report of Scheibe on the absorption spectra of a solution of PIC iodide in water describes the formation of H-aggregates: d) G. Scheibe, *Angew. Chem.* **1936**, *49*, 563.

[2] a) E. E. Jelley, *Nature* **1936**, *138*, 1009 – 1010; b) E. E. Jelley, *Nature* **1937**, *139*, 631 – 632.

[3] It is noteworthy that much earlier Sheppard observed deviations from the Lambert–Beer law in concentration-dependent studies of isocyanine dyes in water: a) S. E. Sheppard, *Proc. R. Soc. London Ser. A* **1909**, *82*, 256 – 270; b) S. E. Sheppard, *Rev. Mod. Phys.* **1942**, *14*, 303 – 340 (see page 312).

[4] a) G. Scheibe, *Kolloid-Z.* **1938**, *82*, 1 – 14; b) for a reinvestigation of the first step of PIC aggregation, that is, the formation of PIC dimers in the concentration range from 10^{-4} to 10^{-3} M, see B. Kopainsky, J. K. Hallermeier, W. Kaiser, *Chem. Phys. Lett.* **1981**, *83*, 498 – 502.

[5] For reviews on cyanine J-aggregates, see a) A. H. Herz, *Adv. Colloid Interface Sci.* **1977**, *8*, 237 – 298; b) D. Möbius, *Adv. Mater.* **1995**, *7*, 437 – 444; c) *J-Aggregates* (Ed.: T. Kobayashi), World Scientific, Singapore, **1996**; d) S. Dähne, *Bunsen-Magazin* **2002**, *4*, 81 – 92; e) V. V. Egorov, *J. Chem. Phys.* **2002**, *116*, 3090 – 3103; f) J. Knoester, *Int. J. Photoenergy* **2006**, *5*, 4; g) S. Kirstein, S. Dähne, *Int. J. Photoenergy* **2006**, *5*, 3; h) B. I. Shapiro, *Russ. Chem. Rev.* **2006**, *75*, 433 – 456; i) V. V. Egorov, M. V. Alfimov, *Phys.-Usp.* **2007**, *50*, 985 – 1029; for the application of cyanine J-aggregates in silver halide photography, see j) *The Theory of Photographic Process* (Ed.: T. J. James), Macmillian, New York, **1977**; k) T. Tani, *Photographic Sensitivity*, Oxford University Press, Oxford, UK, **1995**; l) H. Kuhn, D. Möbius in *Investigations of Surface and Interfaces* (Eds.: B. W. Rossiter, R. C. Baetzold), Wiley, New York, **1993**, pp. 375 – 542.

[6] For a selection of theoretical work on cyanine J-aggregates, see a) H. Fidder, J. Knoester, D. A. Wiersma, *J. Chem. Phys.* **1991**, *95*, 7880 – 7890; b) J. A. Tuszyński, M. F. Jørgensen, D. Möbius, *Phys. Rev. E* **1999**, *59*, 4374 – 4383; c) M. Bednarz, V. A. Malyshev, J. Knoester, *Phys. Rev. Lett.* **2003**, *91*, 217401; d) P. B. Walczak, A. Eisfeld, J. S. Briggs, *J. Chem. Phys.* **2008**, *128*, 044505.

[7] Other publications on cyanine J-aggregates: a) V. Czikkely, H. D. Försterling, H. Kuhn, *Chem. Phys. Lett.* **1970**, *6*, 11 – 14; V. Czikkely, H. D. Försterling, H. Kuhn, *Chem. Phys. Lett.* **1970**, *6*, 207 – 210; b) G. Scheibe, F. Haimerl, W. Hoppe, *Tetrahedron Lett.* **1970**, *11*, 3067 – 3070; c) E. Daltrozzo, G. Scheibe, K. Geschwind, F. Haimerl, *Photogr. Sci. Eng.* **1974**, *18*, 441 – 450; d) A. H. Herz, *Photogr. Sci. Eng.* **1974**, *18*, 323 – 335; e) V. Sundström, T. Gilbro, R. A. Gadonas, A. Piskarskas, *J. Chem. Phys.* **1988**, *89*, 2754 – 2762; f) H. von Berlepsch, C. Böttcher, S. Dähne, *J. Phys. Chem. B* **2000**, *104*, 8792 – 8799; g) H. von Berlepsch, C. Böttcher, *J. Phys. Chem. B* **2002**, *106*, 3146 – 3150; h) I. G. Scheblykin, O. Y. Sliusarenko, L. S. Lepnev, A. G. Vitukhnovsky, M. Van der Auweraer, *J. Phys. Chem. B* **2001**, *105*, 4636 – 4646; i) E. Rousseau, M. M. Koetse, M. Van der Auweraer, *Photochem. Photobiol. Sci.* **2002**, *1*, 395 – 406; j) A. Pawlik, A. Ouart, S. Kirstein, H.-W. Abraham, S. Daehne, *Eur. J. Org. Chem.* **2003**, 3065 – 3080.

[8] a) C. G. Williams, *Trans. R. Soc. Edinburgh* **1856**, *21*, 377 – 401; b) W. Spalteholz, *Ber. Dtsch. Chem. Ges.* **1883**, *16*, 1847 – 1852.

[9] See Ref. [8b], and references cited therein.

[10] A. W. Hofmann, *Proc. R. Soc. London* **1862**, *12*, 410 – 424.

[11] a) N. Tyutyulkov, J. Fabian, A. Mehlhorn, F. Dietz, A. Tadjer, *Polymethine Dyes*, St. Kliment Ohridski University Press, Sofia, **1991**, p. 11; b) R. M. Christie, *Colour Chemistry*, Royal Society of Chemistry, London, **2001**, p. 104; c) H. Zollinger, *Color Chemistry*, 3rd ed., Verlag Helvetica Chimica Acta and Wiley-VCH, Zürich and Weinheim, **2003**, pp. 82 – 84.

[12] a) W. König, *J. Prakt. Chem.* **1906**, *73*, 100 – 108; b) W. König, O. Treichel, *J. Prakt. Chem.* **1921**, *102*, 63 – 74; c) W. König, *Ber. Dtsch. Chem. Ges.* **1922**, *55*, 3293 – 3313, and references therein.

[13] W. König, *J. Prakt. Chem.* **1926**, *112*, 1 – 36.

[14] a) S. Dähne, *Science* **1978**, *199*, 1163 – 1167; b) S. Dähne, *Photogr. Sci. Eng.* **1979**, *23*, 219 – 239.

[15] S. Dähne, D. Leupold, *Angew. Chem.* **1966**, *78*, 1029 – 1039; *Angew. Chem. Int. Ed. Engl.* **1966**, *5*, 984 – 993.

[16] *Chemical Abstracts* also uses the general term cyanine for polymethine.

[17] a) G. Scheibe, L. Kandler, *Naturwissenschaften* **1938**, *24/25*, 412 – 413; b) G. Scheibe, *Z. Elektrochem.* **1948**, *52*, 283 – 292.

[18] G. Scheibe, A. Schöntag, F. Katheder, *Naturwissenschaften* **1939**, *27*, 499 – 501.

[19] a) R. M. Jones, T. S. Bergstedt, C. T. Buscher, D. McBranch, D. G. Whitten, *Langmuir* **2001**, *17*, 2568 – 2571; b) R. M. Jones, L. Lu, R. Helgeson, T. S. Bergstedt, D. W. McBranch, D. G. Whitten, *Proc. Natl. Acad. Sci. USA* **2001**, *98*, 14769 – 14772; c) L. Lu, R. Helgeson, R. M. Jones, D. McBranch, D. G. Whitten, *J. Am. Chem. Soc.* **2002**, *124*, 483 – 488; d) K. E. Achyuthan, T. S. Bergstedt, L. Chen, R. M. Jones, S. Kumaraswamy, S. A. Kushon, K. D. Ley, L. Lu, D. McBranch, H. Mukundan, F. Rininsland, X. Shi, W. Xia, D. G. Whitten, *J. Mater. Chem.* **2005**, *15*, 2648 – 2656; e) D. G. Whitten, K. E. Achyuthan, G. P. Lopez, O.-K. Kim, *Pure Appl. Chem.* **2006**, *78*, 2313 – 2323; f) O.-K. Kim, J. Je, G. Jernigan, L. Buckley, D. Whitten, *J. Am. Chem. Soc.* **2006**, *128*, 510 – 516.

[20] a) C. Fan, S. Wang, J. W. Hong, G. C. Bazan, K. W. Plaxco, A. J. Heeger, *Proc. Natl. Acad. Sci. USA* **2003**, *100*, 6297 – 6301; b) for a recent review on superquenching phenomena in conjugated polymers, see H. Jiang, P. Taranekar, J. R. Reynolds, K. S. Schanze, *Angew. Chem.* **2009**, *121*, 4364 – 4381; *Angew. Chem. Int. Ed.* **2009**, *48*, 4300 – 4316.

[21] T. Förster, *Naturwissenschaften* **1946**, *33*, 166 – 175.

[22] S. F. Mason, *Proc. Chem. Soc.* **1964**, 119.

[23] G. Scheibe, O. Wörz, F. Haimerl, W. Seiffert, J. Winkler, *J. Chim. Phys.* **1968**, *65*, 146 – 151.

[24] a) B. Dammeier, W. Hoppe, *Acta Crystallgr. Sect. B* **1971**, *27*, 2364 – 2370; b) D. L. Smith, *Photogr. Sci. Eng.* **1974**, *18*, 309 – 322.

[25] W. Hoppe, *Kolloid-Z.* **1942**, *101*, 300 – 305.

[26] a) F. Hofmeister, *Arch. Exp. Pharmacol.* **1888**, *24*, 247 – 260; b) R. L. Baldwin, *Biophys. J.* **1996**, *71*, 2056 – 2063; c) Y. Zhang, P. S. Cremer, *Curr. Opin. Chem. Biol.* **2006**, *10*, 658 – 663; for a recent review on the Hoffmeister effect, see d) W. Kunz, P. Lo Nostro, B. W. Ninham, *Curr. Opin. Colloid Interface Sci.* **2004**, *9*, 1 – 18.

[27] a) E. G. McRae, M. Kasha, *J. Chem. Phys.* **1958**, *28*, 721 – 722; b) M. Kasha, R. Rawls, M. A. El-Bayoumi, *Pure Appl. Chem.* **1965**, *11*, 371 – 392.

[28] Note, Kasha's exciton theory is based on ideas of Kautsky, Förster, and others: a) H. Kautsky, H. Merkel, *Naturwissen-*

schaften **1939**, *27*, 195 – 196; b) G. N. Lewis, M. Kasha, *J. Am. Chem. Soc.* **1944**, *66*, 2100 – 2116; c) T. Förster, *Naturwissenschaften* **1949**, *36*, 240 – 245; d) G. L. Levinson, W. T. Simpson, W. Curtis, *J. Am. Chem. Soc.* **1957**, *79*, 4314 – 4320; e) E. G. McRae, M. Kasha, *J. Am. Chem. Soc.* **1958**, *80*, 721 – 722, and Ref. [21].

[29] a) K. Norland, A. Ames, T. Taylor, *Photogr. Sci. Eng.* **1970**, *14*, 295 – 307; b) S. Kirstein, H. Möhwald, *Adv. Mater.* **1995**, *7*, 460 – 463.

[30] W. Cooper, *Chem. Phys. Lett.* **1970**, *7*, 73 – 77.

[31] E. S. Emerson, M. A. Conlin, A. E. Rosenoff, K. S. Norland, H. Rodriguez, D. Chin, G. R. Bird, *J. Phys. Chem.* **1967**, *71*, 2396 – 2403.

[32] H. Bücher, H. Kuhn, *Chem. Phys. Lett.* **1970**, *6*, 183 – 185.

[33] H. Nolte, *J. Chem. Phys. Lett.* **1975**, *31*, 134 – 139.

[34] A. P. Marchetti, C. D. Salzberg, E. I. P. Walker, *Photogr. Sci. Eng.* **1976**, *20*, 107 – 111.

[35] For further publications on the crystal structures of PIC, see Ref. [7b] and L. Dähne, G. Reck, *Z. Kristallogr.* **1995**, *210*, 40 – 43.

[36] K. Misawa, H. Ono, K. Minoshima, T. Kobayashi, *Appl. Phys. Lett.* **1993**, *63*, 577 – 579.

[37] a) T. Kobayashi, K. Misawa, *J. Lumin.* **1997**, *72–74*, 38 – 40; b) T. Kobayashi, *Mol. Cryst. Liq. Cryst.* **1998**, *314*, 1 – 11.

[38] H. Stegemeyer, F. Stöckel, *Ber. Bunsen-Ges.* **1996**, *100*, 9 – 14.

[39] H. Rehage, G. Platz, B. Struller, C. Thunig, *Tenside Surfactants Deterg.* **1996**, *33*, 242 – 248.

[40] B. Herzog, K. Huber, H. Stegemeyer, *Langmuir* **2003**, *19*, 5223 – 5232.

[41] H. von Berlepsch, S. Möller, L. Dähne, *J. Phys. Chem. B* **2001**, *105*, 5689 – 5699.

[42] a) M. Vacha, M. Saeki, O. Isobe, K.-i. Hashizume, T. Tani, *J. Chem. Phys.* **2001**, *115*, 4973 – 4976; b) M. Vacha, M. Saeki, M. Furuki, L. S. Pu, K.-i Hashizume, T. Tani, *J. Lumin.* **2002**, *98*, 35 – 40.

[43] a) P. J. Hillson, R. B. McKay, *Trans. Faraday Soc.* **1965**, *61*, 374 – 382; b) R. B. McKay, *Trans. Faraday Soc.* **1965**, *61*, 1787 – 1799.

[44] V. Czikkely, G. Dreizler, H. D. Försterling, H. Kuhn, P. Sondermann, P. Tillmann, J. Wiegand, *Z. Naturforsch. A* **1969**, *24*, 1821 – 1830.

[45] E. W. Knapp, *Chem. Phys.* **1984**, *85*, 73 – 82.

[46] H. Fidder, J. Terpstra, D. A. Wiersma, *J. Chem. Phys.* **1991**, *94*, 6895 – 6907.

[47] J. Knoester, *J. Chem. Phys.* **1993**, *99*, 8466 – 8479.

[48] J. R. Durrant, J. Knoester, D. A. Wiersma, *Chem. Phys. Lett.* **1994**, *222*, 450 – 456.

[49] D. A. Higgins, P. F. Barbara, *J. Phys. Chem.* **1995**, *99*, 3 – 7.

[50] T. Kobayashi, N. Fukutake, *Chem. Phys. Lett.* **2002**, *356*, 368 – 374.

[51] T. Tani, M. Oda, T. Hayashi, H. Ohno, K. Hirata, *J. Lumin.* **2007**, *122–123*, 244 – 246.

[52] E. Lang, A. Sorokin, M. Drechsler, Y. V. Malyukin, J. Köhler, *Nano Lett.* **2005**, *5*, 2635 – 2640.

[53] Y. Kitahama, T. Yoga, A. Furube, R. Katoh, *Chem. Phys. Lett.* **2008**, *457*, 427 – 433.

[54] T. F. A. De Greef, M. M. J. Smulders, M. Wolffs, A. P. H. J. Schenning, R. P. Sijbesma, E. W. Meijer, *Chem. Rev.* **2009**, *109*, 5687 – 5754.

[55] a) F. Rotermund, R. Weigand, A. Penzkofer, *Chem. Phys.* **1997**, *220*, 385 – 392; b) A. Lohr, M. Lysetska, F. Würthner, *Angew. Chem.* **2005**, *117*, 5199 – 5202; *Angew. Chem. Int. Ed.* **2005**, *44*, 5071 – 5074.

[56] W. West, S. Pearce, *J. Phys. Chem.* **1965**, *69*, 1894 – 1903.

[57] H. Ecker, *Kolloid-Z.* **1940**, *92*, 35 – 70.

[58] G. Scheibe, A. Mareis, H. Ecker, *Naturwissenschaften* **1937**, *25*, 474 – 475.

[59] O. Wörz, G. Scheibe, *Z. Naturforsch. B* **1969**, *24*, 381 – 390.

[60] L. G. S. Brooker, F. L. White, D. W. Heseltine, S. H. Keyes, S. G. Dent, E. J. van Lare, *J. Photogr. Sci.* **1953**, *1*, 173 – 183.

[61] For reviews on cyanine dyes, see Ref. [11a] and a) F. Dietz, *J. Signalaufzeichnungsmater.* **1973**, *1*, 157 – 180; F. Dietz, *J. Signalaufzeichnungsmater.* **1973**, *1*, 237 – 252; F. Dietz, *J. Signalaufzeichnungsmater.* **1973**, *1*, 381 – 382; b) Z. Zhu, *Dyes Pigm.* **1995**, *27*, 77 – 111; c) C. Reichardt, *J. Phys. Org. Chem.* **1995**, *8*, 761 – 773; d) A. Mishra, R. K. Behera, P. K. Behera, B. K. Mishra, G. B. Behera, *Chem. Rev.* **2000**, *100*, 1973 – 2011; e) B. A. Armitage, *Top. Curr. Chem.* **2005**, *253*, 55 – 76.

[62] This procedure, however, is subject to considerable errors, as pointed out by Makio et al., who deduced an association number of eight by similar experiments: S. Makio, N. Kanamaru, J. Tanaka, *Bull. Chem. Soc. Jpn.* **1980**, *53*, 3120 – 3124.

[63] a) J. Moll, S. Dähne, J. R. Durrant, D. A. Wiersma, *J. Chem. Phys.* **1995**, *102*, 6362 – 6370; b) M. van Burgel, D. A. Wiersma, K. Duppen, *J. Chem. Phys.* **1995**, *102*, 20 – 33.

[64] B. Birkan, D. Gülen, S. Özcelik, *J. Phys. Chem. B* **2006**, *110*, 10805 – 10813.

[65] a) H. Hada, C. Honda, H. Tanemura, *Photogr. Sci. Eng.* **1977**, *21*, 83 – 91; b) C. Honda, H. Hada, *Photogr. Sci. Eng.* **1977**, *21*, 91 – 102.

[66] M. A. Drobizhev, M. N. Sapozhnikov, I. G. Scheblykin, O. P. Varnavsky, M. Van der Auweraer, A. G. Vitukhnovsky, *Chem. Phys.* **1996**, *211*, 455 – 468.

[67] a) I. G. Scheblykin, M. A. Drobizhev, O. P. Varnavsky, M. Van der Auweraer, A. G. Vitukhnovsky, *Chem. Phys. Lett.* **1996**, *261*, 181 – 190; b) M. A. Drobizhev, M. N. Sapozhnikov, I. G. Scheblykin, O. P. Varnavsky, M. Van der Auweraer, A. G. Vitukhnovsky, *Pure Appl. Opt.* **1996**, *5*, 569 – 581.

[68] D. M. Basko, A. N. Lobanov, A. V. Pimenov, A. G. Vitukhnovsky, *Chem. Phys. Lett.* **2003**, *369*, 192 – 197.

[69] a) I. G. Scheblykin, O. P. Varnavsky, W. Verbouwe, S. De Backer, M. Van der Auweraer, A. G. Vitukhnovsky, *Chem. Phys. Lett.* **1998**, *282*, 250 – 256; b) I. G. Scheblykin, O. P. Varnavsky, M. M. Bataiev, O. Y. Silusarrenko, M. Van der Auweraer, A. G. Vitukhnovsky, *Chem. Phys. Lett.* **1998**, *298*, 341 – 350; c) I. G. Scheblykin, O. Y. Silusarrenko, S. L. Lepnev, A. G. Vitukhnovsky, M. Van der Auweraer, *J. Phys. Chem. B* **2000**, *104*, 10949 – 10951.

[70] I. G. Scheblykin, M. M. Bataiev, M. Van der Auweraer, A. G. Vitukhnovsky, *Chem. Phys. Lett.* **2000**, *316*, 37 – 44.

[71] E. O. Potma, D. A. Wiersma, *J. Chem. Phys.* **1998**, *108*, 4894 – 4903.

[72] For a detailed discussion of these models, see Ref. [7h].

[73] H. von Berlepsch, C. Böttcher, A. Ouart, C. Burger, S. Dähne, S. Kirstein, *J. Phys. Chem. B* **2000**, *104*, 5255 – 5262.

[74] C. Didraga, A. Pugzlys, P. R. Hania, H. von Berlepsch, K. Duppen, J. Knoester, *J. Phys. Chem. B* **2004**, *108*, 14976 – 14985.

[75] a) J. L. Lyon, D. M. Eisele, S. Kirstein, J. P. Rabe, D. A. Vanden Bout, K. J. Stevenson, *J. Phys. Chem. C* **2008**, *112*, 1260 – 1268; b) D. M. Eisele, J. Knoester, S. Kirstein, J. P. Rabe, D. A. Vanden Bout, *Nat. Nanotechnol.* **2009**, *4*, 658 – 663.

[76] H. von Berlepsch, S. Kirstein, C. Böttcher, *Langmuir* **2002**, *18*, 7699 – 7705.

[77] a) H. von Berlepsch, S. Kirstein, R. Hania, C. Didraga, A. Pugzlys, C. Böttcher, *J. Phys. Chem. B* **2003**, *107*, 14176 – 14184; b) S. S. Lampoura, C. Spitz, S. Daehne, J. Knoester, K. Duppen, *J. Phys. Chem. B* **2002**, *106*, 3103 – 3111.

[78] a) U. De Rossi, S. Dähne, S. C. J. Meskers, H. P. J. M. Dekkers, *Angew. Chem.* **1996**, *108*, 827 – 830; *Angew. Chem. Int. Ed. Engl.* **1996**, *35*, 760 – 763; b) A. Pawlik, S. Kirstein, U. De Rossi, S. Daehne, *J. Phys. Chem. B* **1997**, *101*, 5646 – 5651; c) S. Kirstein, H. von Berlepsch, C. Böttcher, C. Burger, A. Ouart, G. Reck, S. Dähne, *ChemPhysChem* **2000**, *1*, 146 – 150.

[79] a) H. von Berlepsch, C. Böttcher, A. Ouart, M. Regenbrecht, S. Akari, U. Keiderling, H. Schnablegger, S. Dähne, S. Kirstein,

Langmuir **2000**, *16*, 5908 – 5916; b) H. von Berlepsch, M. Regenbrecht, S. Dähne, S. Kirstein, C. Böttcher, *Langmuir* **2002**, *18*, 2901 – 2907.
[80] H. von Berlepsch, S. Kirstein, C. Böttcher, *J. Phys. Chem. B* **2003**, *107*, 9646 – 9654.
[81] K. C. Hannah, B. A. Armitage, *Acc. Chem. Res.* **2004**, *37*, 845 – 853.
[82] a) L. Stryer, E. R. Blout, *J. Am. Chem. Soc.* **1961**, *83*, 1411 – 1418; b) R. F. Pasternack, A. Giannetto, P. Pagano, E. Gibbs, *J. Am. Chem. Soc.* **1991**, *113*, 7799 – 7800; c) Y. Zhang, J. Xiang, Y. Tang, G. Xu, W. Yan, *ChemPhysChem* **2007**, *8*, 224 – 226.
[83] P.-A. Bouit, D. Rauh, S. Neugebauer, J. L. Delgado, E. Di Piazza, S. Rigaut, O. Maury, C. Andraud, V. Dyakonov, N. Martin, *Org. Lett.* **2009**, *11*, 4806 – 4809.
[84] a) N. M. Kronenberg, M. Deppisch, F. Würthner, H. W. A. Lademann, K. Deing, K. Meerholz, *Chem. Commun.* **2008**, 6489 – 6491; b) H. Bürckstümmer, N. M. Kronenberg, M. Gsänger, M. Stolte, K. Meerholz, F. Würthner, *J. Mater. Chem.* **2010**, *20*, 240 – 243; c) U. Mayerhöffer, K. Deing, K. Gruß, H. Braunschweig, K. Meerholz, F. Würthner, *Angew. Chem.* **2009**, *121*, 8934 – 8937; *Angew. Chem. Int. Ed.* **2009**, *48*, 8776 – 8779; d) F. Silvestri, M. D. Irwin, L. Beverina, A. Facchetti, G. A. Pagani, T. J. Marks, *J. Am. Chem. Soc.* **2008**, *130*, 17640 – 17641; e) F. Würthner, K. Meerholz, *Chem. Eur. J.* **2010**, *16*, 9366 – 9373; f) G. Wie, S. Wang, K. Renshaw, M. E. Thompson, S. R. Forrest, *ACS Nano* **2010**, *4*, 1927 – 1934.
[85] a) V. Z. Shirinian, A. A. Shimkin, *Top. Heterocycl. Chem.* **2008**, *14*, 75 – 105; b) F. Würthner, R. Wortmann, K. Meerholz, *ChemPhysChem* **2002**, *3*, 17 – 31.
[86] For a recent review on merocyanine J-aggregates in Langmuir–Blodgett films, see S.-i. Kuroda, *Adv. Colloid Interface Sci.* **2004**, *111*, 181 – 209.
[87] a) F. Würthner, S. Yao, *Angew. Chem.* **2000**, *112*, 2054 – 2057; *Angew. Chem. Int. Ed.* **2000**, *39*, 1978 – 1981; b) F. Würthner, S. Yao, T. Debaerdemaeker, R. Wortmann, *J. Am. Chem. Soc.* **2002**, *124*, 9431 – 9447; c) U. Rösch, S. Yao, R. Wortmann, F. Würthner, *Angew. Chem.* **2006**, *118*, 7184 – 7188; *Angew. Chem. Int. Ed.* **2006**, *45*, 7026 – 7030.
[88] a) For a general review on dye aggregates including merocyanines, see Z. Chen, A. Lohr, C. R. Saha-Möller, F. Würthner, *Chem. Soc. Rev.* **2009**, *38*, 564 – 584; b) for a review on DFT calculations for dimeric π stacks including merocyanine dimers, see S. Grimme, J. Antony, T. Schwabe, C. Mück-Lichtenfeld, *Org. Biomol. Chem.* **2007**, *5*, 741 – 758.
[89] F. Würthner, C. W. Lehmann, E. Duman, unpublished crystallographic data.
[90] F. Würthner, *Synthesis* **1999**, 2103 – 2113.
[91] F. Mizutani, S.-i. Iijima, K. Tsuda, *Bull. Chem. Soc. Jpn.* **1982**, *55*, 1295 – 1299.
[92] a) E. Langhals, H. Balli, *Helv. Chim. Acta* **1985**, *68*, 1782 – 1797; b) M. Kussler, H. Balli, *Helv. Chim. Acta* **1987**, *70*, 1583 – 1595; c) M. Kussler, H. Balli, *Helv. Chim. Acta* **1989**, *72*, 17 – 28; d) M. Kussler, H. Balli, *Helv. Chim. Acta* **1989**, *72*, 295 – 306; e) M. Kussler, H. Balli, *Helv. Chim. Acta* **1989**, *72*, 638 – 647.
[93] Y. Kalisky, D. J. Williams, *Chem. Phys. Lett.* **1982**, *86*, 100 – 104.
[94] S. Yagai, H. Higashi, T. Karatsu, A. Kitamura, *Chem. Mater.* **2005**, *17*, 4392 – 4398.
[95] For recent reviews on squaraines, see a) S. Yagi, H. Nakazumi, *Top. Heterocycl. Chem.* **2008**, *14*, 133 – 181; b) S. Sreejith, P. Carol, P. Chithra, A. Ajayaghosh, *J. Mater. Chem.* **2008**, *18*, 264 – 274.
[96] a) A. Treibs, K. Jacob, *Angew. Chem.* **1965**, *77*, 680 – 681; *Angew. Chem. Int. Ed. Engl.* **1965**, *4*, 694 – 694; b) W. Ziegenbein, H.-E. Sprenger, *Angew. Chem.* **1966**, *78*, 937 – 937; *Angew. Chem. Int. Ed. Engl.* **1966**, *5*, 893 – 894; c) H.-E. Sprenger, W. Ziegenbein, *Angew. Chem.* **1966**, *78*, 937 – 938; *Angew. Chem. Int. Ed. Engl.* **1966**, *5*, 894 – 894.
[97] For publications on J-aggregating squaraine dyes in films, see a) K. Liang, K.-Y. Law, D. G. Whitten, *J. Phys. Chem.* **1994**, *98*, 13379 – 13384; b) H. Chen, K.-Y. Law, D. G. Whitten, *J. Phys. Chem.* **1996**, *100*, 5949 – 5955; c) J.-r. Li, B.-f. Li, X.-c. Li, J. Tang, L. Jiang, *Thin Solid Films* **1996**, *287*, 247 – 251; d) M. Stanescu, H. Samha, J. Perlstein, D. G. Whitten, *Langmuir* **2000**, *16*, 275 – 281; e) O. P. Dimitriev, A. P. Dimitriyeva, A. I. Tolmachev, V. V. Kurdyukov, *J. Phys. Chem. B* **2005**, *109*, 4561 – 4567.
[98] S. Das, T. L. Thanulingam, K. G. Thomas, P. V. Kamat, M. V. George, *J. Phys. Chem.* **1993**, *97*, 13620 – 13624.
[99] S. Alex, M. C. Basheer, K. T. Arun, D. Ramaiah, S. Das, *J. Phys. Chem. A* **2007**, *111*, 3226 – 3230.
[100] J. Wojtyk, A. McKerrow, P. Kazmaier, E. Buncel, *Can. J. Chem.* **1999**, *77*, 903 – 912.
[101] R. S. Stoll, N. Severin, J. P. Rabe, S. Hecht, *Adv. Mater.* **2006**, *18*, 1271 – 1275.
[102] H. Scheer in *Chlorophylls* (Ed.: H. Scheer), CRC, Boca Raton, US, **1991**, pp. 3 – 30.
[103] K. M. Smith, *Photosynth. Res.* **1994**, *41*, 23 – 26.
[104] G. McDermott, S. M. Prince, A. A. Freer, A. M. Hawthornthwaite-Lawless, M. Z. Papiz, R. J. Cogdell, N. W. Isaacs, *Nature* **1995**, *374*, 517 – 521.
[105] J. Koepke, X. Hu, C. Muenke, K. Schulten, H. Michel, *Structure* **1996**, *4*, 581 – 597.
[106] a) X. Hu, K. Schulten, *Phys. Today* **1997**, *50*, 28 – 34; b) X. Hu, A. Damjanovic, T. Ritz, K. Schulten, *Proc. Natl. Acad. Sci. USA* **1998**, *95*, 5935 – 5941.
[107] a) T. Pullerits, V. Sundström, *Acc. Chem. Res.* **1996**, *29*, 381 – 389; b) R. J. Cogdell, A. Gall, J. Köhler, *Q. Rev. Biophys.* **2006**, *39*, 227 – 324.
[108] S. Scheuring, J. N. Sturgis, V. Prima, A. Bernadac, D. Lévy, J.-L. Rigaud, *Proc. Natl. Acad. Sci. USA* **2004**, *101*, 11293 – 11297.
[109] a) A. Satake, Y. Kobuke, *Tetrahedron* **2005**, *61*, 13 – 41; b) C.-C. You, R. Dobrawa, C. R. Saha-Möller, F. Würthner, *Top. Curr. Chem.* **2005**, *258*, 39 – 82; c) J. A. A. W. Elemans, R. Van Hameren, R. J. M. Nolte, A. E. Rowan, *Adv. Mater.* **2006**, *18*, 1251 – 1266; d) Y. Nakamura, N. Aratani, A. Osuka, *Chem. Soc. Rev.* **2007**, *36*, 831 – 845; e) N. Aratani, D. Kim, A. Osuka, *Acc. Chem. Res.* **2009**, *42*, 1922 – 1934.
[110] a) M. I. Bystrova, I. N. Mal'gosheva, A. A. Krasnovskii, *Mol. Biol.* **1979**, *13*, 440 – 451; b) K. M. Smith, L. A. Kehren, J. Fajer, *J. Am. Chem. Soc.* **1983**, *105*, 1387 – 1389; c) J. R. Golecki, J. Oelze, *Arch. Microbiol.* **1987**, *148*, 236 – 241; d) K. Griebenow, A. R. Holzwarth, *Biochem. Biophys. Acta* **1989**, *973*, 235 – 240; e) A. R. Holzwarth, K. Griebenow, K. Schaffer, *Z. Naturforsch.* **1990**, *45*, 203 – 206; f) A. Martinez-Planells, J. B. Arellano, C. M. Borrego, C. López-Iglesias, F. Gich, J. Garcia-Gil, *Photosynth. Res.* **2002**, *71*, 83 – 90; g) G. A. Montaño, B. P. Bowen, J. T. LaBelle, N. W. Woodbury, V. B. Pizziconi, R. E. Blankenship, *Biophys. J.* **2003**, *85*, 2560 – 2565.
[111] a) H. Tamiaki, A. R. Holzwarth, K. Schaffner, *J. Photochem. Photobiol. B* **1992**, *15*, 355 – 360; b) P. Hildebrandt, H. Tamiaki, A. R. Holzwarth, K. Schaffner, *J. Phys. Chem. B* **1994**, *98*, 2191 – 2197; c) H. Tamiaki, M. Amakawa, Y. Shimono, R. Tanikaga, A. R. Holzwarth, K. Schaffner, *Photochem. Photobiol.* **1996**, *63*, 92 – 99; d) "Supramolecular Dye Chemistry" T. S. Balaban, H. Tamiaki, A. R. Holzwarth in, *Topics in Current Chemistry*, *Vol. 158* (Ed.: F. Würthner), Springer, Heidelberg, **2005**, pp. 1 – 38; e) T. S. Balaban, *Acc. Chem. Res.* **2005**, *38*, 612 – 623; f) R. G. Feick, R. C. Fuller, *Biochemistry* **1984**, *23*, 3693 – 3700; g) D. L. Worcester, T. J. Michalski, J. J. Katz, *Proc. Natl. Acad. Sci. USA* **1986**, *83*, 3791 – 3795; h) D. C. Brune, G. H. King, R. E. Blankenship in *Photosynthetic Light-Harvesting Systems* (Eds.: H. Scheer, S. Schneider), Walter de Gruyter, Berlin, **1988**, p. 141; i) T. Nozawa, K. Ohtomo, M. Suzuki, H. Nakagawa, Y. Shikama, H. Konami, Z.-Y. Wang,

Photosynth. Res. **1994**, *41*, 211 – 223; j) J. M. Linnanto, J. E. I. Tommola, *Photosynth. Res.* **2008**, *96*, 227 – 245.

[112] a) A. R. Holzwarth, K. Schaffner, *Photosynth. Res.* **1994**, *41*, 225 – 233; b) V. I. Prokhorenko, D. B. Steensgard, A. R. Holzwarth, *Biophys. J.* **2000**, *79*, 2105 – 2120; c) S. Savikhin, Y. Zhu, R. E. Blankenship, W. S. Struve, *J. Phys. Chem.* **1996**, *100*, 3320 – 3322; d) T. Miyatake, H. Tamiaki, *J. Photochem. Photobiol. C* **2005**, *6*, 89 – 107; e) T. Miyatake, S. Tanigawa, S. Kato, H. Tamiaki, *Tetrahedron Lett.* **2007**, *48*, 2251 – 2254.

[113] a) J. Pšenčik, T. P. Ikonen, P. Laurinmäki, M. C. Merckel, S. J. Butcher, R. E. Serimaa, R. Tuma, *Biophys. J.* **2004**, *87*, 1165 – 1172; b) J. Psencik, J. B. Arellano, T. P. Ikonen, C. M. Borrego, P. A. Laurinmaki, S. J. Butcher, R. E. Serimaa, R. Tuma, *Biophys. J.* **2004**, *91*, 1433 – 1440; c) G. T. Oostergetel, M. Reus, A. G. M. Chew, D. A. Bryant, E. J. Boekema, A. R. Holzwarth, *FEBS Lett.* **2007**, *581*, 5435 – 5439; d) S. Ganapathy, G. T. Oostergetel, P. K. Wawrzyniak, M. Reus, A. G. M. Chew, F. Buda, E. J. Boekema, D. A. Bryant, A. R. Holzwarth, H. J. M. de Groot, *Proc. Natl. Acad. Sci. USA* **2009**, *106*, 8525 – 8530.

[114] V. I. Prokhorenko, A. R. Holzwarth, M. G. Müller, K. Schaffner, T. Miyatake, H. Tamiaki, *J. Phys. Chem. B* **2002**, *106*, 5761 – 5768.

[115] K. M. Smith, D. A. Goff, D. S. Simpson, *J. Am. Chem. Soc.* **1985**, *107*, 4946 – 4954.

[116] a) T. S. Balaban, J. Leitich, A. R. Holzwarth, K. Schaffner, *J. Phys. Chem. B* **2000**, *104*, 1362 – 1372; b) T. S. Balaban, A. D. Bhise, M. Fischer, M. Linke-Schaetzel, C. Roussel, N. Vanthuyne, *Angew. Chem.* **2003**, *115*, 2190 – 2194; *Angew. Chem. Int. Ed.* **2003**, *42*, 2140 – 2144.

[117] a) V. Huber, M. Katterle, M. Lysetska, F. Würthner, *Angew. Chem.* **2005**, *117*, 3208 – 3212; *Angew. Chem. Int. Ed.* **2005**, *44*, 3147 – 3151; b) V. Huber, S. Sengupta, F. Würthner, *Chem. Eur. J.* **2008**, *14*, 7791 – 7807; c) V. Huber, M. Lysetska, F. Würthner, *Small* **2007**, *3*, 1007 – 1014.

[118] a) S. G. Sprague, L. A. Staehelin, M. L. DiBartolomeis, R. C. Fuller, *J. Bacteriol.* **1981**, *147*, 1021 – 1031; b) Y. Miloslavina, A. Wehner, P. H. Lambrev, E. Wientjes, M. Reus, G. Garab, R. Croce, A. R. Holzwarth, *FEBS Lett.* **2008**, *582*, 3625 – 3631.

[119] S. Ganapathy, S. Sengupta, P. K. Wawrzyniak, V. Huber, F. Buda, U. Baumeister, F. Würthner, H. J. M. de Groot, *Proc. Natl. Acad. Sci. USA* **2009**, *106*, 11472 – 11477.

[120] a) C. Röger, M. G. Müller, M. Lysetska, Y. Miloslavina, A. R. Holzwarth, F. Würthner, *J. Am. Chem. Soc.* **2006**, *128*, 6542 – 6543; b) C. Röger, Y. Miloslavina, D. Brunner, A. R. Holzwarth, F. Würthner, *J. Am. Chem. Soc.* **2008**, *130*, 5929 – 5939.

[121] a) X.-F. Wang, O. Kitao, H. Zhou, H. Tamiaki, S. Sasaki, *Chem. Commun.* **2009**, 1523 – 1525; b) X.-F. Wang, O. Kitao, H. Zhou, H. Tamiaki, S. Sasaki, *J. Phys. Chem. C* **2009**, *113*, 7954 – 7961.

[122] a) Y. Kobuke, H. Miyaji, *J. Am. Chem. Soc.* **1994**, *116*, 4111 – 4112; b) A. Satake, Y. Kobuke, *Org. Biomol. Chem.* **2007**, *5*, 1679 – 1691; c) for supramolecular mimicry of the BChl *c* arrangements in green bacteria, see Ref. [111e] and T. S. Balaban, M. Linke-Schaetzel, A. D. Bhise, N. Vanthuyne, C. Roussel, C. E. Anson, G. Buth, A. Eichhofer, K. Foster, G. Garab, H. Gliemann, R. Goddard, T. Javorfi, A. K. Powell, H. Rosner, T. Schimmel, *Chem. Eur. J.* **2005**, *11*, 2267 – 2275.

[123] a) I. W. Hwang, M. Park, T. K. Ahn, Z. S. Yoon, D. M. Ko, D. Kim, F. Ito, Y. Ishibashi, S. R. Khan, Y. Nagasawa, H. Miyasaka, C. Keda, R. Takahashi, K. Ogawa, A. Satake, Y. Kobuke, *Chem. Eur. J.* **2005**, *11*, 3753 – 3761; b) F. Hajjaj, Z. S. Yoon, M. C. Yoon, J. Park, A. Satake, D. Kim, Y. Kobuke, *J. Am. Chem. Soc.* **2006**, *128*, 4612 – 4623.

[124] C. A. Hunter, *Chem. Soc. Rev.* **1994**, *23*, 101 – 109.

[125] E. B. Fleischer, J. M. Palmer, T. S. Srivastava, A. Chatterjee, *J. Am. Chem. Soc.* **1971**, *93*, 3162 – 3167.

[126] a) O. Ohno, Y. Kaizu, H. Kobayashi, *J. Chem. Phys.* **1993**, *99*, 4128 – 4139; b) D. L. Akins, H.-R. Zhu, C. Guo, *J. Phys. Chem.* **1994**, *98*, 3612 – 3618; c) it is noteworthy that the B- and Q-transitions of **44b** are, similar to those for metalloporphyrins, degenerate and polarized orthogonally. Upon aggregation, however, the degeneracy is lifted and different slipping angle dependencies arise for the transitions polarized parallel and orthogonal to the aggregate axis.

[127] L. P. F. Aggarwal, I. E. Borissevitch, *Spectrochim. Acta Part A* **2006**, *63*, 227 – 233.

[128] a) J. M. Ribo, J. Crusats, F. Sague, J. Claret, R. Rubires, *Science* **2001**, *292*, 2063 – 2066; b) R. Rubires, J.-A. Farrera, J. M. Ribó, *Chem. Eur. J.* **2001**, *7*, 436 – 446.

[129] A. S. R. Koti, J. Taneja, N. Periasamy, *Chem. Phys. Lett.* **2003**, *375*, 171 – 176.

[130] V. Gulbinas, R. Karpicz, R. Augulis, R. Rotomskis, *Chem. Phys.* **2007**, *332*, 255 – 261.

[131] H. Kano, T. Saito, T. Kobayashi, *J. Phys. Chem. B* **2001**, *105*, 413 – 419.

[132] A. D. Schwab, D. E. Smith, C. S. Rich, E. R. Young, W. F. Smith, J. C. de Paula, *J. Phys. Chem. B* **2003**, *107*, 11339 – 11345.

[133] K. Hosomizu, M. Oodoi, T. Umeyama, Y. Matano, K. Yoshida, S. Isoda, M. Isosomppi, N. V. Tkachenko, H. Lemmetyinen, H. Imahori, *J. Phys. Chem. B* **2008**, *112*, 16517 – 16524.

[134] Z. Wang, C. J. Medforth, J. A. Shelnutt, *J. Am. Chem. Soc.* **2004**, *126*, 15954 – 15955.

[135] T. Yamaguchi, T. Kimura, H. Matsuda, T. Aida, *Angew. Chem.* **2004**, *116*, 6510 – 6515; *Angew. Chem. Int. Ed.* **2004**, *43*, 6350 – 6355.

[136] a) *Phthalocyanines—Properties and Applications*, *Vol. 1–4* (Eds.: C. C. Leznoff, A. B. P. Lever), VCH, New York, **1989**; b) A. W. Snow, in *The Porphyrin Handbook*, *Vol. 17* (Eds.: K. Kadish, K. M. Smith, R. Guillard), Academic Press, New York, **2003**, pp. 129 – 176.

[137] H. Isago, *Chem. Commun.* **2003**, 1864 – 1865.

[138] a) K. Kameyama, M. Morisue, A. Satake, Y. Kobuke, *Angew. Chem.* **2005**, *117*, 4841 – 4844; *Angew. Chem. Int. Ed.* **2005**, *44*, 4763 – 4766; b) F. Cong, J. Li, C. Ma, J. Gao, W. Duan, X. Du, *Spectrochim. Acta Part A* **2008**, *71*, 1397 – 1401.

[139] a) W. Herbst, K. Hunger, *Industrial Organic Pigments*, 2nd ed., VCH, Weinheim, **1997**; b) *High Performance Pigments*, 2nd ed. (Eds.: E. B. Faulkner, R. J. Schwartz), Wiley-VCH, Weinheim, **2009**; c) P. Erk, H. Hengelsberg in *Handbook of Porphyrins and Phthalocyanines*, *Vol. 19*, (Eds.: K. Kadish, R. Guillard, K. M. Smith), Elsevier, Amsterdam, **2003**.

[140] K. Y. Law, *Chem. Rev.* **1993**, *93*, 449 – 486.

[141] a) W. Hiller, J. Strähle, W. Kobel, M. Hanack, *Z. Kristallogr.* **1982**, *159*, 173 – 118; b) K. Oka, O. Okada, K. Nukada, *Jpn. J. Appl. Phys.* **1992**, *31*, 2181 – 2184.

[142] J. Mizuguchi, H. Yamakami, Y. Kojima, C. Sasaki, Y. Osano, *J. Imaging Sci. Technol.* **2003**, *47*, 25 – 29.

[143] For a general review on perylene bisimides, see F. Würthner, *Chem. Commun.* **2004**, 1564 – 1579.

[144] a) F. Graser, E. Hädicke, *Liebigs Ann. Chem.* **1984**, 483 – 494; b) P. M. Kazmaier, R. J. Hoffmann, *J. Am. Chem. Soc.* **1994**, *116*, 9684 – 9691; c) H.-M. Zhao, J. Pfister, V. Settels, M. Renz, M. Kaupp, V. C. Dehm, F. Würthner, R. F. Fink, B. Engels, *J. Am. Chem. Soc.* **2009**, *131*, 15660 – 15668.

[145] V. Dehm, F. Würthner, unpublished results.

[146] a) The solid-state fluorescence properties of swallow-tail PBIs, for example, **47a**,**b**, were already recognized: L. Langhals, S. Demmig, T. Potrawa, *J. Prakt. Chem.* **1991**, *333*, 733-748; b) for morphological studies on related molecules to **47a**,**b**, see A. Wicklein, A. Lang, M. Muth, M. Thelakkat, *J. Am. Chem. Soc.* **2009**, *131*, 14442 – 14453.

[147] Z. Chen, V. Stepanenko, V. Dehm, P. Prins, L. D. A. Siebbeles, J. Seibt, P. Marquetand, V. Engel, F. Würthner, *Chem. Eur. J.* **2007**, *13*, 436 – 449.
[148] R. Fink, J. Seibt, V. Engel, M. Renz, M. Kaupp, S. Lochbrunner, H.-M. Zhao, J. Pfister, F. Würthner, B. Engels, *J. Am. Chem. Soc.* **2008**, *130*, 12858 – 12859.
[149] F. Würthner, C. Thalacker, S. Diele, C. Tschierske, *Chem. Eur. J.* **2001**, *7*, 2245 – 2253.
[150] Evidence for J-aggregating PBI molecules in a lyotropic liquid-crystalline phase was reported earlier: L. B.-Å. Johansson, H. Langhals, *Spectrochim. Acta Part A* **1991**, *47*, 857 – 861.
[151] a) A. Eisfeld, J. S. Briggs, *Chem. Phys. Lett.* **2007**, *446*, 354 – 358; b) A. Eisfeld, J. S. Briggs, *Phys. Rev. Lett.* **2006**, *96*, 113003; c) A. Eisfeld, J. S. Briggs, *Chem. Phys.* **2002**, *281*, 61 – 70.
[152] E. H. A. Beckers, S. C. J. Meskers, A. P. H. J. Schenning, Z. Chen, F. Würthner, R. A. J. Janssen, *J. Phys. Chem. A* **2004**, *108*, 6933 – 6937.
[153] Z. Chen, U. Baumeister, C. Tschierske, F. Würthner, *Chem. Eur. J.* **2007**, *13*, 450 – 465.
[154] a) T. E. Kaiser, H. Wang, V. Stepanenko, F. Würthner, *Angew. Chem.* **2007**, *119*, 5637 – 5640; *Angew. Chem. Int. Ed.* **2007**, *46*, 5541 – 5544; b) T. E. Kaiser, V. Stepanenko, F. Würthner, *J. Am. Chem. Soc.* **2009**, *131*, 6719 – 6732.
[155] A. R. A. Palmans, E. W. Meijer, *Angew. Chem.* **2007**, *119*, 9106 – 9126; *Angew. Chem. Int. Ed.* **2007**, *46*, 8948 – 8968.
[156] T. E. Kaiser, I. G. Scheblykin, D. Thomsson, F. Würthner, *J. Phys. Chem. B* **2009**, *113*, 15836 – 15842.
[157] H. Lin, R. Camacho, Y. Tian, T. E. Kaiser, F. Würthner, I. G. Scheblykin, *Nano Lett.* **2010**, *10*, 620 – 626.
[158] D. Kurrle, J. Pflaum, *Appl. Phys. Lett.* **2008**, *92*, 133306.
[159] M. Gsänger, J. H. Oh, M. Könemann, H. W. Höffken, A.-M. Krause, Z. Bao, F. Würthner, *Angew. Chem.* **2010**, *122*, 752 – 755; *Angew. Chem. Int. Ed.* **2010**, *49*, 740 – 743.
[160] X.-Q. Li, V. Stepanenko, Z. Chen, P. Prins, L. D. A. Siebbeles, F. Würthner, *Chem. Commun.* **2006**, 3871 – 3873.
[161] F. Würthner, C. Bauer, V. Stepanenko, S. Yagai, *Adv. Mater.* **2008**, *20*, 1695 – 1698.
[162] A. Wicklein, S. Ghosh, M. Sommer, F. Würthner, M. Thelakkat, *ACS Nano* **2009**, *3*, 1107 – 1114.
[163] S. Ghosh, X.-Q. Li, V. Stepanenko, F. Würthner, *Chem. Eur. J.* **2008**, *14*, 11343 – 11357.
[164] X.-Q. Li, X. Zhang, S. Ghosh, F. Würthner, *Chem. Eur. J.* **2008**, *14*, 8074 – 8078.
[165] a) X. Yang, X. Xu, H.-F. Ji, *J. Phys. Chem. B* **2008**, *112*, 7196 – 7202; b) B. Jancy, S. K. Asha, *Chem. Mater.* **2008**, *20*, 169 – 181.
[166] a) F. Würthner, C. Thalacker, A. Sautter, *Adv. Mater.* **1999**, *11*, 754 – 758; b) F. Würthner, C. Thalacker, A. Sautter, W. Schärtl, W. Ibach, O. Hollricher, *Chem. Eur. J.* **2000**, *6*, 3871 – 3885; c) C. Thalacker, F. Würthner, *Adv. Funct. Mater.* **2002**, *12*, 209 – 218.
[167] a) A. P. H. J. Schenning, J. v. Herrikhuyzen, P. Jonkheijm, Z. Chen, F. Würthner, E. W. Meijer, *J. Am. Chem. Soc.* **2002**, *124*, 10252 – 10253; b) F. Würthner, Z. Chen, F. J. M. Hoeben, P. Osswald, C.-C. You, P. Jonkheijm, J. von Herrihuyzen, A. P. H. J. Schenning, P. P. A. M. van der Schoot, E. W. Meijer, E. H. A. Beckers, S. C. J. Meskers, R. A. J. Janssen, *J. Am. Chem. Soc.* **2004**, *126*, 10611 – 10618; c) E. H. A. Beckers, S. C. J. Meskers, A. P. H. J. Schenning, Z. Chen, F. Würthner, P. Marsal, D. Beljonne, J. Cornil, R. A. J. Janssen, *J. Am. Chem. Soc.* **2006**, *128*, 649 – 657; d) E. H. A. Beckers, Z. Chen, S. C. J. Meskers, P. Jonkheijm, A. P. H. J. Schenning, X.-Q. Li, P. Osswald, F. Würthner, *J. Phys. Chem. B* **2006**, *110*, 16967 – 16978; e) F. J. M. Hoeben, J. Zhang, C. C. Lee, M. J. Pouderoijen, M. Wolffs, F. Würthner, A. P. H. J. Schenning, E. W. Meijer, S. De Feyter, *Chem. Eur. J.* **2008**, *14*, 8579 – 8589.
[168] S. Yagai, S. Hamamura, H. Wang, V. Stepanenko, T. Seki, K. Unoike, Y. Kikkawa, T. Karatsu, A. Kitamura, F. Würthner, *Org. Biomol. Chem.* **2009**, *7*, 3926 – 3929.
[169] S. Yagai, T. Seki, T. Karatsu, A. Kitamura, F. Würthner, *Angew. Chem.* **2008**, *120*, 3415 – 3419; *Angew. Chem. Int. Ed.* **2008**, *47*, 3367 – 3371.
[170] J. T. Beatty, J. Overmann, M. T. Lince, A. K. Manske, A. S. Lang, R. E. Blankenship, C. L. Van Dover, T. A. Martinson, F. G. Plumley, *Proc. Natl. Acad. Sci. USA* **2006**, *105*, 9306 – 9320.
[171] a) S. Kirstein, H. von Berlepsch, C. Böttcher, *Int. J. Photoenergy* **2006**, *5*, 7; b) D. M. Eisele, H. v. Berlepsch, C. Böttcher, K. J. Stevenson, D. A. Vanden Bout, S. Kirstein, J. P. Rabe, *J. Am. Chem. Soc.* **2010**, *132*, 2104 – 2105.
[172] a) C. Königstein, R. Bauer, *Int. J. Hydrogen Energy* **1993**, *18*, 735 – 741; b) C. Königstein, M. Neumann-Spallart, R. Bauer, *Electrochim. Acta* **1998**, *43*, 2435 – 2445.
[173] S. Liu, W. M. Wang, A. L. Briseno, S. C. B. Mannsfeld, Z. Bao, *Adv. Mater.* **2009**, *21*, 1217 – 1232.
[174] a) J. Zhao, L. J. Sherry, G. C. Schatz, R. P. Van Duyne, *IEEE J. Quantum Electron. Sel.* **2008**, *14*, 1418 – 1429; b) N. T. Fofang, T.-H. Park, O. Neumann, N. A. Mirin, P. Nordlander, N. J. Halas, *Nano Lett.* **2008**, *8*, 3481 – 3487; c) G. A. Wurtz, P. R. Evans, W. Hendren, R. Atkinson, W. Dickson, R. J. Pollard, A. V. Zayats, *Nano Lett.* **2007**, *7*, 1297 – 1303; d) A. Salomon, C. Genet, T. W. Ebbesen, *Angew. Chem.* **2009**, *121*, 8904 – 8907; *Angew. Chem. Int. Ed.* **2009**, *48*, 8748 – 8751.
[175] a) M. Vacha, M. Furuki, L. S. Pu, K. Hashizume, T. Tani, *J. Phys. Chem. B* **2001**, *105*, 12226 – 12229; b) P. Michetti, G. C. La Rocca, *Phys. Status Solidi B* **2008**, *245*, 1055 – 1058.
[176] J. R. Tischler, M. S. Bradley, V. Bulovic, *Phys. Rev. Lett.* **2005**, *95*, 036401.
[177] J. R. Tischler, M. S. Bradley, Q. Zhang, T. Atay, A. Nurmikk, V. Bulovic, *Org. Electron.* **2007**, *8*, 94 – 113.

